Journal of Controlled Release 336 (2021) 207–232

Contents lists available at ScienceDirect

Journal of Controlled Release

journal homepage: www.elsevier.com/locate/jconrel

Review article

Cellulose nanocrystals in cancer diagnostics and treatment

Ishaq Lugoloobi [a,b,*], Hillary Maniriho [c], Liang Jia [b], Tabbisa Namulinda [b], Xiangyang Shi [a,b], Yili Zhao [d,*]

[a] State Key Laboratory for Modification of Chemical Fibers and Polymer Materials, Donghua University, Shanghai 201620, People's Republic of China
[b] College of Chemistry, Chemical Engineering and Biotechnology, Donghua University, Shanghai 201620, People's Republic of China
[c] Department of Biochemistry and Human Molecular Genetics, Faculty of Medicine, Tel Aviv University, Tel Aviv 6997801, Israel
[d] College of Textile Science and Engineering (International Institute of Silk), Zhejiang Sci-Tech University, Hangzhou 310018, People's Republic of China

ARTICLE INFO

Keywords:
Cellulose nanocrystals (CNCs)
Preparation
Modification
Cancer therapy
Biocompatibility

ABSTRACT

Cancer is currently a major threat to public health, being among the principal causes of death to the global population. With carcinogenesis mechanisms, cancer invasion, and metastasis remaining blurred, cancer diagnosis and novel drug delivery approaches should be developed urgently to enable management and treatment. A dream break-through would be a non-invasive instantaneous monitoring of cancer initiation and progression to fast-track diagnosis for timely specialist treatment decisions. These innovations would enhance the established treatment protocols, unlimited by evasive biological complexities during tumorigenesis. It is therefore contingent that emerging and future scientific technologies be equally biased towards such innovations by exploiting the apparent properties of new developments and materials especially nanomaterials. CNCs as nanomaterials have undisputable physical and excellent biological properties that enhanced their interest as biomedical materials. This article therefore highlights CNCs utility in cancer diagnosis and therapy. Their extraction, properties, modification, *in-vivo/in-vitro* medical applications, biocompatibility, challenges and future perspectives are precisely discussed.

Abbreviations: AA, acrylamide; AMC, 7-amino-4-methylcoumarin; ANC, aminated nanocellulose; APS, ammonium persulfate; ATRP, Atom transfer radical polymerization; 2-BPA, 2-Bromopropanoic acid; CCK, Cell Counting Kit; β CD, β-cyclodextrins; CHPTAC, (3-Chloro-2-HydroxyPropyl) TrimethylAmmonium Chloride; CNCs, cellulose nanocrystals; CNFs, cellulose nanofibrils; CNWBs, cellulose nano-whisker beads; COU, coumarin; CT, computed tomography; CTAB, Cetyl trimethylammonium bromide; CTX, chlorotoxin; CUR, Curcumin; DMAEMA, 2(dimethylamino)ethyl methacrylate; DMSO, dimethyl sulfoxide; DOX, doxorubicin; DOTA, (1,4,7,10-tetraazacyclododecane-1,4,7,10-tetraacetic acid); DTX, docetaxel; DTAF, 5-(4, 6-dichlorotriazinyl) aminofluorescein; DTPA, diethylenetriaminepentaacetic acid; EA, ethanolamine; ETOP, etoposide; FA, Folic Acid; FR, Folate receptor; FITC, fluorescein-5'-isothiocyanate; β-GP, β-glycerophosphate; g, grafted; GA-HA-CNC, Gelatin-hyaluronic acid-cellulose nanocrystals; GSH, glutathione; GTMAC, glycidyltrimethyl ammonium chloride; HCl, Hydrochloric acid; HCT116, human colorectal cancer cell; HL-7702, Human hepatocyte cell line; HMC, 7-hydrazino-4-methylcoumarin; IC_{50}, half maximal inhibitory concentration; ICG, Indocyanine green; KB, human epithelial carcinoma cell line; LbL, Layer-by-Layer; LC, Long chain; LDH, Lactate dehydrogenase; LUS, luteoloside; LUT, luteolin; 3-MPA, 3-Mercaptopropionic acid; MCC, microcrystalline cellulose; MCF-7, Michigan Cancer Foundation-7; MMP-2, Matrix metalloprotease-2; MTS, PromegaCellTiter 96 Aqueous One Solution Cell Proliferation assay; MTT, 3-(4,5-dimethylthiazol-2-yl)-2,5-diphenyltetrazolium bromide; $NaIO_4$, periodate chlorite; NCI H 460, human large cell lung cancer cell line; NPs, Nanoparticles; N/P, nitrogen (N) to phosphate (P) ratio; M_n, the number-average molecular weight; OSO_3, anionic half-ester sulfate; 2-PyA, 2-Propynoic acid; 4-PA, 4-Pentenoic acid; PAA, poly(acrylic acid); PAMAM, polyamidoamine; PCL, Poly-ε-caprolactone; PDMAEMA, Poly(2(dimethylamino)ethyl methacrylate); PE, Pickering Emulsion; PEG, poly(ethylene glycol); PEEP, Poly(ethyl ethylene phosphate); PEI, polyethylenimine; PGEA, (poly (glycidyl methacrylate) (PGMA) functionalized with ethanolamine (EA); PGMA, poly (glycidyl methacrylate); PIPOx, Poly(2-isopropenyl-2-oxazoline); PLGA, poly(lactic-co-glycolic acid)/ Poly-D-L-lactide-co-glycolide; PLA, Polylactic acid; PMMA, Poly(methyl methacrylate); POE, poly(oxyethylene); poly(AEMA), poly(N-(2-aminoethylmethacrylamide)); PPEGEEMA, Poly(poly(ethylene glycol)ethyl ether methacrylate); PTX, paclitaxel; PVA, polyvinyl alcohol; QC, Quaternized cellulose; QDs, quantum dots; RAFT, reversible addition–fragmentation chain transfer; RBCs, red blood cells; RBITC, rhodamine B isothiocyanate; ROP, ring-opening polymerization; ROS, reactive singlet oxygen; SI-ATRP, surface initiated -Atom transfer radical polymerization; SI-SETLRP, surface-initiated single-electron-transfer living radical polymerization; siRNAs, Small interfering RNAs; TEMPO, 2,2,6,6-tetramethyl-1-piperidine-N-oxy; TSPP, trisulfonated tetraphenyl porphyrin; UV, Ultraviolet.

* Corresponding authors at: College of Textile Science and Engineering (International Institute of Silk), Zhejiang Sci-Tech University, Hangzhou 310018, People's Republic of China

E-mail addresses: 318073@mail.dhu.edu.cn (I. Lugoloobi), yzhao@zstu.edu.cn (Y. Zhao).

https://doi.org/10.1016/j.jconrel.2021.06.004
Received 4 February 2021; Received in revised form 2 June 2021; Accepted 3 June 2021
Available online 5 June 2021

1. Introduction

Regardless of the irrefutable recent evolution in medicine and health care, some pathologies including cancer have remained among the most 21st century's dreaded diseases of the global population including patients, experts and health providers alike. Ominously, an estimated 11.4 million death toll from cancer is anticipated in 2030 [1,2]. Cancer is a complex state of illness initiated by alteration and mutation of healthy cells at the molecular level, and it is associated with approximately 200 different types of diseases [3]. However, it is projected that scientific and technological advances could increase likelihood of early diagnosis and consequently treating more cancers as "manageable" chronic diseases, coupled with a favorable pleasing quality of life. Lately, novel cancer research has focused on theranostic as an emerging research field. Theranostics integrate diagnoses and therapies into single systems to allow monitoring of treatment outcomes for efficient therapy of targeted illnesses. Theranostic innovations could hasten the hinderance of cancer growth at diagnosis/screening phases thus, potentiating subsequent specialist treatments [4,5]. Recent findings in nanotechnology have supported, among others, novel molecular imaging and drug/gene delivery methods in cancer treatment by utilizing nanomaterials to develop emerging theranostic systems. Diverse forms of nanomaterials from different sources and preparations, in form of nanoparticles of micelles, liposomes, metal atoms/ions, dendrimers, natural and synthetic polymers, are being/have been explored for biomedical applications [6–11]. These nanoparticles possess appealing properties such as tunable sizes, modifiable surfaces, excellent drug bioavailability, high loading potential, tumor targeting precision, controlled drug release, and thus portray an effectively high therapeutic efficiency and low toxicity [10]. Studies on these nanocarriers have solved limitations of delivery of chemotherapeutics like poor water solubility of most anticancer agents, toxicity to normal cells, poor bioavailability. Nevertheless, we aim at limiting the discussion in this article to plant derived cellulose nanocrystals (CNCs).

Wide spread interest in nano-structured cellulosic materials as biomedical resources is an upshot of their stupendous properties such as sustainability, biodegradability, biocompatibility, remarkable mechanical properties, availability, worldwide variety and abundancy with low cost, renewability and biomass-based economy, low energy consumption, environmentally benign, and low cytotoxicity [12–16]. As a supplement, these structural scaffolds made of green plant cells have great mechanical properties, and could easily be highly functionalized. Therefore, they have precipitously drawn attention of both academia and industry as manifested in the plenteous scientific publications [14]. The various cellulose sources such as trees/plants, bacteria, tunicates (sea squirts) and algae; extraction/production methods and conditions; and the surface chemistry own variations in nanocelluloses as summarized in numerous review papers [14,16–18]. Also, the large differences in the cellulose biosynthesis processes of several raw material sources sway the cellulose chain stacking, and thus result in dissimilar crystallinity degrees, cellulose polymorph, dimensional sizes, particle aspect ratios, and cross-section morphologies of the extracted nanoparticles. Henceforth, deconstruction of wood fibers or other plant structures results in cellulose nanofibers (CNFs) and/or CNCs [15,16,19,20] as amongst the three main nanocelluloses, with bacterial nanocellulose inclusive. As noted above and as portrayed by Foster [21], CNFs differ from CNCs in a way that the former are attained either mechanically or chemically [16] to form much longer (microns) and different nanofibrils, with mixtures of amorphous and crystalline cellulose chains [22] in the same suspension. Nanofibrils also form a gel at very low (averagely 1.5 wt.%) concentrations while a thick paste is formed at relatively higher concentrations (by 10 wt.%). They are also flexible with aspect ratios of 10-100, width range of 6–80 nm, 500–2000 nm long and crystallinity of 40–70% [14,23,24]. While the CNCs are generated *via* chemical treatments to form rice-like crystallites [16,22] that are shorter and much similar in appearance and properties [25], they typically do not independently gel until a concentration of approximately 10-14 wt. % [26]. CNCs therefore, appear organized in achiral nematic way in suspensions that form iridescent films when dried. Furthermore, they are generally stiff, spindle-like, with aspect ratio range of 5-30, 3-50 nm wide, 100-400 nm long, and 60 - 90% variation in crystallinity, depending on the starting material [14,23,24,27–30]. From the available literature, both nanoparticles have immense potential for various applications, however, this review will principally focus on CNCs which are far more abundant and cheaper.

For decades, CNCs have reaped considerable attention in both academic and industrial area. These uniform nanorod-like shaped crystallites are commonly produced *via* acid hydrolysis which interrupts the hydrogen bonding network, leading to cleavage of the cellulose microfiber. This treatment imparts them numerous and unique physicochemical features, optical properties and high aspect ratio. Such properties include high elastic modulus/stiffness (110−220 GPa) due to high surface area (~250 m^2/g), high tensile strength (2-10 GPa) [31,32], low density (1.6 g/cm^3) [31], coupled with unique surface morphology bearing abundant surface hydroxyl groups [15,16,33,34]. These properties make them of a valuable potential as raw materials for future sustainable, renewable and decomposable products. The hydroxyl groups on CNCs surfaces have offered a facile platform for the chemical functionalization with amino, carboxyl, aldehyde, or thiol groups by means of grafting or oxidation [35]. These modifications enable the attachment of smaller chemical moieties such as biomarkers, metal nanoparticles, or larger protein/polymer macromolecules. The hydroxyl groups confer hydrophilicity to CNCs, thus improving their dispersibility in polymer matrices. These superior features coupled with easy chemical modification make CNCs suitable for various applications as functionalized nanoparticles. They are used in systems, such as colloidal complexes, oil-water emulsions, 2-D films and membranes, 3-D hydrogel and aerogels and the yet to be discussed drug delivery and bioimaging. Their importance can be inferred from large-scale production in Japan, Europe, and North America purposely for easy access and affordability of research innovations and development in various sectors [35].

Despite their early discovery in 1949 [35], it was the research in CNCs colloidal suspensions from Gray's laboratory in 1992 [36] that incited curiosity in the materials science community to actively investigate their potential. Modified CNCs were initially explored for use as reinforcing materials before they could be innovatively tested for fluorescence bioimaging applications [37]. This elicited interest for their biomedical applications and other fields by exploiting their chemistry, as documented in several reviews [15,22,33,35,38–41]. The present review examines significant discoveries that utilize CNCs as nanoplatforms for application in cancer therapy. We will analyze CNCs sources, extraction, properties and their application in drug delivery and bioimaging specifically in cancer treatment and diagnosis. Briefly, we highlight the biological and toxicity properties that may limit efficient integration of CNCs in clinical biomedicine.

2. CNCs sources, extraction methods, formation and properties

CNCs were first visualized in the 1950s by Rånby *et al* [42], before being extensively studied in the 1960s [43]. CNCs as termed by the international organization for standardization (ISO) [44] or as a commonly used term, are also synonymously called nanocrystalline cellulose, crystallites, cellulose nano-whiskers, rod-like cellulose microcrystals, whiskers or needles.

2.1. Sources of CNCs

CNCs are crystalline regions of the CNFs, which are also described as the monocrystalline regions of cellulose [45]. Their sources include: wood (such as balsa wood, douglas-fir wood chips, Acacia mangium, bleached eucalyptus kraft pulp, bleached hard wood kraft pulp, poplar) [46–51] that originate from a wide range of forests; industrial cellulosic

products like cotton linter and pulp, whatman, waste office paper, and tetra pak paperboards [30,52,53]; agricultural, fiber and industrial bio-residues such as apple pomace, grape pomace [54], sugar cane, coconut husks, mengkuang leaves, corn husk/ straw [55], pine cones [27], oil palm fronds [56], doum leaves [57], cassava bagasse [58], banana peel, pineapple leaves, coffee skin [59], rice straw, rice husk, bamboo, sugar beets, sugar palm (Arenga pinnata) fibers [60], kenaf bast fiber [61], sisal, mulberry branch bark, , wheat straw or ramie [15,62], Sago seed shells [63]; marine biomass such as bacterial, tunicin, cladophora cellulose [64], sea weeds, red algae [65–69]; microcrystalline cellulose (MCC) [70–72]; among others [62]. These provide a wide range for the exploitation of the high-value and sustainable CNCs, as biomaterials. Generally, sources affect the choice of CNCs, for instance, CNCs from seaweeds are more preferred compared to that from land plants and other sources. This is because they are easily extracted owed to the low matter of other constituent polysaccharides hence less interference to cellulose isolation, grow rapidly and allow a reduced harvest time, contain higher contents of stored carbohydrate for higher CNCs yield [66,67]. However, land derived CNCs sources such as cotton possess a high cellulose content and highly exposed hydroxyl groups [73]. Therefore, their treated fibers are equally modifiable for medical and other applications, in form of either yarns or knitted fabrics [74–76]. With such wide distribution in plants, bacteria, alga, among others, CNCs are among the highly abundant natural nanomaterials.

2.2. Extraction methods of CNCs from raw materials

CNCs are extracted via chemical processes such as acid hydrolysis and chemical oxidation, enzymatic hydrolysis and mechanical treatment (Fig. 1).

Universally, CNCs are isolated chemically by hydrolytic treatment of cellulose with strong acids [16,78,79], as developed in the 1940s and 1950s [42,80–82] after the introduction of the idea by Nickerson and Habrle [80]. Commonly utilized acids such as the typical sulfuric acid [25,52,63,70,83,84], hydrochloric acid [16,71] or phosphoric acid [84] infiltrate into and dissolve the nearby amorphous /disordered domains of the cellulose fibers and fibrils. This leads to cleavage of the glycoside bonds and thus leave behind rigid and highly crystalline CNC nanorods (Fig. 2) [16] that are resistant to acid penetration, and produced at different yields depending on the acid conditions used [15,85–87]. At certain treatment conditions therefore, CNCs tend to retain the same crystal allomorph as the cellulose source.

The other explored acids include: hydrobromic acid, maleic acid [12,52], dicarboxylic acids [88], the more recently developed phosphotungstic acid [89], and combined acid hydrolysis such as sulfuric acid/oxalic acid [46] and sulfuric acid/acetic acid hydrolysis [51] combinations. However, new chemical methods for CNCs preparation have emerged [39,90], that is esterification [88,91–94], ionic liquid treatment [50], subcritical water hydrolysis [95], oxidation chemistry such as oxidation using ammonium persulfate (APS), a strong oxidant [96], Hydrochloric acid (HCl) and 2,2,6,6-tetramethyl-1-piperidine-N-oxy (TEMPO) oxidation [97,98], $NaIO_4$ oxidation [99], DMSO and succinic/acetic anhydride [100,101] and a completely less disadvantaged modern approach utilizing HCl vapor [102–104].

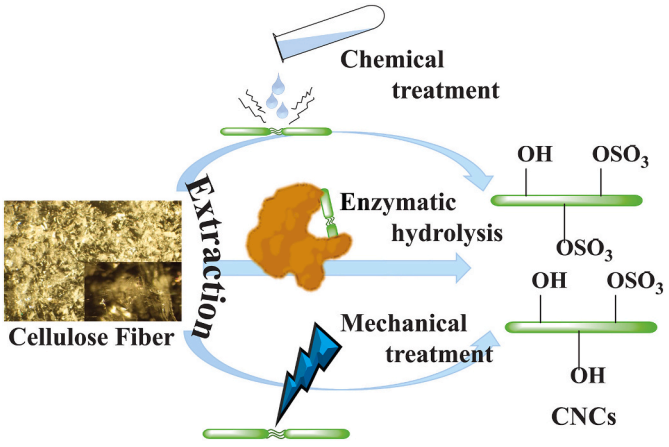

Fig. 1. Illustration of the processes for the extraction of CNCs (green rod-like sulfated/hydroxylated structures) from raw materials (such as cotton nano-whiskers [77]). Reproduced with permission from ref. [77]. Copyright 2013, Engineering.

CNCs can also be biologically extracted from cellulosic microfibers such as MCC through the elimination of amorphous domains by enzyme-assisted hydrolysis or microbial treatment by microorganisms such as Trichoderma reesei, Penicillium oxalicum M12, Aspergillus niger, Caldicellulosiruptor bescii [39,78,105]. Cellulose sources are disintegrated by enzymes such as cellulase, cellobiohydrolase, endoglucanase. The method involves initial hydrolysis of hemicellulose to expose the shielded cellulose, which then undergoes H-bond breakdown to form the CNCs [106]. The cellulose fibers may sometimes be pretreated with substances such as ionic liquids to enhance the enzymatic process for a shorter hydrolysis time. This method is not only environmentally benevolent but also employable together with mechanical fibrillation and chemical pretreatment with substances such as ionic liquids. Enzymatic hydrolysis is also cheap and allows selective degradation of the amorphous regions in the cellulosic fibers, while leaving the crystalline regions unscathed. The numerous hydroxyl groups exposed on the surfaces of produced CNCs allow an easier and wider chemical manipulation and thus enriching the medical industry. However, it faces obstacles such as production of low CNCs yields, requirement of high mechanical energy to disintegrate enzymatically hydrolyzed cellulose fibers, longer time for hydrolysis, requirement of further research to improve its efficiency for application with mechanical fibrillation [78,105,107]. Other challenges include difficulty of dispersing and functionalizing CNCs and limited thermal stability of the enzymatically produced CNCs. These have made the enzymatic process using cellulase to be limited to a pretreatment procedure for enhancing the chemical method.

Abstraction of CNCs using mechanical refining [39] has also been surveyed. The various mechanical methods utilized include high pressure homogenization, ultrasonication, and ball milling [106,108]. During the mechanical extraction, the produced energy in form of mechanical vibration breaks down the amorphous cellulosic bonds to enhance the degradation of the polysaccharide linkages. This energy also causes the isolation of micro- and nano-scale fibrils from the cellulose materials. Disadvantageously therefore, this process requires extreme energy input, however, the raw materials can undergo initial pretreatment before incorporation.

Multi-process integration systems such as oxidative or enzymatic-mechanical, chemical-enzymatic [62], and chemical-mechanical treatments such as mixed chemical-ultrasonic and ball mill assisted solid acid hydrolysis [72,79,83,109] have also been developed.

2.3. Formation of CNCs nanoparticles

CNCs extraction generally consists of three steps including the pretreatment step(s) such as depolymerization and mercerization/alkaline treatment to purify and homogenize the starting material by removing the non-cellulosic contents (wax, hemicellulose, pectin, natural fats), the bleaching/delignification step, followed by the refinement step(s) [14,59,67] which include acid or enzymatic hydrolysis, and mechanical shear/dispersion. Above all, refinement by acid hydrolysis remains the established protocol for CNCs preparation as suggested by the current knowledge on cellulose ultrastructure. Acid hydrolysis owes credit of productivity with high CNCs yields and reasonably economical [14,27,28]. Several sources including those cited in this review, reflect sulfuric acid hydrolysis of cellulose raw materials as an established,

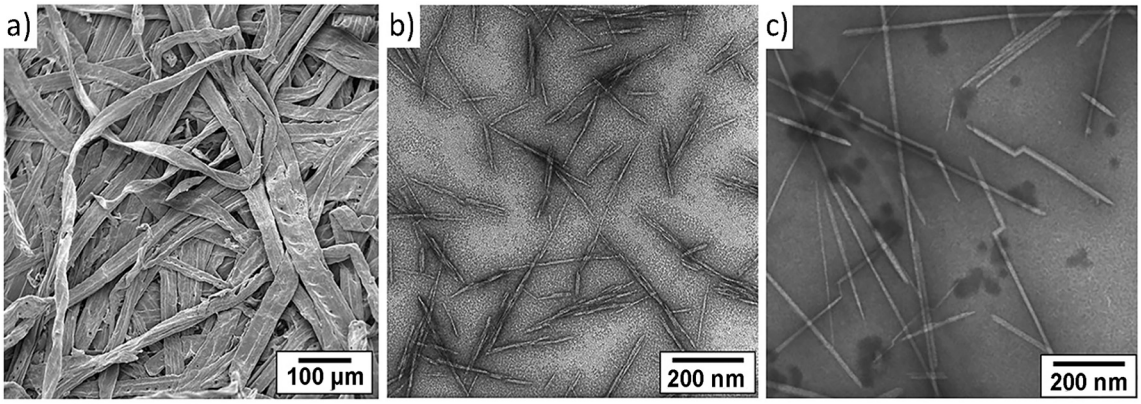

Fig. 2. (a) Scanning Electron Microscopy (SEM) of wood fiber, (b) TEM of wood CNCs, (c) TEM image of tunicate-CNCs. Reproduced with permission from ref. [16]. Copyright 2011, Chemical Society Reviews.

reproducible and widely exploited technique for CNCs preparation in both academia and industry [15]. Sulfuric acid efficiently cleaves the disordered segments in native microfibril and interacts with the surface hydroxyl groups via the esterification reaction to produce crystallites, while simultaneously introducing the OSO_3^- groups on their surface (Fig. 3). These OSO_3^- groups induce repulsive forces between the CNCs, thus leading to an electrostatically stable colloidal suspension in water [15,39,90]. The OSO_3^- content can be obtained by elemental analysis of the present amount of sulfur or using a more simpler method of conductometric titration [110]. While the OSO_3^- content is dependent on sulfuric acid concentration and hydrolysis reaction time, however, the precise location of the OSO_3^- moieties on the CNC molecular surface is yet to be determined [111].

On the other hand, the main concerns associated with using mineral acid hydrolysis especially sulfuric acid include: cumbersome and uneconomical acid recovery; harsh reaction conditions; toxicity of the final product and thus its limited use; low thermal-stability of the yielded sulfate-modified CNCs, but use of sodium exchange and alkali bases such as sodium hydroxide during extraction can increase the thermal stability; potential cellulose degradation which increases the vulnerability to corrosion; advanced functionalization of the sulfate-modified CNCs have remained difficult; and persistently low yields of CNCs, though this is most limited by the acid concentration as a critical parameter [68,109,112].

After hydrolysis, these chemical acids can be neutralized by either washing with water, or dissolving in a base such as sodium hydroxide followed by washing of the formed salts with water. Though retaining of the acids and the low salt concentrations does not affect some of the properties of the prepared CNCs suspension such as the zeta potential, apparent particle size, surface tension, electrophoretic mobility, the performance of their applications such as emulsions [113] are normally influenced by the counterion effect, thus a need for their removal. Furthermore, another hindrance of this process arises at this point with the need of green treatment of the acidic/salty waste water, that may be concentrated and impact the environment. Nevertheless, this traditional process is unceasingly used today in numerous firms for commercial production of CNCs [114]. This has currently limited efforts to elevating pretreatment approaches which are particular to lignocellulosic matter.

For easy handling, transportation and storage, CNCs are normally solidified either by freeze- or spray-drying [21,115]. These are later on redispersed into colloidal suspensions when needed for use.

Several investigations have revealed that the hydrolysis requirements (reaction times, temperature, acid concentration (acid/fiber ratio) and nature) and source of cellulose material are critical parameters that impact most CNCs properties such as morphology and size dimensions, crystallinity, crystallite allomorph structures, thermal resistance, including their overall yield [14,62,85,116]. Other factors may include acid catalyzed hydrolysis by salts of inorganic ions that mainly affect CNCs quality and yield [71]. Generally, CNCs yield is higher at lower acid/chemical concentration and longer hydrolysis time allowed [7,117]. Morphological shapes may include sphere, rod, needle, spike shape and these are important features in CNCs since they relate to inter/intra-molecular hydrogen bonds and crystallinity, as influenced by their source and controlled treatment conditions [22,65,117,118]. For instance, smaller CNCs particles were obtained from sugarcane bagasse by treatment with higher citric acid concentration and longer hydrolysis time. Also, the lateral and length dimensional sizes of CNCs extracted from hard wood are smaller (3-5 nm and 100-300 nm), respectively, where as those of CNCs derived from tunicate are longer (15-30 nm and 1000-1500 nm), respectively [15]. Particle size of CNCs is also influenced by the species level of plant sources [68].

Generally, CNCs are more crystalline as compared to their sources due to the removal of the non-cellulosic parts during the refinement step to release the individually rearranged crystalline components, however, thermal stability varies especially depending on the extraction method and the applied conditions [68]. These factors also vary depending on the group, for instance, as compared to the traditional CNCs sources, seaweed CNCs have a relatively higher crystallinity, are more thermally stable and as well easily accessed [68]. The higher thermal stability of seaweed CNCs compared to their source was due to the removal of the non-cellulosic portions that possess more active sites that can initiate the heating process within the furnace. However, most sources portray a

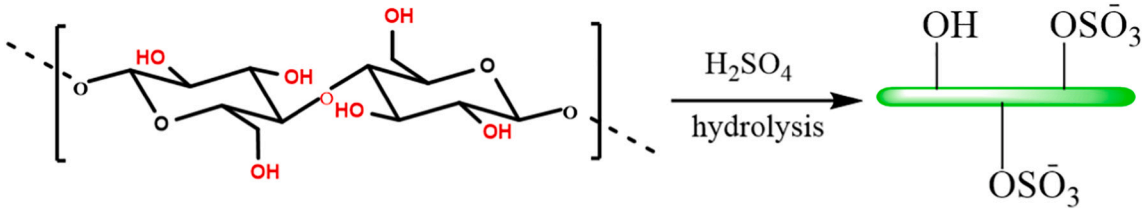

Fig. 3. Preparation of cellulose nanocrystals (CNCs) *via* acid hydrolysis of cellulose; native cellulose (LEFT) and diagrammatic representation of rod-like sulfated/hydroxylated CNCs (green).

lower thermal stability of extracted CNCs due to the rapid decrease in the molecular weight, the increase of the amorphous sulfate ions and the absence of the non-cellulosic domains such as lignin that are not only heat resistant but also act as linkers [62,68]. Also, CNCs with many sulfate groups have weak thermal stabilities because the sulfate groups act as active sites to initiate thermal decomposition [51]. However, extraction using $FeCl_3$-catalyzed deep eutectic solvent system produced more thermally stable CNCs than their original sources. This was due to the efficient and highly selective removal of the cellulose amorphous parts to produce highly crystalline CNCs [50].

Basically, cellulose has two native and common crystalline allomorphs, cellulose I and II and these differ in their self-assembling structure, morphology and performance during applications [119]. Other exhibited allomorphs include cellulose III and IV, as reviewed by Mishra et al [120]. These are identified by X-ray diffraction patterns, showing disparities in the inter and intra-molecular interactions within the matrix of the polymer. Generally, cellulose III is obtained from Cellulose I and II by chemical treatment with agents such as liquid ammonia, while cellulose IV is extracted by thermal treatment from cellulose III. Hydrolysis with dissimilar acids can be manipulated to independently extricate the native polymorphs of CNCs with different morphologies [84,86]. For instance, hydrolysis of cotton with hydrochloric acid and phosphoric acid erected cellulose I and II, respectively, while the use of sulfuric acid generated a mixture of cellulose I and II polymorphs. Sulfuric acid hydrolysis can also permit extraction of specifically cellulose I from cellulose III. Also, spherical shaped CNCs were obtained with phosphoric acid hydrolysis, while the other two acids developed fiber shaped CNCs.

Some researchers proposed a tentative schematic model for the formation of allomorphs CNC-I, CNC-II and CNC-I/CNC-II from eucalyptus CNC-I substrate by controlling various parameters, while studying their state of order during the hydrolysis process [53,85]. In a particular study, the transition of CNC-I supramolecular structure to CNC-II was obtained at 60 wt.% sulfuric acid concentration with a drastic change in CNC yield [85]. CNC-I displayed spindle-shapes, while CNC-II exhibited twisted-strip structures. As well, a high yield of 66.7% CNC suspension was obtained at 60 °C and 58 wt.% acid concentration.

It's also worth noting that CNCs are significantly less flexible compared to other nanocelluloses owed to the disrupted amorphous domains in their ultra-structure [15,121].

2.4. Colloidal stability of CNCs

The choice of acid bestows desired functional moieties on the CNC surface which in turn influences their colloidal stability. For instance, CNCs yielded by hydrolysis with hydrochloric acid are uncharged and thus have poor colloidal stability, while those yielded with sulfuric acid are imparted with negatively charged half-ester sulphate groups that form highly stable colloidal dispersion [22]. Maleic acid together with ball mill pretreatment were also utilized to prepare CNCs with high yield and good colloidal stability. The use of ball mill pretreatment was responsible for the high CNCs yields, while maleic acid reacted with β-1,4-glucosidic linkages/hydrogen bonds of cellulose monomers, hydrolyzed the disordered regions to release the crystals, and then catalyzed the esterification of the exposed hydroxyl groups with maleic anhydride anionic groups to form a colloidally stable CNCs suspension [12]. The colloidal stability was caused by the high charge density due to the formation of carboxyl groups on the CNCs surfaces from the esterification reaction. Deep eutectic solvents and mixed acids such as sulfuric/oxalic acid system have also been utilized to enhance colloidal stability in both aqueous and organic solvents like ethanol, DMF by addition of extra functional groups (esters, carboxyl) on CNCs surfaces [46,50,51]. CNCs colloidal state may contrast several properties such as morphology, surface chemistry, aspect ratio, crystal structure, degree of crystallinity [122–128]. Aggregated CNCs may also affect biological properties such as toxicity to normal cells.

Classically, suspensions in water with $\varsigma > \pm 30$ mV are deemed stable while those with $\pm 10 < \varsigma < \pm 30$ mV attain partial stability, thus dependance on surface charge (ς) [129,130]. However, the hydrolysis environment (temperature, concentration, time) also affects the particle size and thus influencing the stability [16,122,131]. Poor colloidal stability causes hard to break agglomerations due to the strong interparticle forces such as the hydrogen bonds that are induced by high surface area-to-volume ratios of the nanoparticles. The agglomeration strengths are around 10^4-10^9 Pa and therefore, high energetic processes such as ultrasonication, which produces an energy density of 10^6-10^8 Pa is commonly applied. This breaks interparticle bonds of agglomerated or dried solid particles to allow homogeneous dispersion of CNCs in a medium. Ultrasonication has been applied for small suspensions though it normally affects the CNC crystallinity, but high-pressure homogenizers have also disclosed efficacy with nanoparticle dispersion [132,133]. The efficiency of these applied mechanical methods for homogeneous dispersion of suspensions are affected by time, applied energy, medium description (viscosity, concentration, volume, density, temperature), tip diameter of the ultrasonicator, preparation of nanoparticles, homogenization process [122,134].

While pH has little effect on the colloidal stability of the CNCs, presence of salts causes an unstable effect. At low salt concentrations, CNCs form stable colloidal suspensions and these become unstable with increase in salt concentration, with formation of a sudden transition called the critical coagulation concentration (CCC). The addition of salts increases the viscosity of the suspension leading to the aggregation of the solution. This is due to the alteration of the electrostatic interactions that arise from the overlap of the electric double layers around ionic particles, with the rapid reduction in the zeta potential of CNCs [135]. This increases the ionic strengths to form CNC aggregates that morphologically express either sideways lateral associations of CNC particles or cross-linkage with each other, with a fractal dimension of 2.1.

Correspondingly, CNC aggregation varies with difference in charge of salts/ions. For instance, Cao and Elimelech recently showed that monovalent and divalent cations show a similar trend in the magnitude of electrophoretic mobility and CCC values, as reflected by the direct Hofmeister series [135]. Whereby, the magnitudes of CCC values parallels the reverse order of the sizes of cations and thus exhibit specific interaction of these ions with surfaces of CNCs. For trivalent salts however, the authors revealed that destabilization of CNC suspension was found to be more effective. In the case where monovalent and divalent cations show one CCC, trivalent cations show three CCCs in the intermediate concentration regions. This behavior in trivalent cations was due to the charge reversal and re-stabilization of the electrophoretic mobility of CNCs. Additionally, the magnitude of the CCCs of CNCs decreased with increase in the salt counterion valences, and this is in agreement with the predicted Schulze–Hardy rule ([135–137] and the classical DLVO theory [138,139].

As a wrap-up, colloidal stability performs a key role in the application of CNCs in nanotechnology and material science, for example, it affects properties such as catalytic activity, mechanical strength, optical properties of the CNCs-reinforced nanocomposites, hydrogels, aerogels, since these are greatly influenced by the filler dispersibility to form a percolating network [118,140–145]. Thus, percolating networks are normally formed by homogeneously dispersed suspensions. In drug delivery systems, modified CNCs gene carriers with high colloidal dispersion in suspension expressed high efficacy for cancer therapy with negligible cytotoxicity [146]. The high stability was achieved by controlled replacement of the sulphate groups (hydrothermal treatment) via de-esterification. Hydrothermal desulfation is an economical, safe, and environmentally-friendly process for controlling the density of the sulfate groups. Sulfate groups density can also be controlled using traditional chemical procedures such as solvolysis and acid-catalysis by addition of solvents and/or acids, complex reaction, with further purification steps.

3. Modification of CNCs for cancer therapy

CNCs have been prepared by various methods and from different high cellulose content raw materials [15,39]. The common preparation methods include acid hydrolysis [147], enzyme-assisted hydrolysis and oxidation. Depending on the formulation and advanced use, several techniques][118] have been adapted to modify CNCs for suitable utilization. Depending on the initial chemical reagent used in the preparative phase, different chemical groups can be non/covalently bonded on the CNCs surface. For instance, hydrolysis using sulfuric acid yields CNCs with sulphate groups unlike hydrochloric acid which yields CNCs with free -OH groups. As a result, the active chemical groups and the surface charge on the CNCs can be finetuned *via* esterification, de-esterification, oxidation, coordination and nucleophilic substitution reactions. Example of chemical groups that have been used to modify CNCs and its sources like cotton include; alkoxy(ether)-, amido-, carbamyl-, silyl- among others which can be added by their respective reactions and polymer grafting [35,73]. Modification of CNCs with cationic vectors such as chitosan, Poly(2(dimethylamino)ethyl methacrylate) (PDMAEMA), polyethylenimine (PEI) derivatives and poly(L-lysine) has also been of extensive research to exploit their electropositivity and low immunogenicity properties [148–152] which can be suitable for biomedical applications. The bio-functionalization of such agents alleviates the self-agglomeration of CNCs during drying, owed to the breakdown of the formed inter- and intra-molecular hydrogen bonds. Improvement of cell penetration efficiency and inhibiting the activity of tumor cells at certain stages of development are also realized and thus facilitating cancer therapy. By modifying CNCs with precise chemical groups, improved electronic, magnetic, catalytic, acidic, fluorescence, thermal, and optical properties can be imparted. In this review therefore, we thus discuss the modification of CNCs and their derivatives with various agents for cancer therapy (Fig. 4).

3.1. Alternation of surface functional group

Natural sources of CNCs such as cotton possess abundant hydroxyl groups to a tune of 8.13×10^{-3} hydroxyl groups per unit surface area [35,73]. During the extraction of CNCs, these hydroxyl groups can either be maintained or replaced with sulfate, carboxyl, acetyl moieties depending on the chemical or any other treatment utilized. In one of the versatile controlled acid hydrolysis techniques, average-sized 50 nm CNCs with a restored crystallinity and preserved maternal morphology were prepared from MCC by using the compositional mixtures of strong acids (H_2SO_4 and HCl) under varying concentrations [153]. Unlike HCl, H_2SO_4 imparts OSO_3^- groups on CNCs surface. Varying their concentration and ratio also proved formation of either spherical or rod-shaped CNCs. It is much anticipated that these spherical-shape tunable and porous CNCs can circulate in the blood by approximately ten-fold longer time relative to the filament-shaped CNC nanoparticles, thus become potential drug delivery cargo for diseased biological compartments [153]. Further tests with murine embryo fibroblasts (NIH3T3 cells lines) and colon adenocarcinoma cells (HCT116 cells lines) proved their biocompatibility for cancer treatment [154]. Associatively in a modified acid hydrolysis technique, the strong acids (H_2SO_4 and HCl) were replaced with citric acid to yield carboxyl CNCs in one step][117]. The resulting needle-like shaped CNCs of diameter range (20-30 nm) and length range (250-450 nm) had high colloidal stability, at least one carboxyl group, with 32.2% conversion efficiency of the original weight of bagasse pulp. Ultrasonication was utilized to overcome the rigidity of the cellulose fiber and therefore, catalyzing the carboxylation process by the weak edible citric acid. This also caused formation of smaller CNCs compared to non-mechanically treated CNCs. The Carboxyl groups were added through an esterification reaction between free hydroxyl groups of CNCs and carboxyl groups from citric acid, producing up to 0.65 mmol g^{-1} of carboxylate content in the CNCs][117]. This was a high carboxyl content reported. However, Abitbol *et al.* [155] had previously explored the application of carboxylate modification by tagging carboxyl CNCs obtained from APS oxidized wood pulp with CdSe/ZnS semiconductor quantum dots (QDs) *via* carbodiimide chemistry coupling in a one-route water-based covalent modification. This approach yielded morphologically controlled, colloidally stable and highly fluorescent QD-CNC hybrid nanoparticles for a long time. These nanoparticles were utilized for the formation of transparent and powerfully fluorescent QD-CNC/CNCs films for bio-imaging, optical/sensing devices, nanoparticle tracking, and anti-counterfeit applications. In a more recent study involving the preparation of a synergistic chemo-photothermal therapeutic agent for treatment of colon cancer cells, the utilized carboxyl CNCs interacted with aminated nano

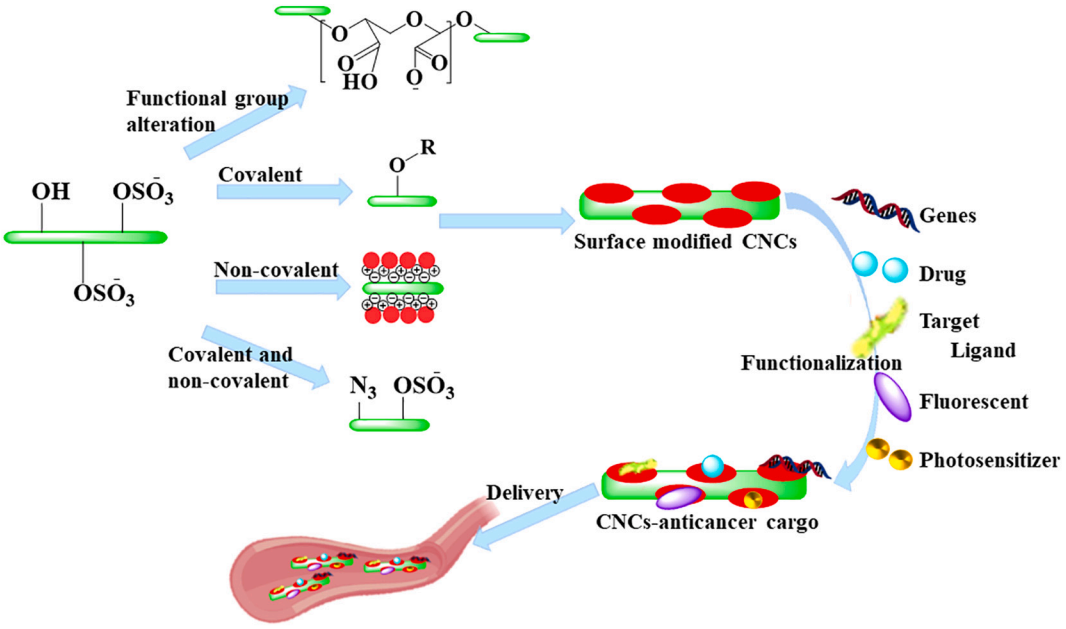

Fig. 4. Summary of the methods for CNCs (green rod-shaped) surface modification and functionalization with anticancer agents for cancer treatment. R=H, alkyl, polymer.

dextran/reduced graphene oxide complex (AD/MGO) via electrostatic bonds to form delivery nanocomposites with characteristic smooth surfaces and minor agglomeration [156]. The carboxylated CNCs anionic polyelectrolyte were prepared by reaction of CNCs with TEMPO to increase the carboxyl group content for an enhanced ionic and hydrogen bonding interaction of the cellulose. Curcumin (CUR) was thereafter loaded onto the nanocomposite surface at pH 8.0 to a capacity of as high as 86.4% via π-π stacking and hydrogen bond interactions to form a drug-nanocarrier with a LbL construction appearance. Furthermore, Herreros-López *et al* [157] covalently grafted photosensitive amino-fullerene C_{60} and fluorescent FITC derivatives to carboxyl CNCs via amide bonds in a one-route reaction to form delivery hybrids for photodynamic cancer therapy. The carboxyl groups were added via TEMPO oxidation of some hydroxyl groups on the CNCs surface followed by HCl acidification.

Functionalization of CNCs with more complex carboxylic acids has also been explored. 2-Propynoic acid (2-PyA), 2-Bromopropanoic acid (2-BPA), 3-Mercaptopropionic acid (3-MPA), 4-Pentenoic acid (4-PA) were used to hydrolyze Whatman paper-derived cellulose fibers yielding their respective modified CNCs (2-PyA-CNC ,2-BPA-CNC, 3-MPA-CNC, 4-PA-CNC). These functionalized CNCs were found to be thermally stable compared to CNCs obtained by hydrolysis with HCl or H_2SO_4. 2-BPA-CNCs were further modified by grafting with Poly(methyl methacrylate) (PMMA), yielding PMMA-g-CNCs. In this case, 2-BPA was utilized as a surface initiated-Atom transfer radical polymerization (SI-ATRP) reagent for the grafting reaction [158]. 3-MPA-CNCs were further treated with Elleman's reagent to obtain thiol-functionalized CNCs while PyA-CNCs were modified by azide-functional dispersed red 13 *via* azide–alkyne Huisgen cycloaddition reaction. Thiol groups can also be introduced on to CNCs reducing end by oxidation to produce carboxyl groups followed by reaction with carbodiimide [159]. Recently, highly stable CNCs functionalized with dicarboxylic acid groups were synthesized by periodate and then chlorite oxidation of bleached birch pulp [160]. Some carboxylic acid groups were then functionalized with arginyl-glycyl-aspartic acid tripeptide up to a degree of 0.12 mmol of the tripeptide/g of dry content, and others with poly (ethylene imine)/pDNA polyplex *via* carbodiimide coupling and electrostatic interactions, respectively, to form a nanofibrillar structure for gene therapy.

Also, CNCs sulfate groups can be replaced with hydroxyl groups by the thermally catalyzed reversible ester hydrolysis. The degree of hydrothermal desulfation can be regulated to control the negative charge on CNCs surfaces, for nanoparticle dispersity in solution [146]. Furthermore, acetyl groups can also be coupled onto CNCs in a one pot approach involving both extraction and modification directly from sources like MCC, using acetic acid and acetic anhydride combination [161]. These reactions expand the realm into which CNCs can be modified and functionalized.

3.2. Covalent modification of CNCs

Besides alteration of the chemical group on CNCs surface, materials have been covalently grafted onto CNCs to form anticancer delivery constructs such as gels, nanocomposite, photosensitizers, fluorescents. Specifically, fluorescent moieties such as fluorescein-5'-isothiocyanate (FITC), Alexa Fluor can be covalently bound to CNCs to form fluorescent conjugates that can be taken up by the cells/ tissues for fluorescence imaging. In one case, FITC was conjugated to CNCs in a sequence of reactions including epoxy activation of nanocrystal surfaces using epichlorohydrin in an alkaline solution, epoxy ring opening with ammonium hydroxide, and then linkage of FITC to the formed primary amino groups [37]. In 2013, Huang *et al.* [162] prepared fluorescent rod-shaped 7-hydrazino-4-methylcoumarin-CNC (HMC-CNC) and 7-amino-4-methylcoumarin-CNC (AMC-CNC) nanoparticles by conjugating CNCs with amino-substituted fluorophores, forming hydrazone and Schiff-base compounds. To build on this innovation for optical imaging application, Colombo *et al.* [163] functionalized CNCs with a fluorophore hydrazine derivative, Alexa Fluor 633 hydrazide bis(triethylammonium) under acetic acid catalysis to yield CNCs-Alexa Fluor 633 hydrazine conjugates, while preserving the rod-like morphology and substitution of a third of the reducing end groups on CNCs. These conjugates were negatively charged, which enabled their specific electrostatic interaction with Ca^{2+} ions in the bone matrix of treated mice. Nevertheless, Grate *et al.* [164] modified CNCs with Alexa Fluor 546 *via* reductive amination reaction with maleimide, to produce labeling reagents for pore network microfluidic devices. Another fluorescent dye 5-(4, 6-dichlorotriazinyl) aminofluorescein (DTAF) was labelled onto CNCs with different sulfur content for studying the uniformity of CNCs dispersed in electro-spun PVA fibers [165]. CNCs have also been grafted with block copolymers such as (1,4,7,10-tetraazacyclododecane-1,4,7,10-tetraacetic acid) (DOTA) and diethylenetriaminepentaacetic acid (DTPA), which can bind tightly with lanthanide ions for radiographic imaging. Reportedly, PEGylated DTPA block copolymers containing different repeating units were prepared and coupled onto amino functionalized CNCs *via* bis-aryl hydrazone conjugation [166]. Tetramethylrhodamine and Alexa Fluor 488 dyes were then attached onto these conjugates *via* covalent bonds.

For biological targeting applications, CNCs have been modified with chemical groups such as receptor peptides, ligands or other precise molecules of biological interest. In one case, folic acid (FA), a folate receptor (FR) ligand was conjugated to CNCs with carboxyl functions *via* amide bonds to form CNC-folate conjugates [167]. The carboxyl groups were formed due to partial oxidation of some hydroxyl groups of CNCs during sulfuric acid hydrolysis.

CNCs have also been modified with photosensitive groups such as ICG, PEI-chlorin P6 derivatives for photodynamic therapy. PEI-chlorin P6 was prepared by reacting Purpurin-18 (synthesized from chlorophyll a) with PEI (of 0.6 kDa, 2 kDa and 25 kDa) in chloroform for 60 min, forming a chlorin P6 moiety that was revealed by a characteristic absorbance at 665 nm. PEI-chlorin P6 was conjugated to cotton wool-derived CNCs *via* reductive amination of PEI amino groups using sodium cyanoborohydride [168]. With a similar aim for phototherapy, CNCs modified with poly(2-oxazoline)s were used to mobilize and deliver Indocyanine green (ICG) for photothermal therapy. CNCs were chemically modified with Poly(2-isopropenyl-2-oxazoline) (PIPOx) in a reaction mixture of freeze-dried CNCs and 2-isopropenyl-2-oxazoline in N, N-dimethylformamide at room temperature under continuous UV light ($\lambda_{max} = 300$ nm) irradiation (UV-induced photopolymerization) for a period of 12-48 h, yielding PIPOx-g-CNCs. PIPOx-g-CNCs were then subjected to living cationic ring-opening polymerization (ROP) reaction which was frozen by introduction of piperidinium moieties. These moieties capped on the side chains as cations to allow further functionalization via ionic interaction. The piperidinium cations were then loaded with negatively charged ICG up to an amount of 8 wt.%, according to the UV standard curve method [169]. Polycationic PEI-modified CNCs prepared with a similar method of reductive amination by sodium cyanoborohydride, were shown to undergo electrostatic interaction and form PEI-CNC-siRNA nanocomplexes which could deliver siRNA to cells. PEI conjugation was confirmed by an increase in the positive charge (+37.9 mV) of the CNCs colloidal suspension while the loading of siRNA caused an increased size of the complex and a lowered net-charge (+2.5 mV) [170]. This provided a simple and faster method for validation of conjugation in chemical reactions.

CNCs have also been modified for delivery of potential anticancer therapeutic peptides such as chlorotoxin (CTX). Chlorotoxin is a content of Leiurus quinquestriatus scorpion venom, with 36 amino acids that can bind specifically with MMP-2/ClC3 protein complex, a component of brain cancers like Glioblastoma Multiforme. Cellante *et al.* [171] reportedly prepared CTX peptide-modified CNCs by utilizing an ionic liquid of Brønsted acid (N-methylpyrrolidinium hydrogen sulfate) as a solvent and as well as a catalyst. 12.5 μM drug load content of CTX was successfully grafted onto CNCs *via* the covalent ester bonds between the

hydroxyl groups of CNCs and the carboxylic acid groups of CTX. For the formation of the fluorescent CNCs-CTX-Cy5, CTX was first conjugated with Cyanine 5-NHS ester (Cy5) *via* amide bonds overnight to form a peptide-fluorophore (CTX-Cy5), which was then reacted with CNCs.

CNC-g-AA gel, as an example of gels has been reportedly prepared by co-polymerization of CNCs with acrylamide (AA), mediated by cross-linker N,N′-methylene bis(acrylamide) under hydrothermal conditions [172]. Hydrothermal treatment over time was thought to be related to the increased activity of -OH and -COOH on CNC surface which increased the cross-linking capacity to form a three-dimensional honey comb network. The resulting aerogel had a high swelling capacity (495:1) and exhibited excellent adsorption capacity [172]. Another group prepared mucoadhesive hydrogels by covalent attachment of a chain of acrylic acid monomers onto CNCs by free radical reaction to form hardcore rod-shaped bottle-brush polymers with numerous carboxylic acid groups. Some of the carboxylic acid moieties complexed with an anticancer drug cisplatin via aquation [145]. The aquation process involved replacement of chloride moieties in cisplatin with the carboxylate moieties in PAA in the presence of sodium bicarbonate. The hydroxyl groups of CNCs were also used to displace the chloride ions for the direct linkage of the drug. In a related preparation, Gelatin-hyaluronic acid-cellulose nanocrystals (GA-HA-CNC) hydrogels were produced by cross-linking, followed by free-drying. This preparation was intended for wound dressing. GA-HA-CNC combination was due to amide and hydrogen bonding, yielding spongy hydrogels with pore diameter of about 80-120 μm [173]. In other applications, various methods including solvent extraction, melt blending and Pickering emulsion [174,175] have been used to reinforce polymeric materials with CNCs to yield nanocomposites of advanced properties. Reportedly, nanocomposites prepared from poly(oxyethylene) (POE) matrix and CNC aqueous suspension were found to be thermally stable with melting point higher than that of POE [176]. The authors attributed the rigid cellulosic network formed within the PEO matrix to have enhanced the thermal stability of the nanocomposites. The ability of CNCs to form such interactions with other materials has been exploited to produce CNC-reinforced nanocomposites such as PVA-CNC reinforced nanocomposites, CNC-stabilized polyvinyl alcohol (PVA) hydrogels, CNC-stabilized Pickering emulsions [174], CNC-generated silver nanoparticles [177,178], CNC-reinforced polyurethane, poly(ε-caprolactone)-grafted-CNC bio nanocomposites [179].

CNC modification can also be tailored to function in particular physiological conditions such as altered redox potential of the cells due to oxidative stress. Hu *et al.* [148] functionalized cotton wool-derived CNCs with disulfide bond-linked PDMAEMA brushes. Atom transfer radical polymerization (ATRP) sites were first introduced on CNC surface by reaction with cystamine to yield CNCs (CNC-SS-NH_2) with disulfide bonds. CNC-SS-NH_2 were reacted with α-bromoisobutyric acid to covalently attach bromoisobutylryl group on CNCs forming CNC-SS-Br. PDMAEMA was then grafted onto CNCs by ATRP at molar reaction ratio of 1:2.5:50 ([copper(I) bromide]/[2,2′-byridine]/[DMAEMA]) to form PDMAEMA-grafted CNC vectors (CNC-SS-PD). CNC-SS-PD were then mixed with DNA plasmids (pDNA) to form CNC-SS-PD/pDNA complexes. Exposure to reducing conditions led to cleavage of PDMAEMA side chains from CNC complexes thus, promoting the release of pDNA [148]. This was experimentally confirmed by complexing CNC-SS-PD with pCMV-cD (Cytomegalo virus promoter base plasmid carrying Cytidine deaminase [cD] cDNA) which induced cytotoxicity in the presence of 5-flourocytidine, both in *in vitro* (reducing conditions) and *in vivo* (in tumor hypoxic areas) [148]. Hence, it was shown that CNC-SS-PD/pDNA could be utilized as an efficient vector for suicide gene therapy. The same group further fabricated Au NP-conjugated heteropolymer brush-coated CNCs, through ATRP and reversible addition–fragmentation chain transfer (RAFT) polymerization methods for an effective and promising model multifunctional therapeutic system. By first amination of CNCs, bi-functional CNC-based polymerization initiators were generated. These initiators were then applied for alternate grafting Poly(poly(ethylene glycol)ethyl ether methacrylate) (PPEGEEMA) and PDMAEMA brushes, before *in situ* insertion of Au Nanoparticles (NPs) as computed tomography (CT) contrast agents [180]. Successful synthesis of polymer brushes was indicated by a substantial change of morphologies of CNCs. Under the same team, the aminated CNCs were further functionalized with dithiolane rings by reaction with lipoic acid [181]. These rings enabled conjugation of spherical and rod-like Au NPs *via* gold-thiolate bonds, and then β-CD-PGEA cationic gene carriers were linked directly to the Au NPs *via* a host-guest interaction. The formed gene carrier expressed a decreased size which indicated shrinkage of polymer chains, and thus proving effective condensing of pDNA within the CNCs complex. In a related study, Li *et al.* [182] attached pre-synthesized cis-aconityl-doxorubicin with carboxylic groups to aminated CNC nanorods *via* amide linkages, to form rod-like cancer drug nanocarriers. The obtained nanocarriers were surprisingly shorter than the parental CNR due to degradation caused by the excessive temperatures applied during modification. Respectively, 0.54 wt.% and 8% of drug loading capacity and efficiency of modified DOX were achieved. These low values were due to the limited preparation process via the heterogenous reaction on the CNCs surface. This reaction has a very low efficiency which directly affects the loading capacity.

3.3. Non-covalent modification of CNCs

The utilized noncovalent bonds including hydrogen bonds, van der Waals and electrostatic interactions are mostly formed via physical adsorption. The surface of non-modified CNCs though bearing polar/ionic chemical groups is largely hydrophobic and therefore may not be suitable for hydrophilic environment. For simple non-covalent hydrophilic complexes, CNCs were modified with phenyl, long alkyl, glycidyl, and diallyl moieties carried on quaternary ammonium cationic groups. CNC complexed quaternary ammonium salts bearing C_{18} alkyl chains had higher water contact angle (71°) relative to the unmodified form (12°) [183]. The resulting nanocomposites had an increased capacity for dispersion in non-polar polymers. In another study, the cationic surfactant Cetyl trimethylammonium bromide (CTAB) was found to increase the zeta potential of CNCs in a concentration dependent manner [184]. This was owed to the ionic interaction of CTAB with the CNC surface bound anionic sulfate groups. The CTAB modified CNCs (CTAB-CNCs) were found to interact with three hydrophobic anticancer drugs; paclitaxel (PTX), docetaxel (DTX), and etoposide (ETOP) to form respective CNC-drug complexes that released the drugs controllably in a period of two hours [184]. The authors also proved direct ionic interaction of doxorubicin (DOX) and tetracycline onto CNCs surface [184]. Therefore, CTAB is a linking surfactant owed to the possession of a cationic part of quaternary ammonium ion that interacts with CNCs and the hydrophobic end of C16 alkyl chain that interacts with non-polar compounds such as drugs. Also, CTAB has antimicrobial properties and thus acts as a pharmaceutical drug as well as an excipient. A critical micelle concentration for adsorption of CTAB onto CNCs exists, whereby below the critical level, CTAB monomers adsorb on the surface. With increase in the concentration of surfactant monomers, the adsorbed surfactants reorganize and associate to induce hydrophobic interactions between C16 alkyl chains to form monomer clusters. However, further increase in concentration of surfactants leads to formation of micelles on CNCs surfaces, which decreases the hydrophobicity of CTAB-CNCs [61]. CTAB modified CNCs were also loaded with hydrophobic and anti-tumorigenic luteolin (LUT) and luteoloside (LUS) model drugs to amounts of 13 and 57 mg g^{-1} [185]. The transformation of the positive charge of CTAB-CNCs into negative charge confirmed its ionic interaction with the negatively charged flavonoids, thus CTAB acting as a cross-linker [185]. The weak acidic drugs were sustainably released at a higher rate and amount over a day. Another hydrophobic and polyphenolic compound from Curcuma longa herb, termed CUR, with anticancer potential was also loaded onto rod-like though colloidally

unstable, CTAB-CNCs. A substantial quantity of CUR in a range of 80 - 96% binding efficiency was bound onto CTAB-CNCs for up to 100 μg of CUR added compared to 27% added onto CTAB-unbound CNCs. This was due to the extremely strong hydrophobic interaction between the nonpolar benzene rings of CUR and the hydrophobic regions of CTAB-CNCs. However, the binding efficiency of CUR decreased at higher concentrations of CUR added due to the decrease in the hydrophobicity of CTAB-CNCs [61].

A more complex modified CNC carrier was prepared by utilizing the cationic interaction of less soluble β-cyclodextrins (β-CD) and negative charges on cotton fiber-derived sulfuric acid hydrolyzed CNCs [186,187]. β-CD was cationized *via* reaction with glycidyltrimethyl ammonium chloride (GTMAC) and loaded onto the CNCs by electrostatic coupling, to form very stable negatively charged β-CD/CNCs complexes [188]. β-CD can also be grafted onto CNCs by either carbodiimide coupling or copper (I) catalyzed click chemistry [189]. The hydrophobic drug, CUR was then successfully inserted into the β-CD cavities of β-CD/CNC up to 10% loading ratio, forming soluble CUR–CD/CNC nanocomposites. The above innovative loading of CUR onto biodegradable CNC nanocarriers provided a solution to their pharmacokinetic challenges like low solubility in aqueous media, rapid metabolism and limited bioavailability, for efficient treatment of various conditions such as cancer, peripheral neurological infections [61,186,190,191]. Additionally, curcumin is a Curcuma longa rhizome polyphenol extract of curcuminoid family with manifold pharmacological characteristics such as antioxidant, anti-inflammatory and neuroprotective potentials. These have attracted its biomedical applications, owed to its oral safety, ability to induce pluripotency, and low-price.

Delivery of DOX hydrochloride (DOX·HCl) and CUR was explored using a Layer-by-Layer (LbL) technique. This approach involved designing nanofibrous multilayer thin films and microcapsules, by alternately depositing positively charged chitosan (CH) and negatively charged CNCs to form $(CH/CNC)_n$ with complementary electrostatic and hydrogen bonding interactions [192]. The water-soluble DOX·HCl was then post loaded in the nano-assemblies by diffusion and interacted with CNCs *via* hydrogen bonds and electrostatic interactions. While as for the hydrophobic CUR, a stable water-dispersion was first prepared *via* noncovalent interaction with CNCs as portrayed by molecular docking studies, followed by incorporation into the LbL nano-assembly [192]. This approach is thus suitable for delivery of lipophilic drugs that can be ably incorporated in the microcapsule walls without interfering the ability of the microcapsule aqueous core to further load a hydrophilic drug.

3.4. Covalent and non-covalent modification of CNCs

More complex conjugates that utilize both covalent and noncovalent interactions onto CNCs have been also assembled for cancer therapy. These have mostly involved the use of linkers that primarily form covalent bonds with CNCs by “grafting to” or “grafting from” approaches and noncovalent bonds with small molecules, surfactants, hydrophobic polymers and anticancer agents/drugs such as DOX, MTX, CUR. For instance, a CNC conjugate of PEEP-modified CNCs (CNC-g-PEEP) was prepared for the delivery of DOX to cancer cells [193]. 2-ethoxy-2-oxo-1,3,2-dioxaphospholane (EOP) monomers were exploited to synthesize Propargyl-terminated PEEP (g-PEEP) *via* ROP reaction. The obtained g-PEEP was then subjected to Cu(I)-catalyzed azide–alkyne cycloaddition (CuAAC) “click” reaction with the azide-modified-CNC ($CNC\text{-}N_3$) to graft Poly(ethyl ethylene phosphate) (PEEP) onto CNCs [193]. $CNC\text{-}N_3$ was initially prepared from partially desulfated CNCs and then chlorinated with p-toluenesulfonyl chloride (TsCl) to form CNC-Cl. CNC-Cl was then reacted with sodium azide to yield azide-modified CNCs. DOX was then loaded onto negatively charged CNC-g-PEEP forming CNC-g-PEEP-DOX by electrostatic interactions owing to DOX protonated amine groups. In another study, CNC-Cl operated as a macroinitiator to prepare CNC grafted polyacrylamide chains (PA-g-CNC) using polyacrylamide via ATRP technique. For the first time, transamidation method was used to attach amine pendant groups onto PA-g-CNC copolymer to enable further functionalization with anticancer agents [194]. FA was attached both directly and indirectly using CD to the copolymer. The indirect process involved initial grafting of carboxymethyl-β-cyclodextrin (CM-β-CD) onto the copolymer via amide bonds, followed by introduction of folic acid (FA) into the CD cavity via the host-guest interaction. DOX was loaded into the nanocarrier spheres via ionic interaction. However, the mass of drugs loaded on the polymer substrate was restricted by the CNCs complexity and its lateral groups.

Negatively charged CNCs have been modified via charge reversal by attachment of positively charged species. This is aimed at carriage of negatively charged anticancer NPs that are electrostatically repelled by the unmodified CNCs. For instance, CNCs were modified with poly(N-(2-aminoethylmethacrylamide)) (poly(AEMA)) and poly(2-aminoethylmethacrylate) (poly(AEM)) for charge reversal [195]. Poly (AEMA) is a cationic core utilized in the construction of nanogels for delivery of proteins and genes such as siRNA and plasmid DNA while poly(AEMA) is a linking polymer for delivery of DNA vaccine and genes (*in vitro*) [195]. These cationic CNCs were synthesized by reacting 2-bromoisobutyryl bromide (BriB) with CNCs, followed by grafting with poly (AEMA) and poly(AEM) by the surface-initiated single-electron-transfer living radical polymerization (SI-SETLRP) reaction. Negatively charged Au NPs were then incubated with the modified CNCs to catalyze the electrostatic interaction among the species. The deposition of Au NPs onto the cationic CNCs was controlled by Brownian motion and monitoring the net charge reduction of the aggregated CNCs. CNC-reinforced injectable hydrogels were also investigated for DOX delivery. Quaternized cellulose (QC) obtained through cellulose quaternization in LiOH/urea aqueous solution was reacted with β-glycerophosphate (β-GP) and hence forming an *in-situ* gelling solution (QC/β-GP). Treatment of cationic QC/CCNCs with QC/β-GP yielded QC/CCNC/β-GP hydrogel complexes. Where β-GP acted as a cross-linker between QC and CCNCs, thus increasing the mechanical strength and the dimensional stability of the resultant hydrogel [31]. CCNCs was prepared using CHPTAC via epoxidation and etherification for CNCs charge reversal. DOX was loaded directly into QC/CCNC/β-GP hydrogels and created interactions with the sulfonate and hydroxyl groups of CNCs *via* electrostatic interactions and hydrogen bonds, respectively. And then easily released when injected to the tumor proximity of mice bearing liver cancer xenografts. This indicated successful *in vivo* anti-cancer therapy with low toxicity.

For advanced studies involving charge reversal, negatively charged CNCs were functionalized with 3-amino propyl-3-methoxy silane (APTMS) via etheric linkages [6]. The amine groups of the modified CNCs were then conjugated with N, N′-Dicyclohexylcarbodiimide (DCC)-activated carboxylic acids of the amino acid L-lysine via amide bonds. A positively charged system with APTMS as a bridging molecule was formed. Also, the addition of the amino acids provided a prolonged fluid circulation of the nanocarriers and an effective resistance against biological barriers. Via electrostatic interactions, anticancer drugs CUR and MTX spread in a suspension were stacked onto the pH-sensitive NPs by dispersion in the solution to form nanoparticles for combination therapy [6]. Dispersion is a simple co-loading method that has also been utilized elsewhere for loading of DOX onto cellulose/MXene hydrogels [196]. More specifically, CUR and MTX were loaded onto the NPs surfaces mostly via hydrophobic interactions and surface adsorption. That is, the carboxylic acid groups of MTX and the amine groups of the NPs were converted into COO^- and NH_3^+, respectively, at pH 7.4 to allow hydrogen bonding amongst them. While the hydrophobic interactions were attributed to the hydrogen bonds formed between the ammonium groups of NPs and the enolate groups of CUR [6,197,198]. This led to entrapment of 33% MTX and 75% CUR onto the nanocarriers. A group of trimethylamine-rich cationic molecules, CHPTAC were covalently attached to hydrothermally desulfated CNCs via epoxidation and etherification reactions to enhance inversion of surface charge, for

preparation of spindle-shaped cationic CNCs [146]. Desulfation of CNCs was enabled via reversible ester hydrolysis by detachment and regeneration of sulfate and hydroxyl groups, respectively, on the CNCs surfaces. This enabled preparation of highly dispersed CNCs and less turbid cationic CNCs. Polymeric siRNAs were then prepared via sequential synthetic processes and purified by Mg^{2+} chelation. By electrostatic interaction, the anionic polymeric siRNAs were then complexed with the spindle-like cationic CNCs to form branched and spindle-shaped nanocomplexes with high colloidal stability. Different weight ratios of polymeric siRNAs were used to optimize the formation of nanocomplexes and the complexation efficiency was enhanced with increase in the weight ratio at particularly beyond 5 wt.% [146]. With carefully controlled biocompatibility studies, this charge reversal potential portrayed ability of wider application of cationic CNCs in treatment of cancers like breast cancer. This is owed to its ability to not only enable delivery of several negatively charged or hydrophobic anticancer agents like drugs, genes, but also combination therapy. Another group prepared nanohydrogels (PDA/Fe@CNC and ALA/Fe@CNC) with functional polymeric chains of either 5-aminolevulinic acid (ALA) or dopamine (DPA), conjugated to carboxylated CNCs via iron ions coordination, prior to loading of the hydrophobic anticancer drug PTX [100]. 28% of carboxyl groups were created on CNCs via oxidation by DMSO and succinic anhydride. The formed system is described as a nanoscale metal-organic framework or nanoscale coordination polymer in which organic ligand moieties such as the polyphenols derivatives, benzothiazole complexes, dihydroartemisinin form coordination bonds with metal ions such as Fe^{3+} [199–202]. The metal ions then act as cross-linking ligands to bridge the system to other supporting polymer surfaces such as CNCs, disylase for effective drug delivery [203].

Exploration of CNCs modification for cancer therapy through oil in water emulsion approach has also been undertaken. In a recent study, Ngwabebhoh *et al.* [204] aminated CNCs prepared by H_2SO_4 acid hydrolysis of MCC powder before formulation of coumarin (COU) and CUR conjugated Pickering Emulsion (PE). The amine groups further acted as active sites for loading of CUR or COU through hydrogen bonds [204]. Similarly, CUR-encapsulated CNCs stabilized PE for colorectal cancer therapy was prepared by using MCNC composites as solid emulsifiers to stabilize an oil layer of β-carotene rich red palm olein with dissolved CUR [205]. The MCNC nanocomposites were synthesized through an *in-situ* ultrasound-facilitated coprecipitation method by depositing Fe_3O_4 magnetic nanoparticles onto CNCs surfaces via covalent bonding.

4. CNCs as dispensers for cancer theranostic agents

Much as chemotherapy has been one of the common modes of cancer treatment since the first use of a rather successful chemotherapeutic agent-Nitrogen mustard in 1940's [206], several deleterious anti-cancer agent-associated toxicities have been reported. The toxicity-associated side effects include; neurotoxicity and neuropathy, ototoxicity, hepatotoxicity, anorexia, cachexia, cardiotoxicity, cognitive deficits, nephrotoxicity, fatigue and motivational deficit, neuro-inflammation among others [207,208]. The task of medicinal chemists has been therefore to modify some of the established drugs into more potent but less toxic ones whilst exploring drug delivery agents that decrease off target delivery without affecting their homing to the target cells/tissues. Generally, an ideal drug delivery agent with probable clinical translation has been characteristically described with nano-sizes for easier passage across biological barriers and subsequent accumulation in malignant cells, potential of binding reversibly to both hydrophilic and hydrophobic drugs, stability, prolonged blood circulation, body macrophage resistance, non-toxicity, biocompatibility, non-invasiveness to normal body cells, vessel extravasation, tumor penetration, sensitivity to extrinsic (light, magnetic field, radiofrequency) or intrinsic (pH, temperature, redox reactions) stimuli or both, degradability in living cells. These properties also minimize the side effects from these nanocarriers [209]. pH sensitivity is among the most essential stimuli because drug delivery in cancer cells is normally enhanced by their acidic environment which arises chiefly from the buildup of metabolic end products and the poor edifice of blood vessels in the cells. Among the anti-cancer delivery materials [210] that are in research for clinical translation today, CNCs have arose wide attention [211]. Despite the reported toxicities [212], CNCs have been drug delivery materials under active research today. CNCs are under intense research as future nanomaterials for targeted delivery of drugs especially for cancer cure, owed to their excellent physical properties like the nano size and spindle shaped structure that possesses abundant hydroxyl groups on the surface, and degradability in living cells [213–218]. In detail, the spindle-like shape as compared to the sphere-like provides a high aspect ratio which causes a lengthened fluid circulation, improved cellular binding and uptake, rapider internalization, and high accumulation in the targeted tumours [7,8,182,211,213]. While as the hydroxyl groups on CNCs not only favour chemical functionalization with anti-tumour agents, but also allow a prolonged blood circulation and low cytotoxicity, owed to their hydrophilic surfaces on a favourable elongated shape.

Depending on the cells/tissues being targeted for delivery of drugs, genes, bioimaging agents for cancer treatment *via* numerous methods such as utilization of radiations among others, the utility of CNCs has been exploited as simple CNCs or CNC conjugates, as illustrated in Fig. 5 below.. Both non-conjugated and conjugated CNCs are thought to enter the cells by endocytosis just like other polysaccharide-based nanoparticles. The endocytic mechanism can be non-specific (micropinocytosis or phagocytosis) or facilitated (caveolae or clatharin-mediated) [215,217–219]. Both phagocytosis and micropinocytosis are actin-dependent processes. While phagocytosis is carried out by specialized cells (professional phagocytes), micropinocytosis is dependent on actin-driven formation of invaginations on the surface of the membrane to take up particulate material [215,219]. Clathrin-mediated uptake is a form of receptor mediated uptake of molecules (such as iron-loaded transferrin, LDL) at the specialized sites of the membrane known as coated pits. These coated pits are sites of assembly and recruitment of protein complexes that mediate trafficking of the cargo from the cell membrane into other cytosolic compartments [215]. Caveolae-mediated endocytosis occurs at specialized areas on the cell membrane 'lipid rich' sites known as 'lipid rafts' mediated by the associated protein caveolin. This process involves cellular uptake facilitated by flask-shaped membrane invaginations called caveolae (little caves) [220]. All these pathways may not be active in cell depending on the cell type, the size and nature of the particulate material [219,221]. Confirmation of the delivery of the drug into the intracellular compartments is initially quantified by tagging the particulate material understudy such as nanoparticles with fluorochromes like FITC which can be monitored by live imaging.

4.1. CNCs for bioimaging

CNCs have been applied for therapeutic bioimaging of tumors by use of acoustic signals from nanoparticles after penetration into the tumors or fluorescent agents such as rhodamine B isothiocyanate (RBITC) and FITC. These may be non-conjugated onto CNCs and therefore, taken up non-specifically by endocytosis. For instance, photoacoustic imaging of mouse ovarian cancer models was carried out using non-conjugated CNCs, after *ex vivo* signal quantitative experiments [216]. These biodegradable nanoparticles with peak photoacoustic signal at 700 nm and *ex vivo* detection limit of 0.02 mg/mL competently produced photoacoustic signals at doses below 1.2 mg/mL when applied to the carcinomatous cells.

For an effective cancer therapy through bioimaging, fluorescent agents have been designed to enter the membranous cells passively or to trigger cell internalization actively with no or insignificant toxicity. This is because large water-soluble biomarkers cannot easily cross the cell membranes. Nevertheless, their transportation is controlled by the mechanism of cell endocytosis. For instance, Mahmoud *et al.* evidenced

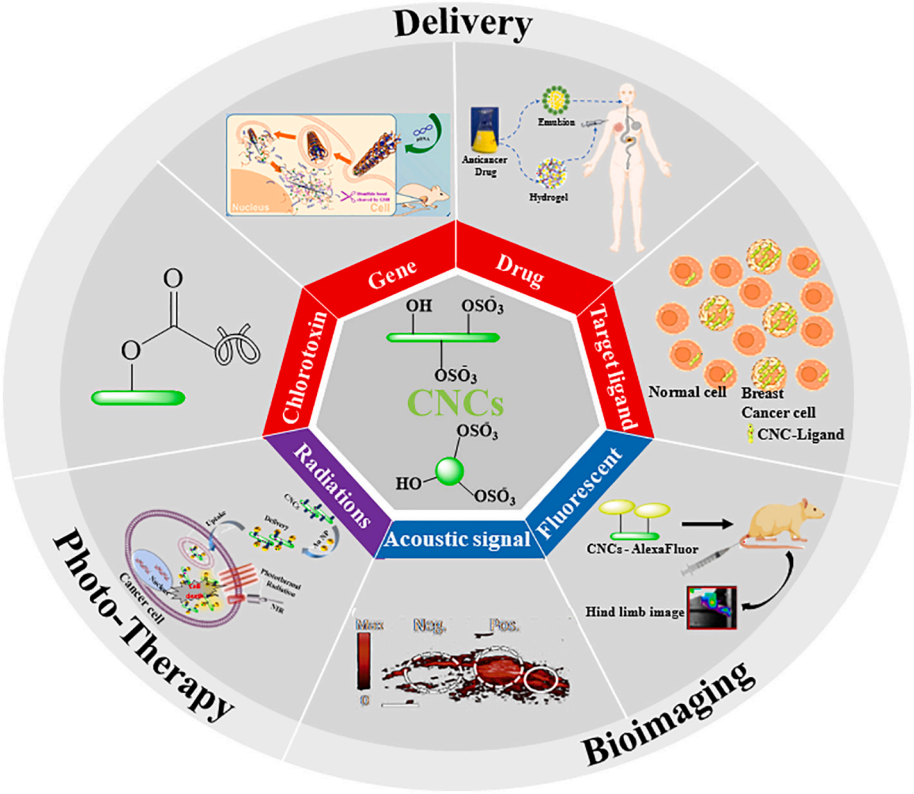

Fig. 5. Summary of the applications of CNCs (green rod/spherical shaped) modified with anticancer agents (genes, drugs, chlorotoxin), target ligands, fluorescent (Hind limb image [163]) Reproduced with permission from ref. [163]. Copyright 2015, Biomacromolecules, and photosensitive elements (acoustic signal [216]) for cancer treatment. Reproduced with permission from ref. [216]. Copyright 2014, Photoacoustic.

the capability of fluorescent CNCs, FITC and RBITC to penetrate cells. Without marked sign of toxicity and no effect of cell membrane integrity, the positively charged CNC-RBITCs were internalized by the anionic cellular membrane of both Spodoptera frugiperda (Sf9) and human embryonic kidney 293 (HEK 293) cells. However, there was no uptake of CNC-FITC due to its negative charge, thus confirming the relevance of the surface charge of nanocarriers [222]. In another study, CNC- Alex flour 633 conjugates were found to transiently migrate into the bones and then penetrate cells without eliciting material-related cytotoxic effect [163]. This ability of CNCs conjugates to infiltrate cancer cells, coupled with rapid excretion and tolerance, can allow the conjugates be exploited as theragnostic imaging nanodevices for bone tumors. Furthermore, CNCs can be decorated with hydrophilic block copolymers such as DOTA and DTPA. These polymers are capable of chelating with radioactive lanthanide ions such as Gd^{3+} for magnetic resonance bioimaging and $^{177}Lu^{3+}$ for radiotherapy to enable cancer diagnostic imaging and radiography. For example, Guo *et al* [166] prepared PEGylated DTPA block copolymers with attached fluorochromes-rhodamine and Alexa Fluor 488. These fluorescent-labelled polymer-CNCs conjugates were taken up by ovarian cancer cells (HEYA8) with non-toxicity limit of up to 0.0035 wt.%. This portrayed low toxicity was owed to shielding of the poly(ethylene glycol) (PEG) corona. Besides diagnosis, biomarkers can also be important in monitoring the delivery of other therapeutic agents such as targeting agents, drugs, and genes among others.

4.2. CNCs for cargo delivery

4.2.1. CNCs for target agent delivery

In some studies, CNCs have been conjugated to suitable agents either to increase the adsorptive capacity, passive endocytosis or receptor-mediated endocytosis where targeting of the drug is required to specific cells/tissues with minimal toxicity. Specifically, agents such as FA (Vitamin B_9) are an important cause, given their function in facilitating proliferation of all living cells by acting as vital vitamins for cell division. Proliferation involves rapid division of cells, and cancer cells being characteristic, they immensely take up FA passively or actively by the numerous folate receptors and thus its overexpression on their plasma membranes (Fig. 5). Types of cancer cells such as breast, brain, ovarian, kidney, lung, and endometrial cancer, have a high affinity for FA, unlike the normal cells [223]. For instance, FA conjugated CNCs (FA-CNCs) were reported to be capable of targeted delivery of chemotherapy to cancer cells (rat brain tumor (C6) cells and human (DBTRG-05MG, H4) cells) that are FR-positive, as monitored with a fluorescent moiety, FITC (Fig. 6) [224]. The non-neuronal DBTRG-05MG and C6 cells bound FA-CNC conjugates internalized primarily *via* caveolae-mediated endocytosis while the neuronal human H4 cells internalized the conjugates chiefly *via* clatharin mediated endocytosis. This indicated that FA-CNC conjugates could also be loaded with chemotherapeutic drugs to increase their uptake in the respective cells given that the binding/uptake for C6, H4, and DBTRG-05MG cells was 46, 975, and 1452 times higher, respectively, as compared to untargeted CNCs [224].

The same group further used FA-CNCs conjugates with a fluorescent imaging agent (FITC) for targeting human breast (MDA-MB-468) and human epithelial carcinoma cell line (KB) cancer cells. These FA-CNCs conjugates showed a remarkably high affinity for FR-positive human breast (MDA-MB-468) and KB cancer cells with momentously high uptake. As caveolae FR-mediated endocytosis was the only expressive cellular internalization mechanism in MDA-MB-468 cells, clathrin FR-mediated endocytosis was substantial in both cell types. This was attributed to the small size of the internalized NPs and specific cell-type dependence, as the major factors for NPs internalization. MDA-MB-468 and KB cells had substantively greater levels of FR-αmRNA and protein expression as compared to the negative control of human aortic

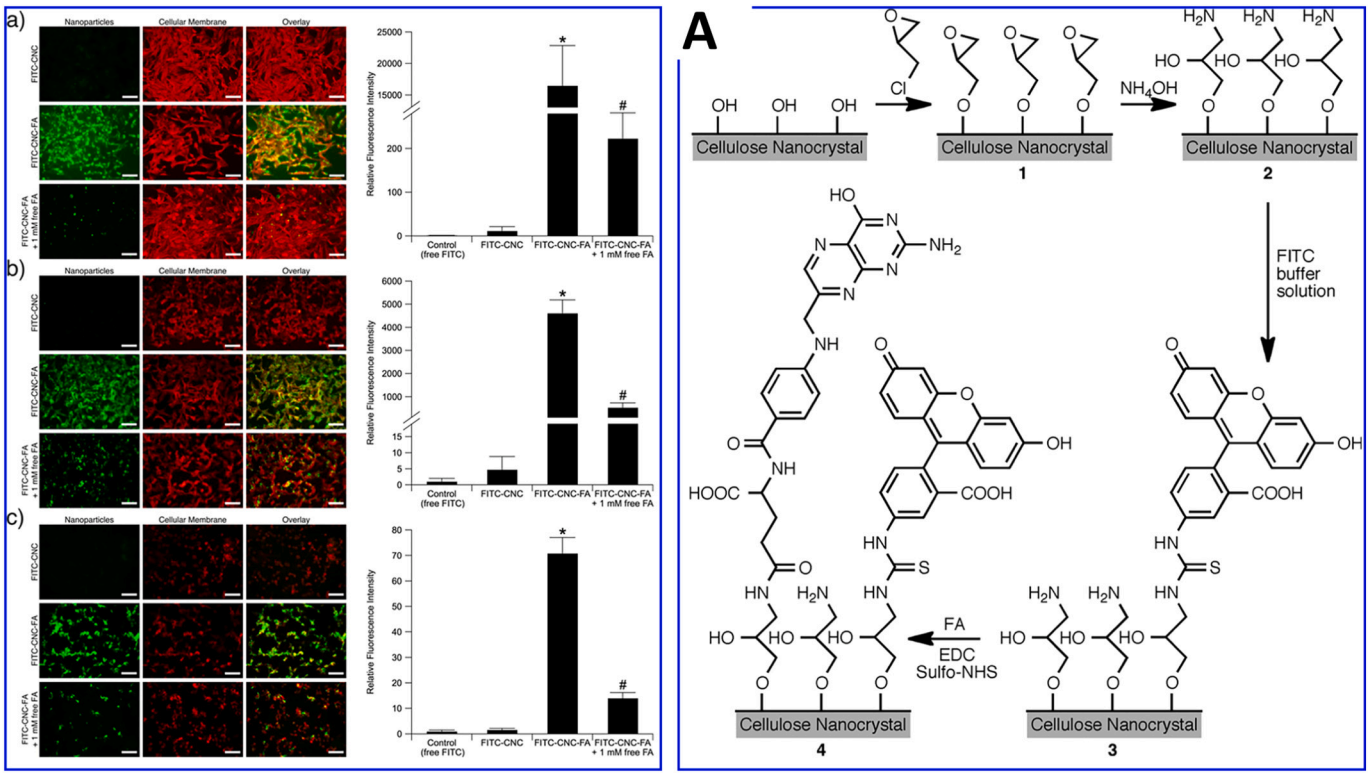

Fig. 6. Cellular binding/uptake of FITC-CNC and FITC-CNC-FA in the absence and presence (1 mM) of free folic acid by (a) DBTRG-05MG, (b) H4, and (c) C6 cells. (A) Synthesis of the FITC-labeled FA-conjugated CNCs (Sulfo-NHS, N-hydroxysulfosuccinimide; EDC, 1-ethyl-3-(3-dimethylaminopropyl)carbodiimide). Reproduced with permission from ref. [224]. Copyright 2014, American Chemical Society.

endothelial cells (HAEC) [223]. This research team therefore, demonstrated the attachment of these negatively charged nanoscale delivery vehicles to specific membranes for timely discovery and treatment of tumors. These FA-conjugated CNCs were also reported to significantly potentiate the cytotoxicity of Irreversible Electroporation on the MDA-MB-468 and KB cells, with no effect on FR-negative cancer cells (A549) realized [167]. Thus, proving that FA selectively binds to FR. In brief, these noninvasive, and passive screening strategies are likely to enhance early-stage diagnoses of cancer and thus increasing survival chances by minimizing the avoidable risks to patients.

4.2.2. *CNCs for drug delivery*

CNCs have also been surveyed as nanocarriers for the delivery of cancer drugs singly or in multiple for combined therapy. Specifically, combination chemotherapy is a promising strategy involving synchronized delivery of more than one anticancer agent to express different mechanisms of action during cancer treatment to simultaneously achieve a synergetic effect and asphyxiate the undesirable side effects associated with single-drug therapy. The delivery cargos have been designed in several forms such as attaching the drug directly onto CNCs as a non-conjugated surfactant or conjugated compound, indirect attachment *via* a spacer moiety, or encapsulation. The delivery cargo may exist as hydrogels, emulsions, thin films made using LbL approach. CNC drug nanocarriers that are non-conjugated tend to enter cells non-specifically by endocytosis. For example, surfactant-modified CNCs were reported to form complexes with three anticancer drugs such as PTX, DTX, and ETOP that were controllably released in a duration of two hours. The initial release profile (20-26%) was quite similar for the three drugs, only differing on the total period release up to 75% [184]. However, since these drugs are hydrophobic, solubilization had to be facilitated by coating CNCs with a surfactant CTAB to increase the zeta potential of CNCs in accordance to the concentration. The CTAB-coated CNC-drug complexes were reported to strongly associate with bladder cancer cells (KU-7) [184]. Non-CTAB modified CNCs could easily conjugate significant amounts of the ionizable water soluble drugs such as tetracycline and doxorubicin. Non-conjugated CNCs could also be suitable for control of the drug release for transdermal patch application [225]. In a related study, torispherically shaped and negatively charged CNCs were bound with CTAB to enhance the loading efficiency of hydrophobic anticancer drugs LUT and LUS into the hydrophobic CTAB domains [185]. CNCs solutions formed were well-dispersed and remained stable with a high zeta potential of 21.5 mv. At pH 7.4, 57% and 72% of the drugs were sustainably released in one day from LUT-CTAB-NCC and LUS-CTAB-NCC, respectively. This finding underlines a CNC-based drug delivery system, capable of modulating loading and release of drugs.

For directly conjugated drug delivery systems of CNC nanocarriers, Colacino *et al* [226] designed various CNC conjugates, such as CNCs linked with FITC, without (FITC-CNC) or with FA (FITC-CNC-FA), and CNCs linked with DOX and without (DOX-CNC) or with FA (DOX-CNC-FA) and investigated using FR-positive MDA-MB-468 and KB cancer cells. Expectedly, there was increased cellular internalization of FITC-CNC-FA (as indicated by the fluorescence). The uptake was not commensurate with cell viability status on treatment with DOX-CNC-FA, as compared to free DOX or DOX-CNC treatment [226]. The significantly lower cell viability of DOX-CNC-FA treated cancer cells was suggestive of increased delivery of DOX to the cells than mere free DOX or DOX-CNC treatment. In another study, porous nanofibrous multilayer thin films and microcapsules composed of CNCs were fabricated following the LbL approach. For drug delivery application, these nanocarriers were loaded with DOX·HCl and CUR. DOX was successfully released sustainably, higher at acidic pH than at physiological conditions since diffusion is enhanced by protonation of the amine groups [192]. This property is commendable for cancer therapy given the lower extracellular pH of tumor cells, as well as delivery of the lipophilic drugs.

CNC-g-PEEP have been reported to be capable of encapsulating DOX

and its subsequent delivery to the tumor micro-environment [193]. Polyphosphoesters (PPEs) such as PEEP, just like CNCs are known to be biocompatible [15] and therefore show negligible toxicity. The half maximal inhibitory concentration (IC_{50}) of DOX-loaded CNC-g-PEEP (9.95 mg DOX equiv L^{-1}) was slightly higher than that of free DOX (6.38 mg DOX equiv L^{-1}) due to slow release of DOX from CNCs [193]. This slow release was even more noticeable at pH 7.4 compared to pH 5.0 which could be advantageous for use at cellular physiological conditions. However, over 40 h sustained and high DOX release of up to 80% at pH 5.0 was realized when DOX·HCl was conjugated onto rod-like CNCs [182]. The high DOX release was attributed to a greatly low pH which stimulated the carboxylic acid (C-4) catalyzed splitting of cis-aconityl amide bonds. The enhanced DOX release was further confirmed by the 1.75 times higher efficiency of IC_{50} of the prodrug carrier with no NH_4Cl (lysosomotropic weak base) present, against NCI H 460 cells. This DOX release was activated by the lysosome in the microenvironment, which was highly acidic with pH 5.0 and thus provided a prolonged and gradual drug release. Unlike the DOX·HCl, the prodrug nanocarriers exhibited enhanced cellular internalization *via* the endocytosis route. The cellular uptake was further proved by incubation of the prodrug nanocarrier with Human hepatocyte cell line (HL-7702), KB, human large cell lung cancer cell line (NCI H 460) and Michigan Cancer Foundation-7 (MCF-7) cell lines, where a visible red fluorescence was observed. The authors attributed the fluorescence drug delivery potential of the prodrug nanocarriers to its rod-like shape, appropriate aspect ratio, preferential NPs uptake, and acidic pH-activated drug release potential. The above findings suggest that pH sensitivity potentially controls, prolongs and enhances release of anticancer drugs in low pH-characterized tumor sites while hindering their untimely release in physiological environments with normal pH values.

More complex CNC conjugates have also been explored. For example, CNCs were functionalized with cationic β-CD to form β-CD/CNCs complexes that encapsulated CUR [186]. This CUR–CD/CNCs complex inhibited proliferation of cancer cells of prostatic and colorectal origin, though with lower IC_{50} compared to that of free CUR [186]. The enhanced effect could be attributed to higher solubility of CUR–CD/CNCs, its internalization into the cell by endocytosis before spontaneous release of CUR into the intracellular membrane compartments such as lysosomes. Antimitotic anticancer chalcone drugs, 3-hydroxy-3′,4,4′,5′-tetramethoxychalcone and 3′,4,4′,5′-tetramethoxychalcone were also encapsulated into β-CD/CNCs complexes [227]. The obtained β-CD/CNCs/chalcone complexes presented high solubility and invitro antiproliferative effect against prostate (PC3 and DU145) and colon (HT29 and HCT-116) cancer cells. The authors attributed these results to successful encapsulation of the hydrophobic chalcones by the β-CD/CNCs, which led to their increased internalization into the malignant cells. Therefore, improved water solubility and bioavailability of hydrophobic anticancer agents is likely to enhance specificity to malignant cells which will deter toxicity to healthy cells. Ehsanimehr et al [194] prepared a complex CNC (FA-CM-β-CD/aminated (PA-g-CNC)) copolymer system with nanospheres for loading and release of DOX. The system had a high loading capacity and encapsulation efficiency of about 8.08% and 88%, respectively. This was attributed to the high chain length of the polymeric shell and the effective interaction between the electronegative atoms in the polymeric system and the carbonyl, amine, and carboxylic acid groups of DOX. Though the CNC complexity limited the loading process. A high DOX release of about 89% was also identified especially in a low pH media [194]. The authors attributed it to the decreased ionic interaction between the drug and carrier due to protonation of the electronegative groups in the nanocarrier system, as well as breakdown of the hydrogen bonds attached to DOX. The high DOX release caused a low IC_{50} of 0.216 μgmL^{-1} when exposed to MCF-7 cancer cells thus, portraying a high tumor control compared to the free drug. The conjugated FA portrayed a high internalization rate with a complete cellular uptake in 3 h. In yet another CNC conjugate system, a colon-target drug release nanocarrier was designed by linking the model drug (tosufloxacintosilate, TFLX) with maleic anhydride CNC using a spacer moiety of L-leucine. This drug nanocarrier exhibited a high encapsulation efficiency of 99.84% and could release about 72.55% of the drug satisfactorily loaded to a maximum of approximately 29.14% to avoid leakage. The enhanced drug release potential of the nanocarrier was credited to the breakdown of CNCs and cleavage of the CNCs-drug amide bond by the protein enzyme, lysozyme. This releasing efficiency could be close to *in vivo* value since the experiment was conducted in a colon fluid containing lysozyme for 30 hours, in which no drug was detected when simulated with pepsin and hence indicating selective drug release in the colon [228]. This could be a potential chemotherapeutic delivery agent for colon cancer if TFLX, an antibiotic, would be replaced with an anti-cancer agent that would otherwise be activated in the gastric fluids. In a finding involving combination chemotherapy, a biocompatible nano-system comprising of CNCs and amino acid L-lysine was constructed for high loading and co-delivery of model anticancer drugs, MTX and CUR to MCF-7 and MDA-MB-231 breast cancer cells [6]. The non-drug loaded nano-systems expressed ideality for intravenous injection by maintaining the normal discocyte form of erythrocytes and cancer cells, thus portraying a negligible hemolytic and cytocompatibility effect, moreover at various concentrations. The enhanced biocompatibility of the NPs was mainly due to the decorated amino acid L-lysine [6,229]. In the acidic tumor environment, the pH-sensitive nanocarriers released the drugs sustainably, which lessened the chances of untimely drug release and adverse side effects during blood transit, while allowing high penetration into the tumor for enhanced toxicity. The pH enhanced release of CUR and MTX was due to the protonation of the enolate and methotrexate carboxylate groups of CUR and MTX, respectively. This eliminated their electrostatic interactions with the protonated ammine groups of the nanocarriers by reduction of the surface charge. However, the strong hydrophobic interactions of CUR with the nanocarriers enabled a sustained release of the anticancer drugs. The duple-drug cargo nanocarriers presented a superior anticancer efficiency against human breast tumors, in which the adjuvant drug CUR synergized the therapeutic efficiency of MTX by cell growth inhibition and induction of apoptotic cell deaths of the malignant tumors. This synergy arises from activation of the dissimilar signal pathways in which MTX prevents the conversion of dihydrofolate (DHF) to tetrahydrofolate (THF) by outcompeting DHFR to inhibit dihydrofolate reductase (DHFR) enzyme, and thus causing cell apoptosis. The affinity of MTX to DHFR is higher than that of folate, which is important for DNA synthesis. While CUR induced apoptosis through numerous signaling pathway. The MTX/CUR combination therapy also lowered the proper dosage of MTX, and thus preventing the severe toxicity of chemotherapeutic MTX to systemic parts [6,230]. Thus, an effective performance compared to free-drug or single-drug loaded NPs in liquidating tumors. Also, CUR selectively killed human HCT-116 cells when 89.0% of the drug was released in 2 days, owed to the presence of an acidic environment (pH 5.5) that enabled the breakdown of the drug-nanocarrier [156]. This was eased by the decrease of the static interaction between CUR and the nanocarrier (CNCs-AD/MGO), as well as decrease of the negative charge deposit with protonation of the carboxyl and amino groups of CNCs and AD respectively. These led to electrostatic repulsons in the drug-nanocarrier and thus their breakdown to release CUR. The drug-nanocarriers also expressed antibacterial and biocompatibility potential [156].

Pickering emulsion kind of suspension stabilization by solid particles at oil-water interfaces, has as well drawn attention in pharmaceuticals and nanomedicine for drug delivery in the blood and gastro-intestinal systems. The plan of emulsion properties enables irreversible binding of particles at the interface, which provides a prolonged colloidal stability and drug protection against macrophages and enzymes and thus, empower controlled release of bioactive encapsulations [175,205,231]. For instance, CNCs were designed to form aminated nanocellulose (ANC) particles to act as stabilizers of COU and CUR loaded PEs with different compositions of Tween 80 and medium chain triglyceride

(MCT) oil phases [204]. Above 90% encapsulation efficiencies of both COU and CUR were obtained due to strong molecular interactions of hydrogen bonds between ANC polar groups and bioactive CUR and COU. Both encapsulated systems displayed elevated stability and sustained release, higher with CUR than COU due to the high solubility of the latter, thus easy diffusion of the bioactive compounds. Besides, half-life estimates of CUR presented results similar to the reported encapsulations by chitosan-tripolyphosphate nanoparticles (half-life of 5 days) and silica nanoparticles (half-life of 5.2 days) stabilized PEs. Demonstration with human cell lines (MCF-7 and L929) showed that these uniform, regular and spherically shaped PEs are promising candidates for selective targeting of tumor cells to normal ones [204]. In a related study, magnetically-triggered Fe_3O_4-CNC stabilized PEs containing oil soluble CUR were recently prepared for controlled drug release and in-vitro therapy of colon cancer. Exposure of the micron-sized (≈ 7 μm) Fe_3O_4-CNC PEs to external non-invasive oscillating magnetic field (EMF) of 0.7 T induced *in-vitro* release of the highly stable encapsulated CUR as experimented in a buffered solution (pH 7.5). The release was as high as 53.30 ± 5.08% in 4-days, out of the initial 99.35% loading efficiency. The drug release was facilitated by the EMF magnetization of the adsorbed Fe_3O_4-CNC NPs, where they get attracted towards the direction of the magnetic field. This disorders the emulsions by induction of dilatational deformation of the fluid interface to facilitate the escape of the NPs into the water phase, while exposing the CUR-loaded oil to amplify their release. This mode of cargo delivery not only lowered overdosage induced side effects, but also effectively caused the human colorectal cancer cell (HCT116) deaths of up to 82 ± 2% after 96 hours of treatment, as mediated by apoptosis. This validated the effective cellular uptake and magnetically-induced hyperthermia cell cytotoxicity of the emulsions. In a 3-D culture model, the same nanoparticle formulation reduced the volume of the multicellular spheroids of HCT116 by two-folds as compared to the control sample, and yet non-toxic to brine shrimp [205]. Though the palm-based Fe_3O_4-CNC PEs still require improvement on the drug protection ability, they are however promising and could be an effective biocompatible stimuli-responsive colloidal drug delivery system for intracellular release of bioactive materials and therapeutics. Furthermore, a mixture of CNCs and an equal amount of CNF were employed for physical stabilization of Astaxanthin - α-tocopherol nano emulsions *via* hydrogen bonds, for skin cancer treatment [232]. With no cytotoxicity, the synthesized sample disclosed enhanced cell proliferation and viability by producing more amounts of singlet aerobic oxygen and antioxidant species [232–234]. The 24 h LDH exposure also caused damage of plasma membrane integrity, given that bioactive molecules and time are major factors for cell viability. The samples also confirmed that intracellular signaling pathways in NIH3T3 (mouse embryonic) and L929 (mouse fibroblast) cell lines were regulated during the combined treatment. This occurred with high levels of protein expression, owed to stimulation by precise molecules for cell proliferation, migration, and differentiation in cancer cells. The researchers therefore portrayed photocytotoxicity by laser irradiation for enhancement of cell proliferation of malignant cells [232,235–237]. CNCs can also act as co-stabilizers for polymeric excipients of butyl methacrylate, ethyl acrylate and methyl methacrylate as pharmaceutical acrylic beads synthesized by suspension co-polymerization reactions [238]. The resulting cellulose nano-whisker beads (CNWBs) were shown to be nontoxic and could be used to prepare tablets by compression with propranolol hydrochloride. Further analysis indicated that CNWBs could be useful in matrix tablets as potential excipients for control of drug release [238], which could be of great utility in cancer therapy.

CNCs have been utilized to reinforce mechanical properties of cellulose-based hydrogels for improved biomedical use including anti-tumor therapy [3,239]. Hydrogels are multicomponent systems with organo-polymeric three-dimensional networks and water, as the basic physical constituent. Hydrogels possess a hydrophilic and insoluble cross-linked structure, for absorption of immense water amounts or other biological fluids without affecting their structural integrity. The ability to accommodate high water amounts provide hydrogels a swelling response and high biocompatibility potential and thus possessing numerous excellent choices for application [38,74,240–243]. For instance, QC and rigid rod-shaped cationic CNCs (CCNCs) were cross-linked with β-GP to form nanocomposite hydrogels. These nanocomposites displayed enhanced mechanical strength, extended degradation time (higher half-life) and sustained release time. The biocompatible QC/β-GP/CCNCs hydrogels did not cause cytotoxicity and inflammation. When DOX-encapsulated QC/β-GP/CCNC hydrogels were injected besides tumors of mice having liver cancer xenografts, depots for subcutaneous and sustained release of anti-cancer drugs for anti-tumor therapy were displayed [31]. Like *et al.* [101] utilized slender carboxylated CNCs and long chains of hexadecyl amine, as the network to assemble a pH sensitive CNCs-nanohydrogel for controlled PTX delivery. With the created solvophobic area, the reticular hydrogel could effortlessly load the hydrophobic drug, PTX to a capacity of 13.7% with an efficacy of 59%. The nanohydrogel expressed high stability at pH 7.4 but the structure was altered/destroyed at the acidic pH 5.5, which enabled a sustained release of PTX. In vitro studies expressed high cytotoxicity of PTX loaded nanohydrogel towards A549 and HepG2 tumor cells with an inhibitory effect of 30% and 34%, respectively, compared to free PTX. A549 in particular expressed an apoptosis rate of 90.5% after 12 h. Intracellular PTX uptake was also greatly improved as expressed by the red influorescence of ICG loaded nanohydrogels in the nucleus and cytoplasm of the malignant cells after 1.5 h. This proved a lowered drug resistance [101]. The same group further prepared a multifunctional nanohydrogel of ALA/PDA/Fe@CNC loaded with PTX to obtain PTX-PDA/ALA/Fe@CNC, for pH-responsive antitumor therapy via a combined chemotherapy and ROS-mediated oxidative damage [100]. PTX-PDA/ALA/Fe@CNC exhibited a greatly high cytotoxic effect against MCF-7 cells of only 2.7% cell viability and 33.05% apoptosis rate, after 24 h incubation. The very high antitumor cytotoxicity was due to the high cellular uptake of over 2-folds, given the great adhesion effect of the nanogel-attached PDA molecules to living cells. The authors also attributed the anticancer oxidative effect to the highly toxic $O^{\bullet}H$ ions from the greatly effective ROS production of over 8.0-folds, due to incorporation of photosensitizer protoporphyrin IX ALA precursor, and Fe^{3+}catalysis of intracellular hydrogen peroxide, after their release from the CNC nanohydrogel. The Fe^{3+}ions also caused the pH-triggered release of antitumor drugs as a result of the destruction of the Fe^{3+}-ligand coordination structure by the low pH environment. The high decrease of the mitochondrial membrane potential also caused an increased ROS production. The loading of the anticancer drug PTX greatly added the chemotherapeutic antitumor effect of the nanohydrogels thus, efficiently killing the tumor cells. An excellent biocompatibility was also portrayed by the antitumor nanohydrogels. Additionally, the nanohydrogel exhibited a much reduced cytotoxic effect on normal cells, thus portraying a reduced side effect of PTX [100]. This represented an enhanced antitumor efficacy of pH targeting nanogels to construct hydrogels with a mucoadhesive and localized delivery potential, PAA and platinum antitumor drugs, cisplatin were conjugated with CNCs for therapy against human HCT-116 colorectal cancer cells [145]. The hydrogel expressed a superior muco-rheological behavior thus demonstrating relevant mucoadhesive properties. Hydrogel viscosity has generally been utilized for determination of the mucoadhesive property of nanocellulose [145,244]. The authors attributed this observation to the presence of carboxylic acid groups that allowed interaction between hydrogel and mucin. The anticancer hydrogel exhibited a slow release of ~ 10% of cisplatin after 6 h, causing > 3-fold increase in IC_{50} of the drugs against HCT116 cells. This was attributed to the spacious cavity provided by PAA branches for loading of enough cisplatin via relatively strong cross-linkages. The hydrogel also showed negligible intrinsic cytotoxicity, thus proving biocompatibility. Much as more examination for cancer diagnoses and treatment using CNC based hydrogels is still demanding, the use of other delivery

podiums such as aerogels should be worthy exploring. This is attributed to their returns over hydrogels for instance, remarkable weightier degree of swelling, rapider stacking of bioactive molecules, more effective interaction with the matrix of polymers, and easy entry into the inner matrix regions [245]. These hydrogels are thus described as potential localized and non-invasive depot materials for sustained drug delivery in chemotherapy.

CNC-peptide conjugates have also been explored for delivery of Chlorotoxin to cancer cells. Chlorotoxin-CNC (CNC-CTX) conjugate prepared using an ionic liquid was reported to be internalized selectively by U87 MG, a glioblastoma cell line [171]. Analysis showed stable and sustained internalization of CNC-CTX by U87MG cell line due to higher expression of Matrix metalloprotease-2 (MMP-2), a CTX target, as compared to MMP-2 negative MCF-7 breast cancer cell line. The internalization was sustained by the high affinity of CTX towards MMP-2. CTX reduce MMP-2 expression and increase sensitivity to radiotherapy. CTX are also delivered to cells *via* cationic vector-modified NPs [246].

4.2.3. CNCs for gene delivery

CNCs have been applied for the delivery of suicidal genes to various tumors. In a novel innovation but for a less complex conjugate, CNCs were utilized for transfection of Small interfering RNAs (siRNAs). siRNAs are future anticancer agents with the ability of silencing undruggable target genes in a specific and sequential manner [247,248]. siRNAs exist as either monomeric or the highly stable polymeric with enhanced therapeutic efficiency. They face restrictions like efficient carriage into the tumor cell cytoplasm with negligible toxicity, degradation by blood stream enzymes such as RNase A, erosion via the kidney or liver. siRNAs mute genes of malignant cells by apoptosis via activation of internal and external stimuli by triggering Caspase 9 and Caspase 8 gene code signals, respectively. PEI was covalently bound to CNCs by reductive amination producing CNC-PEI conjugates that were later loaded with siRNA forming strongly stabilized CNC-PEI-siRNA particles [170]. These particles showed no toxicity but instead protected siRNA from degradation, thus PEI form a good gene linker. However, siRNA release was pH-dependent since it was highly enhanced at low pH. The conjugates increased delivery of siRNA killer resulting into significant cell cycle arrest and apoptosis. The apoptotic pathway was typically intrinsic, given that siRNA was delivered into the cytoplasm, as expressed by signaling of caspase 9. CNC-PEI-siRNA particles could be a future alternative for non-viral siRNA delivery vehicles for tumor therapy [170]. Nanocomplex delivery vehicles (siRNAs-CNCs) of polymeric siRNA (Ps) and cationic CNCs were also prepared for cancer therapy [146]. For high drug loading, controlled release and efficient biological functioning in the cytoplasmic environment, the complexation efficiency of these nano-vehicles was optimized by choosing the most suitable physicochemical property of CNCs. siRNAs-CNCs were enormously well-protected compared to the free polymeric siRNAs, whereby at least a weight ratio of 5 siRNAs-CNCs portrayed 6-fold higher resistance to nuclease mediated degradation by RNase A than monomeric siRNAs [249]. This was due to the condensed structure of siRNAs-CNCs that efficiently entrapped polymeric siRNAs and thus lessened their exposure to RNase A. These gene vehicles showed 84.4% successful internalization efficiency into SKOV3 cancer cells at 40 nM, significantly improved enzymatic stability against RNase degradation, 72.7% target regulation of luciferase gene expression, and in vitro therapeutic effect of apoptosis-induced cancer cell proliferation [146]. This release rate proved that RNA interference was efficaciously enabled by the transported polymeric siRNAs in a dose-dependent mode, and thus proficient silencing of the target genes. These nanocarriers exhibited a promising approach for satisfactorily inducing anticancer potential without cytotoxicity. Significantly, the nanocarrier properties disclosed possibility of combined therapy via delivery of multiple biologically active cargos, which should be timely manipulated for faster clinical translation. In another study for nanoparticle-mediated gene delivery, CNCs were functionalized with polycationic PDMAEMA *via* disulfide linkage to form CNC-PDMAEMA (CNC-SS-PDs) brushes (Fig. 7a) [148]. Since disulfide linkages can be reduced by cellular glutathione (GSH), several redox responsive bio-cleavable nanocomposites (CNC-SS-PD) were designed for the study [148]. Anti-tumor evaluation of CNC-SS-PD by using suicide gene systems for *in vitro* and *in vivo* experiments showed increased suppression growth of cancer cells (HePG-2) and tumors in mice [148]. Thus, such redox responsive nanocomposites could be utilized as future novel smart prodrug/gene delivery systems. In a similar study of DNA delivery system, Au NP-conjugated heteropolymer brush-coated CNCs were designed *via* alternate grafting of PPEGEEMA and PDMAEMA brushes (Fig. 7b) [180]. For not only reduction and protection of Au, the cationic PDMAEMA chains also effectively complexed the plasmid DNAs, whereas the outward neutral and biocompatible PPEGEEMA brushes induced the shielding effect and significantly reduced cytotoxicity. All the gene carriers presented high transfection efficacies and internalization rates of up to 75.8%. The polymer brushes also portrayed better CT imaging ability with treated HepG2 cancer cells.

4.3. CNCs for photo-therapy

Photodynamic therapy (PDT) is an advanced method that involves initiation of photochemical reactions using photosensitisers, light and oxygen for treatment of a number of conditions including cancer, arthritis, and skin disorders. The presence of activators such as oxygen and light stimulate the photosensitizer agents to generate reactive oxygen species (ROS), which are directly or indirectly released for easy killing/destruction of cancer cells. Therefore, combination of photosensitizers with nanocarriers enable their efficient delivery thus enhanced efficacy in cancer healing. For instance, CNC-PEI based nanoconjugates have been modified further for application in anti-tumor resistance by photodynamic therapy. Soluble and stable photosensitizer nanoconjugates (PS-CNCs) constituting of CNCs covalently associated with polyaminated chlorin p6 [168] were reported to have a nanomolar range IC_{50} when tested with HaCat cell line under exposure of 570-670 nm wavelength light. These Chlorin-PEI-labelled CNCs also showed minimal cytotoxicity to HaCat (human keratinocyte) cell line in the dark. In another related study, poly(2-oxazoline) modified CNCs were utilized to immobilize ICG *via* electrostatic interactions, forming nanorods that exhibited low toxicity in dark [169]. These nanorods however unveiled competent photothermal therapeutic efficacy when internalized by HeLa cells and irradiated with 808 nm wavelength near infrared laser [169]. HeLa cells treated with ICG-loaded nanorods under radiation were more obliterated than free ICG after internalization, thus proving the photothermal-induced cytotoxicity. The enhanced cell lethality was due to the high photostability expressed by the amphiphilic poly(2-oxazoline) polymer strings that effectively stabilized ICG via electrostatic interactions. Also, the irreversible degradation of ICG affects its photocytotoxicity. The poly(2-n-propyl-2-oxazoline) amphiphilic arms on these CNCs are known to be efficient in stabilizing ICG compared to the hydrophilic poly(2-methyl-2-oxazoline), which makes such CNCs suitable for designing related CNC-based drug nanocarrier systems. Additionally, these nanocarriers have potential of delivery of multiple antitumor prodrugs. Hu *et al* [181] synthesized multifunctional hetero-nanocomposites of CNC-gold nanorod and nanospherical hybrid particles, enveloped with less-toxic hydroxyl-enriched polycationic gene carriers, β-CD-PGEA (composed of β-CD cores and EA-functionalized PGMA arms) for tumor photocytotoxicity (Fig. 8a). The subsequent CNC-Au-PGEA hetero-nanocomposites displayed excellent gene transfection efficiency of 35 ± 1% due to high cell internalization rates of ~74±1%. The high rates of cell internalization were facilitated by the rod-shaped structure of the nanocarriers. The enhanced gene transfection was enabled by the PGEA supported polycations, which were shipped into the lysosomes to provide a buffering environment for efficient mediating of acid-triggered escape of pDNA. Via interexchange

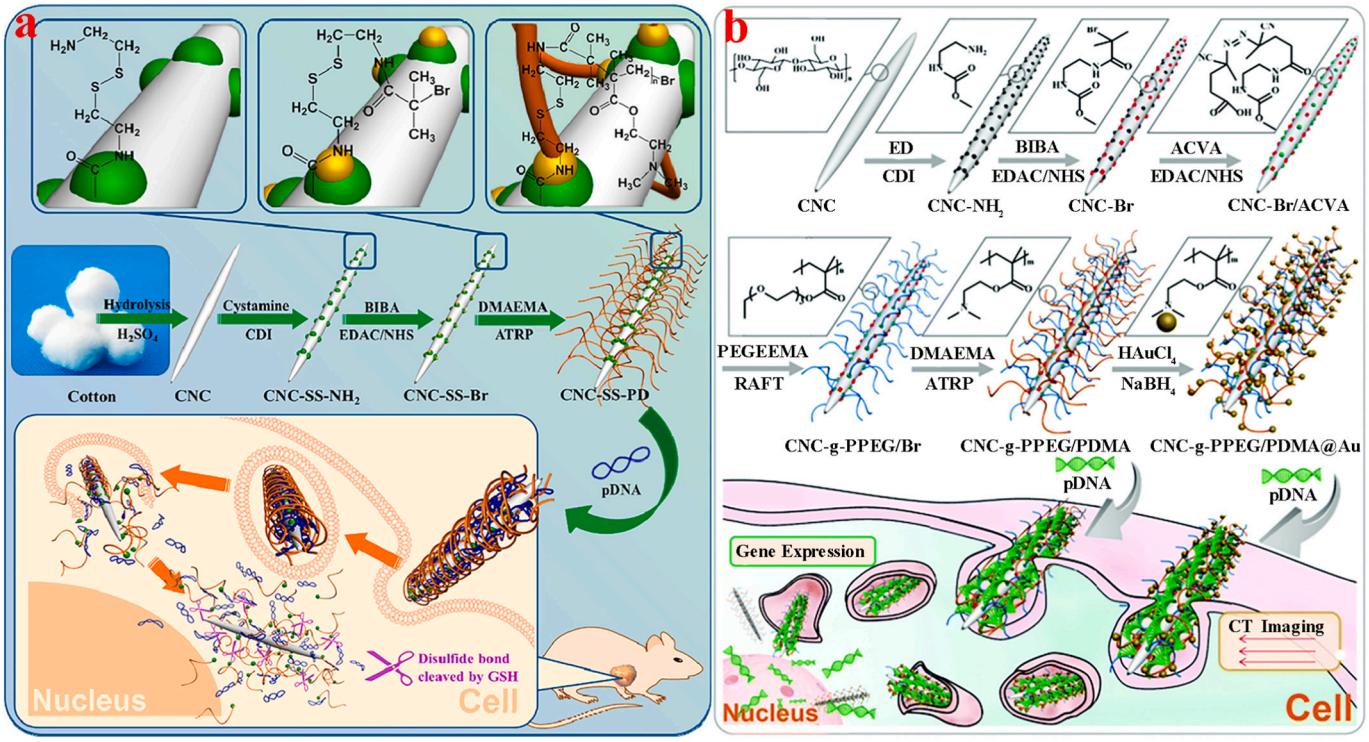

Fig. 7. (a) Schematic diagram illustrating the preparation of CNC-graft-PDMAEMA (CNC-SS-PD) via ATRP and the resultant gene delivery process. Reproduced with permission from ref. [148]. Copyright 2015, ACS Applied Materials & Interfaces. (b) Preparation and schematic illustration of pDNA delivery via CNC-g-PPEG/PDMA@Au nanoparticles. Reproduced with permission from ref. [180]. Copyright 2016, Polymer Chemistry.

with counter polyanions, the complexes were swiftly decondensed to induce release of pDNA. Furthermore, the nanorod hetero-structures expressed satisfactory optical absorption characteristics which led to excellent photothermal (PT) (Fig. 8b, d-f) and photoacoustic (PA) imaging properties (Fig. 8g-i) with low cytotoxicity. Thanks to the perfect conjugation of Au NPs that are excellently characteristic of both photoacoustic imaging and photothermal therapy, in addition to the faster delivery of CNCs nanocarriers. The authors also realized that both photothermal and photoacoustic imaging were enhanced with increase in the concentration of the nanorod hetero-structures (Fig. 8c). For combined gene/photothermal therapy of the nanorod hetero-structures, reduction of the viability of C6 cells to 20% during *in-vitro* studies and total suppression of tumor in mice using plasmid p53 under irradiation, confirmed the high antitumor efficacy of these nanorod hetero-structures.

5. Biocompatibility and nanotoxicity of CNCs and their derivatives

CNCs are external agents to the body and therefore, their 'foreignness' should be examined before any biomedical application that would require their direct contact with the body cells. The foreignness is evaluated based on the nature of host response when the CNCs come into contact with human tissues. For CNCs to be biocompatible, they should be chemically and biologically inert to elicit minimal/tolerable or no response at all from the host. Biocompatibility loosely refers to the ability of a biomaterial to perform as expected while eliciting a proper host response in a specified condition(s) [250]. Generally, the biomaterial has to perform the envisioned function without merely being passively available in cells. The elicited reaction to its presence and the nature of the reaction should be appropriate to the specified application and thus, making its suitability different from one context to another [251]. Although biocompatibility has been defined based on the biomaterials in question such as implantable devices, scaffolds and matrices [250], the principle factor of biocompatibility is the host response. The biomaterial molecular, physical and topological characteristics influence the nature of the host response. Host responses can be diverse depending on factors such as sex, age, general health, lifestyle features, physical mobility and pharmacological status. They however include protein adsorption and desorption properties, neutrophil and macrophage activation, general cytotoxic effects, fibrosis, microvascular changes, activation of the clotting process and platelet adhesion, maladaptive cell-specific responses, complement activation and immune responses, hypersensitivity, genotoxicity, reproductive toxicity and carcinogenesis [250]. Generally, high biocompatibility is achievable when biomaterials interact with host tissues/cells to induce tolerable or nontoxic, thrombogenic, immunogenic, and carcinogenic responses. Smaller biomaterials such as nanoparticles including CNCs, usually bind/adsorb proteins forming nanoparticle-protein complexes. The nature of such complexes depends on the surface chemical properties of the NPs. The extent of binding/adsorption of proteins significantly determines the biocompatibility and biodistribution of the NPs [252]. Basing on biocompatibility considerations, biodegradable NPs or CNC coated with biodegradable materials are preferred for biomedical (including drug delivery) applications. PLGA, PLA, PCL, Chitosan and Gelatin are some of the materials that can be used to prepare biodegradable NPs [253], unlike non-biodegradable NPs which can be phagocytosed and accumulated by polymorphonuclear leukocytes [251]. Although some of these materials may stimulate inflammatory responses involving release of free radicals [254], there are no significant clinical outcomes since the NPs are eventually eliminated by the system. For instance, in mouse and human macrophages, a mild inflammatory response characterized by interleukin-1β (IL-1β) secretion and surge in mitochondrial free radicals was evoked by cationic CNC derivative (CNCs grafted with poly(AEMA) [255]. Most CNCs conjugated to these biodegradable materials have been found to be biocompatible [256]. Some of the conjugates such as PEG and PAMAM dendrimer-glucosamine induce immunosuppression [251] leading to

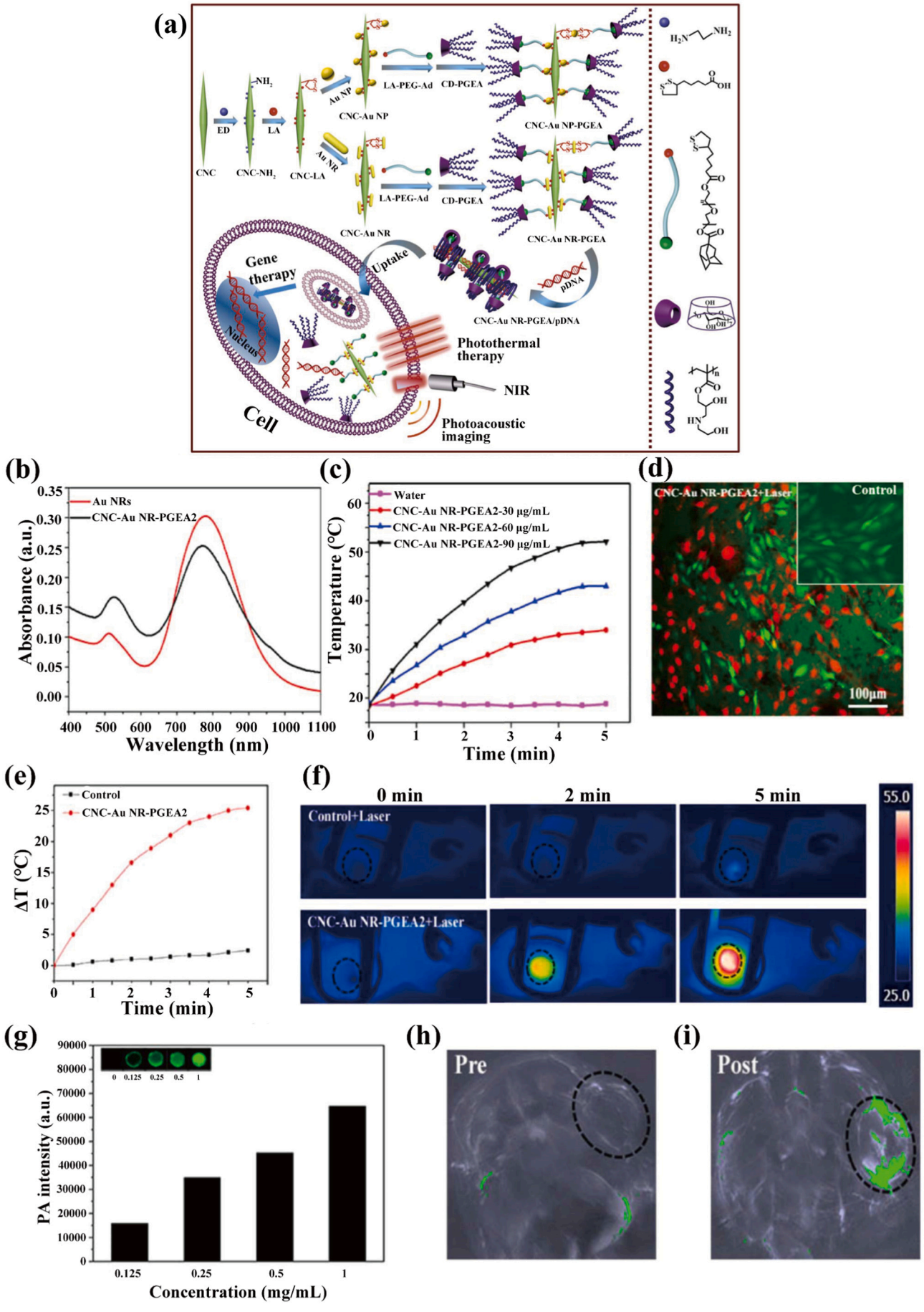

(caption on next page)

Fig. 8. (a) Schematic illustration of the preparation of CNC-Au NP-PGEA and CNC-Au NR-PGEA and the resultant PA imaging and combined gene/PT therapy. (b) Vis-NIR absorption spectra of Au NR and CNC-Au NR-PGEA2. (c) Temperature elevation of water and CNC-Au NR-PGEA2 solutions with different concentrations as a function of irradiation time. (d) Fluorescence images of FDA-PI stained C6 cells with and without CNC-Au NR-PGEA2 after irradiation at 808 nm (2 W/cm^2). (e) Temperature variation, (f) infrared thermal images of C6 tumor-bearing mice exposed to 808 nm laser (2 W/cm^2) after injection with PBS or CNC-Au NR-PGEA2. (g) PA intensity and images (inset) of CNC-Au NR-PGEA2 solutions at different concentrations. PA images of mice (h) before and (i) after intratumoral injection with CNC-Au NR-PGEA (tumor regions were highlighted by black circles). NR-nanorod. Reproduced with permission from ref. [181]. Copyright 2017, Journal of Controlled Release.

blunting of the immune response to the CNCs thus, rendering them biocompatible. Though the fate of unmodified CNCs is not known in the cells and human system [257], CNCs have been reported to be significantly environmentally biodegradable as deduced from their theoretical oxygen demand [258]. In spite the fact that CNCs are generally known to have low toxicity and low environmental risk [259], they can interact with the host cells/tissues to elicit an exacerbated response resulting into CNC toxicity. Although most of the CNCs toxicity studies in context of drug delivery have mainly evaluated cytotoxicity [41,54,256], with most indicating no or non-significant toxicity, some reports have profiled CNC-induced toxicities in various cells/tissues and organs [212,260,261]. For instance, carboxylated CNCs prepared from softwood pulp *via* sodium periodate oxidation, exerted cytotoxicity stress to various cells at 3.8 mmol g^{-1} threshold [262]. This was caused due to the high charge density of the NPs.

Due to increasing use of CNCs, there has been rise of their inhalation exposure to humans during CNC commercial production, commercial CNCs applications, mixing CNCs with other products and incidental contact [263]. Much as inhalation of CNCs would be the major occupational exposure relative to consumption of CNC-made products and contact (skin, eye), the minimum dose required to elicit a biological response at a given time (chronic or acute) is not known [263]. Most of the current CNCs toxicity studies have been carried out using varied models such as mice, aquatic organisms such as zebra fish, cell lines (kidney, breast cancer, fibroblast, insect, macrophage) to evaluate pulmonary outcomes, genotoxicity, reproductive fitness, inflammatory response, cytotoxicity (apoptosis and necrosis) and growth [260]. By the virtue of CNCs being in the range of fine/ultrafine particulate matter of less than 2.5 μm/0.1 μm ($PM_{2.5/0.1}$), they present a great health risk of cardiovascular and pulmonary irritation if inhaled [264] and therefore pulmonary CNC toxicity has been one of the important focus of investigations. Pulmonary toxicity occurs due to adverse effects of foreign materials in the respiratory tract.

Available reports indicate that CNCs can induce a proinflammatory phenotype associated with oxidative stress and tissue damage [261]. Yanamala *et al.* exposed the NPs to adult female C57BL/6 mice in form of CNC suspension (10%w/v) and powder by pharyngeal aspiration in doses of 0.05, 0.1, or 0.2 mg in about 0.04 mL. Both CNC suspension and powder showed dose dependent increase in oxidative stress and tissue damage. Oxidative stress markers such as protein carbonyl and 4-hydroxynonenal were approximately twice that of control at 0.2 mg dose. These findings were in agreement with *in-vitro* observations from the human epithelial airway barrier designed in a three-dimensional triple cell co-culture model [265], in which CNCs elicited a significantly lower cytotoxicity and (pro-)inflammatory reaction as compared to multiwalled carbon nanotubes and crocidolite asbestos fibers. Although CNCs modified with different ligands, regardless of the chemical modification induced relatively low incidences of developmental impairment and mortality at concentrations below 1000 mg/L [266], CNC suspension and powder seem to induce differential pulmonary toxicity. CNC powder induced higher extent of tissue damage in mice while CNC suspension upregulated higher levels of proinflammatory cytokines and oxidatively modified proteins [261]. Additionally, though both induce a common plethora of pro-inflammatory cytokines, CNC suspension uniquely elevated IL-4, 10, 12p70 and IFNγ as compared to RANTES and 1L-13 for CNC powder [261]. This emphasizes the influence of physical state on the activity of CNCs.

Despite noted respiratory tract CNC toxicity, studies conducted so far in rats show no significant orogastrointestinal toxicity. No toxicity was found for aerosolized CNCs in Sprague-Dawley stock-derived albino rats subjected to CNCs inhalation to a maximum concentration of 0.26 mg/L for 4 hrs [212]. This is a suitable property for CNC application in drug delivery *via* the oral route of administration. No significant CNC dermal toxicity has been reported yet. In the past review, Roman [212] reported that CNCs were neither found to be skin sensitizers nor dermal irritators and corrosives. When 1.1 mg/mL CNC suspension was intradermally injected into Crl:(HA) BR guinea pigs followed by 103 mg/mL CNC topical application, it did not cause lymphocyte recruitment as a sign of sensitization at the site of application, even after more than two weeks. In a murine model, consecutive topical application of 25 μL of CNC suspension (ranging from 2.5 to 10.7%) on the ear dorsa of CBA/J mice did not indicate that CNCs could be dermal sensitizers at the tested concentrations. In a related study, CNC gel with 0.5 g of dried CNC was topically applied with a gauge patch for 4 h on Crl:KBL(NZW)BR albino rabbits and monitored for 14 days for erythema and oedema. The scores (scale of 0-4) for the skin response obtained at different time points; 60 min, 24 h, 48 h, and 72 h suggested that CNCs may not induce corrosive effects on the skin [212]. However, CNCs may influence the activity of myeloid cells when conjugated to some chemical agents. According to Sunasee *et al.*, CNCs-β-CD do not elicit a strong immunological response (elevated secretion of IL-1β and TNFα) to human monocytes (THP-1 cell line) and mouse macrophage-shaped cells (J774A.1), although in high concentrations, they enhance the production of mitochondrial ROS, without affecting antioxidant defense [267].

CNC cytotoxicity investigations have been done more extensively *in vitro* than available *in vivo* animal model studies, most of which show no cytotoxicity effects (as per ISO standard 10993-5, i.e., reduction of not more than 30% cell viability). For instance, Table 1 shows the toxicities of CNCs and its derivatives in various cancer cells, where they show low or no toxicity at different concentrations, thus proving their biocompatibility during cancer therapy. One notable finding reports that CNCs were not cytotoxic to nine dissimilar cell lines (PC-3 and C6, KB, HBMEC, MCF-10A, bEnd.3, RAW 264.7, MDA-MB-468, MDA-MB-231) as evaluated by MTT and LDH assays at the concentration ranges of 0-50 μg/mL for exposure duration of 48 h [268].

There are however other studies that report dose dependent cytotoxicity of CNCs with most notable effects at higher concentrations in some cell lines [41,212,263]. The conflicting results of cytotoxicity have been attributed to variable conditions such as the source of CNCs, preparation technique, aggregation of CNCs in culture medium, presence of toxins and variable responses from different cell lines. Some CNC treatment conditions may also influence their cytotoxicity; for instance autoclaving of sulfuric acid-hydrolyzed CNCs could lead to loss of CNC sulfate groups releasing sulfuric acid which lowers their pH, causing decreased viability [212]. In another scenario, FITC-labelled CNCs (0.1 mg/mL) elicited cytotoxicity in insect ovary cells (Sf9) and human embryonic kidney cells (HEK 293) while no measurable cytotoxicity was induced by a comparable concentration (0.01–0.05 mg/mL) of FITC-labelled CNCs in diverse barrier and immune cell types for *in vitro* studies [263]. Similarly, CNCs obtained from hemp and flax caused less inhibition on Sf9 cells when pre-treated with enzymes such as pectate lyase than if hemp and flax were not enzymatically treated [272]. Despite these inconsistences and conflicting observations, it is suggestive that CNCs may cause cytotoxicity at higher doses to some cell lines. In another study, Mahmoud *et al.* investigated the uptake and toxicity of two fluorescent CNCs; CNC-RBITC and CNC-FITC. Unlike the positively

Table 1
Summary of the toxicities of CNCs and its derivatives for cancer treatment.

Modified CNCs	Chemical modifier(s) group	Nanoparticle shape/length (nm)	Theranostic Application	Cell line	Biocompatibility/ Cytotoxicity	Examination method	Ref.
CNC	–	rod-like 181 ± 9		HBMEC, RAW264.7, bEnd.3, MCF-10A (not tumor), MDA-MB-231, KB, MDA-MB-468, PC-3 and C6	No cytotoxicity ≤ 50 μgmL^{-1}	MTT and LDH Assay	[268]
CNCs-poly(AEMA) CNCs-poly(AEM)	poly(AEMA) poly(AEM)	rod-like 100−200		J774A1 MCF-7 Nine Mammalian cells	Negligible cytotoxicity25-100 μgmL^{-1}	MTT Assay	[195]
CNC	–	rod-shaped 100-1200	Nanomedicine Biotechnology	NIH3T3 HCT116	Low cytotoxicity ≤ 250 μgmL^{-1}	WST-1 assay	[154]
CNCs	–	spherical shape 63 ± 16	Diagnotherapy	A549 cells	Low cytotoxicity ≤ 62.5 μgmL^{-1}	MTT assay	[269]
CNPs	–	amorphous and anisotropic 160 - 200	Photoacoustic imaging	OV2008	Low cytotoxicity ≤ 0.31 mgmL^{-1}	Presto Blue assay	[216]
CNC	–	Rod-like 10-100		human brain microvascular endothelial cells (HBMECs)	Non-toxicity 10-50 μgmL^{-1}	MTT assay	[270]
CNC-Alexa Fluor 633	Alexa Fluor 633	rod-like 200−300		HeLa cells.	No cytotoxicity 14-140 μgmL^{-1}	MTS assay	[163]
Rho-CNCs or AF488-CNCs	Alexa Fluor 488 (AF488) rhodamine (Rho)	rod-like shape 170 ± 30	Fluorescent imaging	HEYA8 cells	No cytotoxicity ≤ 0.0035 wt. %	Acid phosphatase (APH) assay	[166]
CNC-RBITC CNC-FITC	RBITC FITC	rod-like 120-300nm (for CNC-RBITC)		HEK-293 Sf9	Noncytotoxic (CNC-RBITC) Cytotoxicity (CNC-FITC) ≤ 100 μgmL^{-1}	Trypan blue exclusion assay MTT assay	[222]
CNC CNC-g-PEEP	PEEP	nanorod-like 200−300		HeLa cells L929 cells	No significant cytotoxicity≤1mgmL^{-1}	MTT assay	[193]
MGO-AND/CNC MGO-AND/CNC-CUR		MGO-AND/CNC Irregular (158)		RBCs	Little hemolytic activity 12.5-100 μgmL^{-1}	In vitro hemolysis assay	[156]
MGO-AND/CNC	CUR MGO AND	MGO-AND/CNC-CUR regular		HCT-116	Nontoxicity 6.25-25 μgmL^{-1}	MTT assay	
Fe_3O_4@cellulose nanocrystal (MCNC)	Fe_3O_4 (≈9 nm)	rod-like 150-200		Brine shrimp Artemia	Non-toxic 1.5-100 μgmL^{-1}	Brine shrimp lethality assay	[205]
CNC/CNF/AS-AT (Emulsion)	Astaxanthin (AS) - α-tocopherol (AT)	spherical 200-210		L929 NIH3T3	No photocytotoxicity and chemotoxicity 100 μgmL^{-1}	MTT and LDH assay	[232]
QC/CCNC/β-GP (Hydrogel)	β-GP QC	rod-like shape for only CCNC 427	Drug delivery	COS-7 cells	Low in vitro cytotoxicity ≤ 5 mgmL^{-1}	MTT assay	[31]
CNC-APTMS-Lysine	APTMS Lysine	rod-like 240.68 ± 124.58		RBCs	Negligible hemolysis 1000 μgmL^{-1}	In vitro hemolysis assay	[6]
CNC-g-PAA (Hydrogel)	Poly(acrylic acid)	rod shape215 for CNCs		HCT-116	Negligible toxicity 7-450 μgmL^{-1}	MTT Assay	[145]
CNR	–	rod-like 188		NCI H 460	Low cytotoxicity 300 mgL^{-1}	MTT Assay	[182]
CNC FITC-CNC	FITC	spherical 39 ± 9	Drug delivery, Fluorescent imaging	C6 NIH3T3	Low cytotoxicity 1.56-25 μgmL^{-1} for all ≤50 μgmL^{-1} for C6	MTT assay	[271]
PA-g-CNC	PA	irregular		human red blood cells	Negligible hemolysis 10-1600 μgmL^{-1}	in vitro hemolysis assay	[194]
CNCs–CTX	Chlorotoxin	rod-like 8000–10,000	Targeted drug delivery	U87MG MCF7	Non-cytotoxic 6-200 μgmL^{-1}	MTS assay	[171]
CNC-SS-PD/pDNA	PD (PDMAEMA) pDNA	needle-shape 200−250		COS7 HepG2 cells	Low toxicity 88.1-203.6 mg of PD	MTT assay	[148]
CNC-based cationic vectors/pDNA complexes	PPEGEEMA PDMAEMA pDNA	rod-like 150–200		HepG2 HEK293	Lower toxicity dependent on N/P ratio (5-15) and PDMAEMA M_n	MTT assay	[180]
CNC-Au-PGEAs/ pDNA complexes	Au PGEA pDNA	rod-shaped <200		HEK293 C6	Low cytotoxicity 10-30 W/W ratios	MTT assay	[181]
CNCs CationicCNCs PsCNCs	CHPTAC polymeric siRNA (Ps)	spindle-like CNCs 215-360		SKOV3	negligible cytotoxicity 40 nM	CCK	[146]

(*continued on next page*)

Table 1 (*continued*)

Modified CNCs	Chemical modifier(s) group	Nanoparticle shape/length (nm)	Theranostic Application	Cell line	Biocompatibility/ Cytotoxicity	Examination method	Ref.
		spindle-like and branched 293 ±28	Gene delivery				
ICG-PIPOx-g-CNCs	ICG PIPOx	rod-like 100–140	Photothermal therapy	HeLa cells	Above 80% viability in dark $\leq 25\ \mu gmL^{-1}$	MTT assay	[169]
CNC-PEI-chlorin P6	PEI chlorin P6600 Da	rod-shape 100–200	Photodynamic therapy	HaCat	Low cytotoxicity (dark)1.95 nM - 2 μM	MTT assay	[168]
NCC-LC- C_{60} and NCC-SC- C_{60}	C_{60}	whisker-like 150-200	Photodynamic cancer therapy		No (dark) andlow (light) cytotoxicity ≤ 20 μM		[157]
NCC- TSPP(Zn)	TSPP(Zn)	whisker-like 132 ± 52	Drug delivery	MCF-7	Cytotoxicity (light) ≤ 20 μM	Resazurin assay	

charged CNC-RBITC (ζ-potential 8.7 mV) which was taken up by *Spodoptera frugiperda* (Sf9) and human embryonic kidney 293 (HEK 293) cells without a significant toxic effect on the cell membrane integrity, negatively charged CNC-FITC (0.1 mg/mL, ζ-potential -46.4 mV) were not observed to be internalized at physiological pH. Instead, CNC-FITC surrounded the cells eventually leading to membrane rapture [222]. It is however important to note that very high concentrations of CNCs (0.25-5 mg/mL) with respect to mammalian cell culture were used and for such levels of CNCs, similar toxicities have been observed, some with even impaired metabolic activity and reduced cell proliferation as reviewed [263]. Hanifah *et al.* [154] reported a portion of variable size of CNCs that caused substantial cytotoxicity at much higher concentrations of 500 g/mL and 1000 g/mL to HCT116 colon carcinoma and NIH3T3 fibroblast cell lines as evaluated by WST-1 assay. However, none of the CNCs of varying size showed any significant cytotoxicity to either cell line at lower concentrations in the range of 10 g/mL to 250 g/mL (and even 500 g/mL). Similarly, CNCs had low cytotoxicity to L929 cells at 0.01-0.2% concentration, the cytotoxic tendency increased with increased concentration as evaluated by MTT assay and cell morphology [273]. In the same line, porphyrin conjugated CNCs (CNC-TSPP(Zn)) in the concentration range of 5-50 μM lowered the metabolic activity of MCF-7 human breast cancer cells to approximately 55% of the untreated cells, while up to 20 μM concentrations of NCC-LC-C_{60} slightly reduced the metabolic activity of the same cells to 70% of control cells [157]. For both dose-dependent phototoxicity tests, irradiation of light at the fluence of 7.2 J/cm^2 was applied.

Unlike the nanorod, nano-disk, and nano-cube particles, spherically shaped nanoparticles manifest enhanced cellular uptake [274]. This is attributed to their geometry described by a high length normalized curve, thus enabling cellular internalization. Their small sizes also allow protection from opsonization by immune host cells, which enhances their bioavailabity. On this note, Liebert *et al.* attempted to prepare spherically shaped CNC nanoparticles directly from commercial trimethylsilylcellulose, and conjugated with FITC [275]. Investigation of the cytotoxicity of these nanocarriers during untargeted drug delivery, expressed a rapid cellular uptake *via* adsorptive endocytosis. This showed their unsuitability to development of safe targeted nanocarriers because the targeted property is only attained after functionalization of surfaces with precise ligands. As a remedy, Shazali *et al.* [271] improvised a preparation technique of negatively charged CNC from CNF of oil palm fruit by using acid-hydrolysis, before conjugation with FITC. The spherically shaped FITC-CNC manifested low cytotoxicity and poor untargeted cell internalization into C6 rat glioma and NIH3T3 normal fibroblasts cells thus, can be potentially applied as nanocarriers of anticancer drugs, DNA, or other macromolecules. The authors attributed these observations to the negative surface charge and hydrophobicity of the nanocarriers, in addition to their spherical shape.

Some studies have reported CNCs to be genotoxic agents [41,263] based on the observed DNA double strand breaks (DNA DSB), micronuclei formation and mutagenicity potential. Farcas *et al.* [276] reported that pulmonary exposure resulted into significant decrease in spermatozoa count (40%), reduction in sperm motility (50%) and higher abnormality score compared to the controls. Apart from increased DNA fragmentation index (from 2.61-3.32%) in the exposed mice, there were increased sperm anatomical abnormalities including club-shaped head (1.5-fold), thin and elongated head (2.67-fold), bent mid-piece (2.37-fold), and looping midpiece (1.57-fold). They also reported increased oxidative stress, about 20% increase myeloperoxidase activity and a significant increase in the levels of proinflammatory cytokines [276]. The increased oxidative stress could be responsible for exacerbation of DNA damage by free radicals. These findings indicate the potential role of CNCs in reproductive toxicity. However, CNCs are simply taken potential genotoxic agents due to mixed results from different studies with both significant positive and negative results [263]. According to the current reports of available literature, it can be strongly noted that CNC-induced toxicity is likely at high concentrations and it could be roughly consistent to conclude that such toxicity may manifest as an inflammatory response characterized by elevated secretions of pro-inflammatory cytokines. This may exacerbate further damage due to oxidative stress leading to cytotoxicity, genotoxicity, immunotoxicity among others. More investigations are therefore required in this direction to resolve the inconsistencies and conflicting conclusions that have been reported in literature. This is very paramount given the importance of CNCs in drug delivery and other biomedical applications.

6. Current challenges and future perspectives

The large scale production of CNCs for marketing is facile, however its commercial application in cancer diagnoses and treatment still suffers some drawbacks. These range primarily from their sources to application systems. Noticeably, CNCs sources and processing techniques influence their properties such as elastic moduli, colloidal stability, which determine modification easiness and feasibility, appropriate routes for preparation of nanocarriers, storage and incubation time. Though some research works [61] have made survey, a weighty examination of the impact of origin and isolation techniques to CNCs properties will improve interaction with anticancer agents and malignant cells, and stability during delivery. Also, the use of cationic agents for charge reversal has eased attachment of negatively charged functional moieties onto CNCs. However, positively charged NPs degrade slowly and also catalyze interaction with the negatively charged albumin in the plasma hence causing cytotoxic effects. Nevertheless, enhanced biocompatibility and degradability studies, and effectively green preparation techniques will provide safer nanocarriers.

Several anticancer agents are liable to normal cell side effects during delivery. For instance, platinum-based chemotherapeutics are characteristic of healthy organ toxicities such as ototoxicity, nephrotoxicity and myelosuppression [207], DOX expresses severe systemic toxicities [182]. Also, siRNA agents possess restrictions to clinical trials like influencing gene mutations, stimulation of immunological reactions, undesirable tissue deposition, instability in the bloodstream, and inefficient intracellular delivery [146,277]. But delivery of stimuli-

responsive NPs for either one or more preferably both internal stimulants such as pH, temperature, redox potential, enzymes, and external stimulants such as ultrasound, radiofrequency, infra-red irradiation, light, magnetic field [6,205,278] and application of combination therapy will minimize toxicities with retention of a high nanocarrier efficacy. For instance, Tao et al. [214] utilized both pH and near infra-red (NIR) irradiation as intrinsic and extrinsic stimuli, respectively, for the delivery of DOX in malignant cells. They recorded high biocompatibility and degradability of the nanocarriers with deep tumour penetration of sufficiently high drug amounts at a controlled rate, owed to the excellent stimuli response. Henceforth, the application of various stimuli, photosensitizers including 2D inorganic nanosheets (antimonene, borophene, silicene [214]), target ligands and biomarkers (nucleic acids, proteins, and circulating tumor cells [279]) onto CNC nanocarriers will enable targeting tumor cells for a timely pharmacokinetics feedback, effective dosaging, provide enhanced sensitivity, monitoring of the tumor progression, therapeutic invasions, drug treatment, and surgical predictions [280].

Drug resistance by tumor cells develops in different ways including metabolizing specific anticancer target drugs, tolerating unusually high drug toxicities, dormancy, and active extrusion of multiple drugs. For example, breast tumors form lumps of mixed malignant cell populations in which only drug-sensitive cells respond to therapy while resilient cancer cells repopulate. The approach to counter drug resistance in most protocols is combination treatment by precise co-administration of several anti-cancer agents such as PTX and DOX/DSF (disulfiram)/marimastat [10,281], docetaxel (DTX) and gemcitabine (GEM) [9], CUR and methotrexate [282], or combination with physical therapies such as phototherapy, magnetic therapy. This novel therapy may promote synergistic cytotoxicity to drug resistant tumors at various growth stages via distinct mechanisms of action. Besides, combination therapy can subordinate the cruel side effects due to high doses of single drugs, given that dose reduction is prospective [281]. For efficient delivery, CNCs can be exploited as suitable biocompatible platform. Similarly, high IC_{50} are executed with slow or controlled drug release process for efficient cytotoxicity of tumors, while minimizing evolution of drug evasive/resistant clones that can arise in a short and stochastic bout of drug exposure. CNCs-mediated controlled drug release can be tuned by altering the potency of interaction of drugs with CNCs nanocarriers, incorporation of stimuli-receptive elements, controlling the nanocarrier morphology, manipulation of biocompatible and strong adhesive agents such as poly(acrylic acid) (PAA), and coalescence of erodible and swellable skeletal parts for hydrogel-based nanocarriers. This will alleviate drug dilution effect by cell division and erosion by tissue fluids and hence increasing half-life and localization in/on cellular and tissue surfaces.

FDA approved some anticancer chemoagents and materials for clinical use, while others are still under clinical phases [219,283]. A few of them such as gold nanorods, DOX, PTX, CUR have been successfully studied for delivery by CNCs. To fast-track translation of the clinical use of CNCs for delivery, more FDA anticancer acceptable agents should be characterized. Furthermore, enhancement effect with use of precise in vivo diagnostic methodologies should be critically analyzed to realize their translation with the reasonably set criteria. Market potential such as drug affordability to realize a reliable clinical validity in accordance to the throughput systems by the regulatory authorities is also obligatory. This will allow lawful investigation of the drug performance by appropriate monitoring authorities for licensing.

In brief, the earlier knowledge acquired about the synthetic and functionalization potential of CNCs allowed the birth of novel modifications for delivery of anticancer agents. This is coupled to their remarkable mechanical features for drug cargo. Hence, exploration of alternative therapies such as targeted therapy, photodynamic and hyperthermia therapies have been realized at the nano-level. Therefore, intensifying devotion to exertions of controlling the clinical translation of antitumor CNCs nanocarriers by timely unravelling the associated challenges, will further exploit the new systems for assembly of therapeutics that highly fulfil forecasts. Especially that CNCs drug-payloads seem ready for transformation into injectable formulations, ointments, given the great necessity of a novel anticancer therapy for clinical translation.

7. Conclusion

Recently, CNCs have gained popularity from industrial and scientific communities mostly due to their appealing physico-chemical characteristics that confer them low cost extraction from renewable sources, low biotoxicity, biodegradability and desirable mechanical properties. They can also be subjected to a wide range of chemical modification to facilitate conjugation with therapeutic drugs for diverse applications. Though there has been a significant rise in the number of CNC-related publications in the last years according to the Web of Science®, it can eminently be noticed that CNCs application in the biomedical field is still precocial.

As per the discourse presented herein and in other literature, CNCs can be magnificently modified and conjugated to other nanomaterials and chemical moieties such as dyes, therapeutic drugs, toxins, genes among others, yielding new nanocomposites for oncological drug and gene delivery, bioimaging and biosensing applications among others. Though some scientific and technological progress has been achieved, bottlenecks for clinical translation of CNCs still exist. Therefore, it should be of considerable value to innovate controllable chemical or physical modification methods for CNCs surfaces, preferably by exploiting mild or green chemistry conditions. To follow suite, methods for ultrastructural detail characterization of such CNCs are necessary to allow investigations of all their chemical characteristics which are useful for full-scale application.

Currently, nanotoxicity/ biocompatibility of CNC-based materials is not fully defined, some publications that have considered in-vitro studies have described it to be very low/non-existent under their respective experimental conditions. Such data is clearly inadequate for clinical translational studies given their inordinate potential for biomedical applications of CNCs in oncology. As one of the ultimate goals in the field of nanomedicine, more studies on cellular-to-organismal toxicity, biodistribution, epi-and intracellular interactions and ecotoxicity of CNCs are still required to explore their size, morphological and surface chemistry determinants of biotoxicity. On contrary, ineffective delivery, genotoxicity, inflammation, oxidative stress, lack of dosage and other hazardous profiles as discussed above, are also major blockades for clinical translation of CNCs. Thus, a necessity of special scientific investigations of CNC-based nano-agents for cancer therapy.

Finally, there are numerous CNCs-based patents and innovations, highlighting significant scientific and technological impacts of this natural-based material with attributes that may revolutionize cancer diagnosis and treatment. We would like to believe that this article will intensify the attention of research community towards advanced innovative preparation, modification, characterization, biocompatibility and nanotoxicological evaluation of CNCs for cancer diagnosis and treatment.

Declaration of Competing Interest

The authors report no declaration of interest.

Acknowledgements

This work was funded by the Fundamental Research Funds of Zhejiang Sci-Tech University (2021Q002), State key Laboratory for Modification of Chemical Fibers and Polymer Materials, Donghua University (KF2020), and the Shanghai Education Commission through the Shanghai Leading Talents Program, the Science and Technology

Commission of Shanghai Municipality (19XD1400100). We also appreciate the contribution by the college of chemistry, chemical engineering and biotechnology, Donghua university.

References

[1] S. Wang, J. Li, Z. Ye, et al., Self-assembly of photosensitive and chemotherapeutic drugs for combined photodynamic-chemo cancer therapy with real-time tracing property, Coll. Sur. A Physicochem. Eng. Aspects 574 (2019) 44–51.

[2] Y. Li, S. Wang, F.X. Song, et al., A pH-sensitive drug delivery system based on folic acid-targeted HBP-modified mesoporous silica nanoparticles for cancer therapy, Coll. Sur. A Physicochem. Eng. Aspects 590 (2020) 124470.

[3] H. Chen, W. Zhang, G. Zhu, et al., Rethinking cancer nanotheranostics, Nat. Rev. Mater. 2 (7) (2017).

[4] C.C. Horgan, M.S. Bergholt, A. Nagelkerke, et al., Integrated photodynamic Raman theranostic system for cancer diagnosis, treatment, and post-treatment molecular monitoring, Theranostics 11 (4) (2021) 2006–2019.

[5] H. Huang, J.F. Lovell, Advanced functional nanomaterials for theranostics, Adv. Funct. Mater. 27 (2) (2017).

[6] S.V. Moghaddam, F. Abedi, E. Alizadeh, et al., Lysine-embedded cellulose-based nanosystem for efficient dual-delivery of chemotherapeutics in combination cancer therapy, Carbohydr. Polym. 250 (2020) 116861.

[7] J. Choi, S.-E. Lee, J.-S. Park, et al., Gold nanorod-photosensitizer conjugates with glutathione-sensitive linkages for synergistic cancer photodynamic/photothermal therapy, Biotechnol. Bioeng. 115 (5) (2018) 1340–1354.

[8] L. Zhang, Y. Wang, D. Yang, et al., Shape Effect of Nanoparticles on Tumor Penetration in Monolayers Versus Spheroids, Mol. Pharm. 16 (7) (2019) 2902–2911.

[9] V. Kushwah, S.S. Katiyar, A.K. Agrawal, et al., Co-delivery of docetaxel and gemcitabine using PEGylated self-assembled stealth nanoparticles for improved breast cancer therapy, Nanomedicine 14 (5) (2018) 1629–1641.

[10] Z. Zhao, S. Lou, Y. Hu, et al., A nano-in-nano polymer–dendrimer nanoparticle-based nanosystem for controlled multidrug delivery, Mol. Pharm. 14 (8) (2017) 2697–2710.

[11] M. Rahimi, K.D. Safa, R. Salehi, Co-delivery of doxorubicin and methotrexate by dendritic chitosan-g-mPEG as a magnetic nanocarrier for multi-drug delivery in combination chemotherapy, Polym. Chem. 8 (47) (2017) 7333–7350.

[12] F.T. Seta, X. An, L. Liu, et al., Preparation and characterization of high yield cellulose nanocrystals (CNC) derived from ball mill pretreatment and maleic acid hydrolysis, Carbohydr. Polym. 234 (2020) 115942.

[13] H. Bian, L. Chen, H. Dai, et al., Effect of fiber drying on properties of lignin containing cellulose nanocrystals and nanofibrils produced through maleic acid hydrolysis, Cellulose 24 (10) (2017) 4205–4216.

[14] S. Ventura-Cruz, A. Tecante, Nanocellulose and microcrystalline cellulose from agricultural waste: Review on isolation and application as reinforcement in polymeric matrices, Food Hydrocoll. 118 (2021) 106771.

[15] Y. Habibi, L.A. Lucia, O.J. Rojas, Cellulose nanocrystals: chemistry, self-assembly, and applications, Chem. Rev. 110 (6) (2010) 3479–3500.

[16] R.J. Moon, A. Martini, J. Nairn, et al., Cellulose nanomaterials review: structure, properties and nanocomposites, Chem. Soc. Rev. 40 (7) (2011) 3941–3994.

[17] A. Farooq, M.K. Patoary, M. Zhang, et al., Cellulose from sources to nanocellulose and an overview of synthesis and properties of nanocellulose/zinc oxide nanocomposite materials, Int. J. Biol. Macromol. 154 (2020) 1050–1073.

[18] R.J. Moon, G.T. Schueneman, J. Simonsen, Overview of cellulose nanomaterials, their capabilities and applications, JOM-US 68 (9) (2016) 2383–2394.

[19] L.R. Arcot, A.H. Groschel, M.B. Linder, O.J. Rojas, O. Ikkala, Self-Assembly of native cellulose nanostructures, in: H. Kargarzadeh, S. Thomas, A. Dufresne (Eds.), Handbook of Nanocellulose and Cellulose Nanocomposites, 2017, pp. 123–174.

[20] H. Zhu, W. Luo, P.N. Ciesielski, et al., Wood-derived materials for green electronics, biological devices, and energy applications, Chem. Rev. 116 (16) (2016) 9305–9374.

[21] E.J. Foster, R.J. Moon, U.P. Agarwal, et al., Current characterization methods for cellulose nanomaterials, Chem. Soc. Rev. 47 (8) (2018) 2609–2679.

[22] N. Grishkewich, N. Mohammed, J. Tang, et al., Recent advances in the application of cellulose nanocrystals, Curr. Opin. Colloid Interface Sci. 29 (2017) 32–45.

[23] S.S. Ahankari, A.R. Subhedar, S.S. Bhadauria, et al., Nanocellulose in food packaging: A review, Carbohydr. Polym. 255 (2021) 117479.

[24] R.A. Ilyas, Sapuan* S M, Sanyang M L, et al., Nanocrystalline cellulose as reinforcement for polymeric matrix nanocomposites and its potential applications: a review, Curr. Anal. Chem. 14 (3) (2018) 203–225.

[25] M.S. Reid, M. Villalobos, E.D. Cranston, Benchmarking cellulose nanocrystals: From the laboratory to industrial production, Langmuir 33 (7) (2017) 1583–1598.

[26] K.J. De France, T. Hoare, E.D. Cranston, Review of hydrogels and aerogels containing nanocellulose, Chem. Mater. 29 (11) (2017) 4609–4631.

[27] D. García-García, R. Balart, J. Lopez-Martinez, et al., Optimizing the yield and physico-chemical properties of pine cone cellulose nanocrystals by different hydrolysis time, Cellulose 25 (5) (2018) 2925–2938.

[28] C. Zinge, B. Kandasubramanian, Nanocellulose based biodegradable polymers, Eur. Polym. J. 133 (2020) 109758.

[29] S. Rashid, H. Dutta, Characterization of nanocellulose extracted from short, medium and long grain rice husks, Ind. Crop. Prod. 154 (2020) 112627.

[30] X.Q. Chen, G.X. Pang, W.H. Shen, et al., Preparation and characterization of the ribbon-like cellulose nanocrystals by the cellulase enzymolysis of cotton pulp fibers, Carbohydr. Polym. 207 (2019) 713–719.

[31] J. You, J. Cao, Y. Zhao, et al., Improved mechanical properties and sustained release behavior of cationic cellulose nanocrystals reinforeced cationic cellulose injectable hydrogels, Biomacromolecules 17 (9) (2016) 2839–2848.

[32] R. Scaffaro, L. Botta, F. Lopresti, et al., Polysaccharide nanocrystals as fillers for PLA based nanocomposites, Cellulose 24 (2) (2017) 447–478.

[33] Y. Si, H. Luo, F. Zhou, et al., Advances in polysaccharide nanocrystals as pharmaceutical excipients, Carbohydr. Polym. 262 (2021) 117922.

[34] M.D. Xue, D.G. Gray, Induced circular dichroism of isotropic and magnetically-oriented chiral nematic suspensions of cellulose crystallites, Langmuir 13 (11) (1997) 3029–3034.

[35] R. Sunasee, U.D. Hemraz, Synthetic strategies for the fabrication of cationic surface-modified cellulose-nanocrystals, Fibers 6 (1) (2018) 15 ((19 pp.)-15 (19 pp.)).

[36] J.F. Revol, H. Bradford, J. Giasson, et al., Helicoidal self-ordering of cellulose microfibrils in aqueous suspension, Int. J. Biol. Macromol. 14 (3) (1992) 170–172.

[37] S. Dong, M. Roman, Fluorescently labeled cellulose nanocrystals for bioimaging applications, J. Am. Chem. Soc. 129 (45) (2007) 13810.

[38] J. Shojaeiarani, D. Bajwa, A. Shirzadifar, A review on cellulose nanocrystals as promising biocompounds for the synthesis of nanocomposite hydrogels, Carbohydr. Polym. 216 (2019) 247–259.

[39] D. Trache, M.H. Hussin, M.K.M. Haafiz, et al., Recent progress in cellulose nanocrystals: sources and production, Nanoscale 9 (5) (2017) 1763–1786.

[40] H. Golmohammadi, E. Morales-Narvaez, T. Naghdi, et al., Nanocellulose in sensing and biosensing, Chem. Mater. 29 (13) (2017) 5426–5446.

[41] A.B. Seabra, J.S. Bernardes, W.J. Favaro, et al., Cellulose nanocrystals as carriers in medicine and their toxicities: A review, Carbohydr. Polym. 181 (2018) 514–527.

[42] B.G. Rånby, E. Ribi, Recent advances in nanocellulose for biomed appln.pdf- Über den Feinbau der Zellulose, Experientia 6 (1) (1950) 12–14.

[43] R.H. Marchessault, F.F. Morehead, N.M. Walter, Liquid crystal systems from fibrillar polysaccharides, Nature 184 (4686) (1959) 632–633.

[44] L.L.H. Bergeson, N. Carla, Nanotechnologies — Standard terms and their definition for cellulose nanomaterial, Edition 1, ISO, 2017.

[45] O. Kose, A. Tran, L. Lewis, et al., Unwinding a spiral of cellulose nanocrystals for stimuli-responsive stretchable optics, Nat. Commun. 10 (1) (2019) 510.

[46] H. Xie, Z. Zou, H. Du, et al., Preparation of thermally stable and surface-functionalized cellulose nanocrystals via mixed H2SO4/Oxalic acid hydrolysis, Carbohydr. Polym. 223 (2019) 115116.

[47] L. Jasmani, S. Adnan, Preparation and characterization of nanocrystalline cellulose from Acacia mangium and its reinforcement potential, Carbohydr. Polym. 161 (2017) 166–171.

[48] L. Du, J. Wang, Y. Zhang, et al., A co-production of sugars, lignosulfonates, cellulose, and cellulose nanocrystals from ball-milled woods, Bioresour. Technol. 238 (2017) 254–262.

[49] A. Isogai, Y. Zhou, Diverse nanocelluloses prepared from TEMPO-oxidized wood cellulose fibers: Nanonetworks, nanofibers, and nanocrystals, Curr. Opinion Solid State Mater. Sci. 23 (2) (2019) 101–106.

[50] X. Yang, H. Xie, H. Du, et al., Facile extraction of thermally stable and dispersible cellulose nanocrystals with high yield via a green and recyclable FeCl3-catalyzed deep eutectic solvent system, ACS Sustain. Chem. Eng. 7 (7) (2019) 7200–7208.

[51] H. Wang, H. Xie, H. Du, et al., Highly efficient preparation of functional and thermostable cellulose nanocrystals via H2SO4 intensified acetic acid hydrolysis, Carbohydr. Polym. 239 (2020) 116233.

[52] F. Yeganeh, R. Behrooz, M. Rahimi, The effect of sulfuric acid and maleic acid on characteristics of nano-cellulose produced from waste office paper, Int. J. Nano Dimension 8 (3) (2017) 206–215.

[53] L. Xing, J. Gu, W. Zhang, et al., Cellulose I and II nanocrystals produced by sulfuric acid hydrolysis of Tetra pak cellulose I, Carbohydr. Polym. 192 (2018) 184–192.

[54] C.C.S. Coelho, M. Michelin, M.A. Cerqueira, et al., Cellulose nanocrystals from grape pomace: Production, properties and cytotoxicity assessment, Carbohydr. Polym. 192 (2018) 327–336.

[55] C.C. Hernandez, F.F. Ferreira, D.S. Rosa, X-ray powder diffraction and other analyses of cellulose nanocrystals obtained from corn straw by chemical treatments, Carbohydr. Polym. 193 (2018) 39–44.

[56] R. Dungani, A.F. Owolabi, C.K. Saurabh, et al., Preparation and fundamental characterization of cellulose nanocrystal from oil palm fronds biomass, J. Polym. Environ. 25 (3) (2017) 692–700.

[57] M. Fardioui, A. Stambouli, T. Gueddira, et al., Extraction and characterization of nanocrystalline cellulose from doum (chamaerops humilis) leaves: a potential reinforcing biomaterial, J. Polym. Environ. 24 (4) (2016) 356–362.

[58] A.P. Travalini, E. Prestes, L.A. Pinheiro, et al., Extraction and characterization of nanocrystalline cellulose from cassava bagasse, J. Polym. Environ. 26 (2) (2018) 789–797.

[59] S.H. Sung, Y. Chang, J. Han, Development of polylactic acid nanocomposite films reinforced with cellulose nanocrystals derived from coffee silverskin, Carbohydr. Polym. 169 (2017) 495–503.

[60] R.A. Ilyas, S.M. Sapuan, M.R. Ishak, Isolation and characterization of nanocrystalline cellulose from sugar palm fibres (Arenga Pinnata), Carbohydr. Polym. 181 (2018) 1038–1051.

[61] N. Zainuddin, I. Ahmad, H. Kargarzadeh, et al., Hydrophobic kenaf nanocrystalline cellulose for the binding of curcumin, Carbohydr. Polym. 163 (2017) 261–269.
[62] Listyanda R.F. Kusmono, M.W. Wildan, et al., Preparation and characterization of cellulose nanocrystal extracted from ramie fibers by sulfuric acid hydrolysis, Heliyon 6 (11) (2020) e05486.
[63] S. Naduparambath, T.V. Jinitha, V. Shaniba, et al., Isolation and characterisation of cellulose nanocrystals from sago seed shells, Carbohydr. Polym. 180 (2018) 13–20.
[64] U.P. Agarwal, Raman spectroscopy in the analysis of cellulose nanomaterials, in: Nanocelluloses: Their Preparation, Properties, and Applications, ACS, 2017, pp. 75–90.
[65] M. El Achaby, Z. Kassab, A. Aboulkas, et al., Reuse of red algae waste for the production of cellulose nanocrystals and its application in polymer nanocomposites, Int. J. Biol. Macromol. 106 (2018) 681–691.
[66] Y.W. Chen, H.V. Lee, J.C. Juan, et al., Production of new cellulose nanomaterial from red algae marine biomass Gelidium elegans, Carbohydr. Polym. 151 (2016) 1210–1219.
[67] Z. Liu, X. Li, W. Xie, et al., Extraction, isolation and characterization of nanocrystalline cellulose from industrial kelp (Laminaria japonica) waste, Carbohydr. Polym. 173 (2017) 353–359.
[68] H. Doh, M.H. Lee, W.S. Whiteside, Physicochemical characteristics of cellulose nanocrystals isolated from seaweed biomass, Food Hydrocoll. 102 (2020) 105542.
[69] R.M. Parker, G. Guidetti, C.A. Williams, et al., The self-assembly of cellulose nanocrystals: hierarchical design of visual appearance, Adv. Mater. 30 (19) (2018).
[70] J. Yang, O. Dahl, K. Vanhatalo, Manufacturing of nanocrystalline cellulose, in: Master's Programme in Chemical, Biochemical and Materials Engineering Major in Biomass refining, 2017.
[71] M. Cheng, Z. Qin, Y. Chen, et al., Efficient extraction of cellulose nanocrystals through hydrochloric acid hydrolysis catalyzed by inorganic chlorides under hydrothermal conditions, ACS Sustain. Chem. Eng. 5 (6) (2017) 4656–4664.
[72] R. Rohaizu, W.D. Wanrosli, Sono-assisted TEMPO oxidation of oil palm lignocellulosic biomass for isolation of nanocrystalline cellulose, Ultrason. Sonochem. 34 (2017) 631–639.
[73] I. Lugoloobi, H. Memon, Chemical structure and modification of cotton, in: W. Hua, H. Memon (Eds.), Cotton Science and Processing Technology, Springer Nature, 2020, pp. 417–432.
[74] I. Lugoloobi, M. Shahriari Khalaji, H. Memon, Advanced biological applications of modified cotton, in: W. Hua, H. Memon (Eds.), Cotton Science and Processing Technology, Springer Nature, 2020, pp. 473–500.
[75] I. Lugoloobi, M. Tebyetekerwa, H. Memon, et al., Advanced chemical applications of modified cotton, in: W. Hua, H. Memon (Eds.), Cotton Science and Processing Technology, Springer Nature, 2020, pp. 501–527.
[76] M. Shahriari Khalaji, I. Lugoloobi, Biomedical application of cotton and its derivatives, in: W. Hua, H. Memon (Eds.), Cotton Science and Processing Technology, Springer Nature, 2020, pp. 393–416.
[77] J.V. Edwards, N. Prevost, A. French, et al., Nanocellulose-based biosensors: design, preparation, and activity of peptide-linked cotton cellulose nanocrystals having fluorimetric and colorimetric elastase detection sensitivity, Engineering 05 (09) (2013) 20–28.
[78] J.M. Yarbrough, R. Zhang, A. Mittal, et al., Multifunctional cellulolytic enzymes outperform processive fungal cellulases for coproduction of nanocellulose and biofuels, ACS Nano 11 (3) (2017) 3101–3109.
[79] K. Song, Y. Ji, L. Wang, et al., A green and environmental benign method to extract cellulose nanocrystal by ball mill assisted solid acid hydrolysis, J. Clean. Prod. 196 (2018) 1169–1175.
[80] R.F. Nickerson, J.A. Habrle, Cellulose intercrystalline structure, Ind. Eng. Chem. Res. 39 (11) (1947) 1507–1512.
[81] O.A. Battista, Hydrolysis and crystallization of cellulose, Ind. Eng. Chem. Res. 42 (3) (1950) 502–507.
[82] S.M. Mukherjee, H.J. Woods, X-ray and electron microscope studies of the degradation of cellulose by sulphuric acid, Biochim. Biophys. Acta 10 (4) (1953) 499–511.
[83] C.L. Pirich, G.F. Picheth, J.P.E. Machado, et al., Influence of mechanical pretreatment to isolate cellulose nanocrystals by sulfuric acid hydrolysis, Int. J. Biol. Macromol. 130 (2019) 622–626.
[84] M.M. Mahmud, A. Perveen, R.A. Jahan, et al., Preparation of different polymorphs of cellulose from different acid hydrolysis medium, Int. J. Biol. Macromol. 130 (2019) 969–976.
[85] L. Xing, C. Hu, W. Zhang, et al., Transition of cellulose supramolecular structure during concentrated acid treatment and its implication for cellulose nanocrystal yield, Carbohydr. Polym. 229 (2020) 115539.
[86] J. Gong, J. Li, J. Xu, et al., Research on cellulose nanocrystals produced from cellulose sources with various polymorphs, RSC Adv. 7 (53) (2017) 33486–33493.
[87] A. Khan, Y. Wen, T. Huq, et al., Cellulosic nanomaterials in food and nutraceutical applications: a review, J. Agric. Food Chem. 66 (1) (2018) 8–19.
[88] L. Chen, J.Y. Zhu, C. Baez, et al., Highly thermal-stable and functional cellulose nanocrystals and nanofibrils produced using fully recyclable organic acids, Green Chem. 18 (13) (2016) 3835–3843.
[89] Q. Lu, Z. Cai, F. Lin, et al., Extraction of cellulose nanocrystals with a high yield of 88% by simultaneous mechanochemical activation and phosphotungstic acid hydrolysis, ACS Sustain. Chem. Eng. 4 (4) (2016) 2165–2172.
[90] K.-Y. Lee, Nanocellulose and sustainability _ production, properties, applications 1, CRC Press, 2018.
[91] E. Fischer, A. Speier, Darstellung der ester, Ber. Dtsch. Chem. Ges. 28 (3) (1895) 3252–3258.
[92] B. Braun, J.R. Dorgan, Single-step method for the isolation and surface functionalization of cellulosic nanowhiskers, Biomacromolecules 10 (2) (2009) 334–341.
[93] L. Tang, B. Huang, Q. Lu, et al., Ultrasonication-assisted manufacture of cellulose nanocrystals esterified with acetic acid, Bioresour. Technol. 127 (2013) 100–105.
[94] C.Q. Yang, W. Xilie, Formation of cyclic anhydride intermediates and esterification of cotton cellulose by multifunctional carboxylic acids: an infrared spectroscopy study, Text. Res. J. 66 (9) (2016) 595–603.
[95] L.P. Novo, J. Bras, A. García, et al., A study of the production of cellulose nanocrystals through subcritical water hydrolysis, Ind. Crop. Prod. 93 (2016) 88–95.
[96] M.M. Bashar, H. Zhu, S. Yamamoto, et al., Highly carboxylated and crystalline cellulose nanocrystals from jute fiber by facile ammonium persulfate oxidation, Cellulose 26 (6) (2019) 3671–3684.
[97] Q. Wu, J. Xu, Z. Wu, et al., The effect of surface modification on chemical and crystalline structure of the cellulose III nanocrystals, Carbohydr. Polym. 235 (2020) 115962.
[98] R. Salminen, M. Reza, T. Pääkkönen, et al., TEMPO-mediated oxidation of microcrystalline cellulose: limiting factors for cellulose nanocrystal yield[J], Cellulose 24 (4) (2017) 1657–1667.
[99] B. Sun, Q. Hou, Z. Liu, et al., Sodium periodate oxidation of cellulose nanocrystal and its application as a paper wet strength additive, Cellulose 22 (2) (2015) 1135–1146.
[100] C. You, L. Ning, H. Wu, et al., A biocompatible and pH-responsive nanohydrogel based on cellulose nanocrystal for enhanced toxic reactive oxygen species generation, Carbohydr. Polym. 258 (2021) 117685.
[101] L. Ning, C. You, Y. Zhang, et al., Synthesis and biological evaluation of surface-modified nanocellulose hydrogel loaded with paclitaxel, Life Sci. 241 (2020) 117137.
[102] Y. Zhang, L. Cui, H. Xu, et al., Poly(lactic acid)/cellulose nanocrystal composites via the Pickering emulsion approach: Rheological, thermal and mechanical properties, Int. J. Biol. Macromol. 137 (2019) 197–204.
[103] F. Wang, Y. Zhang, X. Li, et al., Cellulose nanocrystals-composited poly (methyl methacrylate) encapsulated n-eicosane via a pickering emulsion-templating approach for energy storage, Carbohydr. Polym. 234 (2020) 115934.
[104] E. Kontturi, A. Meriluoto, P.A. Penttilä, et al., Degradation and crystallization of cellulose in hydrogen chloride vapor for high-yield isolation of cellulose nanocrystals, Angew. Chem. Int. Ed. 55 (46) (2016) 14455–14458.
[105] T. Yang, Y. Guo, N. Gao, et al., Modification of a cellulase system by engineering Penicillium oxalicum to produce cellulose nanocrystal, Carbohydr. Polym. 234 (2020) 115862.
[106] A. Sharma, M. Thakur, M. Bhattacharya, et al., Commercial application of cellulose nano-composites – A review, Biotechnol. Rep. 21 (2019), e00316.
[107] X. An, Y. Wen, D. Cheng, et al., Preparation of cellulose nano-crystals through a sequential process of cellulase pretreatment and acid hydrolysis, Cellulose 23 (4) (2016) 2409–2420.
[108] P. Phanthong, P. Reubroycharoen, X. Hao, et al., Nanocellulose: extraction and application, CRC 1 (1) (2018) 32–43.
[109] N. Pandi, S.H. Sonawane, Kishore K. Anand, Synthesis of cellulose nanocrystals (CNCs) from cotton using ultrasound-assisted acid hydrolysis, Ultrason. Sonochem. 70 (2021) 105353.
[110] S. Beck, M. Methot, J. Bouchard, General procedure for determining cellulose nanocrystal sulfate half-ester content by conductometric titration, Cellulose 22 (1) (2015) 101–116.
[111] C.H. Lemke, R.Y. Dong, C.A. Michal, et al., New insights into nano-crystalline cellulose structure and morphology based on solid-state NMR, Cellulose 19 (5) (2012) 1619–1629.
[112] S. Afrin, Z. Karim, Isolation and surface modification of nanocellulose: necessity of enzymes over chemicals, ChemBioEng Rev. 4 (5) (2017) 289–303.
[113] L. Liu, Z. Hu, X. Sui, et al., Effect of counterion choice on the stability of cellulose nanocrystal pickering emulsions, Ind. Eng. Chem. Res. 57 (21) (2018) 7169–7180.
[114] D. Haldar, M.K. Purkait, Micro and nanocrystalline cellulose derivatives of lignocellulosic biomass: A review on synthesis, applications and advancements, Carbohydr. Polym. 250 (2020) 116937.
[115] Q. Beuguel, J.R. Tavares, P.J. Carreau, et al., Ultrasonication of spray- and freeze-dried cellulose nanocrystals in water, J. Colloid Interface Sci. 516 (2018) 23–33.
[116] S. Dong, M.J. Bortner, M. Roman, Analysis of the sulfuric acid hydrolysis of wood pulp for cellulose nanocrystal production: A central composite design study, Ind. Crop. Prod. 93 (2016) 76–87.
[117] H. Ji, Z. Xiang, H. Qi, et al., Strategy towards one-step preparation of carboxylic cellulose nanocrystals and nanofibrils with high yield, carboxylation and highly stable dispersibility using innocuous citric acid, Green Chem. 21 (8) (2019) 1956–1964.
[118] J. Tang, J. Sisler, N. Grishkewich, et al., Functionalization of cellulose nanocrystals for advanced applications, J. Colloid Interface Sci. 494 (2017) 397–409.
[119] J. Gong, L. Mo, J. Li, A comparative study on the preparation and characterization of cellulose nanocrystals with various polymorphs, Carbohydr. Polym. 195 (2018) 18–28.

[120] R.K. Mishra, H. Sung Kyu, K. Verma, et al., Recent progress in selected bio-nanomaterials and their engineering applications: an overview, J Sci Adv. Mater. Dev. 3 (3) (2018) 263–288.
[121] R. Sunasee, U.D. Hemraz, K. Ckless, Cellulose nanocrystals: a versatile nanoplatform for emerging biomedical applications, Expert Opin Drug Deliv. 13 (9) (2016) 1243–1256.
[122] M. Girard, D. Vidal, F. Bertrand, et al., Evidence-based guidelines for the ultrasonic dispersion of cellulose nanocrystals, Ultrason. Sonochem. 71 (2021) 105378.
[123] K. Sahlin, L. Forsgren, T. Moberg, et al., Surface treatment of cellulose nanocrystals (CNC): effects on dispersion rheology, Cellulose 25 (1) (2018) 331–345.
[124] H. Oguzlu, C. Danumah, Y. Boluk, Colloidal behavior of aqueous cellulose nanocrystal suspensions, Curr. Opin. Colloid Interface Sci. 29 (2017) 46–56.
[125] Y. Esparza, T.-D. Ngo, C. Fraschini, et al., Aggregate Morphology and Aqueous Dispersibility of Spray-Dried Powders of Cellulose Nanocrystals, Ind. Eng. Chem. Res. 58 (43) (2019) 19926–19936.
[126] R. Nigmatullin, M.A. Johns, J.C. Muñoz-García, et al., Hydrophobization of cellulose nanocrystals for aqueous colloidal suspensions and gels, Biomacromolecules 21 (5) (2020) 1812–1823.
[127] M. Mazloumi, L.J. Johnston, Z.J. Jakubek, Dispersion, stability and size measurements for cellulose nanocrystals by static multiple light scattering, Cellulose 25 (10) (2018) 5751–5768.
[128] S. Lombardo, A. Gençer, C. Schütz, et al., Thermodynamic study of ion-driven aggregation of cellulose nanocrystals, Biomacromolecules 20 (8) (2019) 3181–3190.
[129] A. Kumar, C.K. Dixit, 3 - Methods for characterization of nanoparticles, in: S. Nimesh, R. Chandra, N. Gupta (Eds.), Advances in Nanomedicine for the Delivery of Therapeutic Nucleic Acids, Woodhead Publishing, 2017, pp. 43–58.
[130] S. Bhattacharjee, DLS and zeta potential – What they are and what they are not? J. Control. Release 235 (2016) 337–351.
[131] J. Huang, D. Alain, L. Ning, Nanocellulose: From Fundamentals to Advanced Materials, First edition, Wiley-VCH Verlag GmbH & Co. KGaA, 2019, p. 486.
[132] H.-J. Lee, H.-S. Lee, J. Seo, et al., State-of-the-art of cellulose nanocrystals and optimal method for their dispersion for construction-related applications, Appl. Sci. 9 (3) (2019) 426.
[133] J. Shojaeiarani, D. Bajwa, G. Holt, Sonication amplitude and processing time influence the cellulose nanocrystals morphology and dispersion, Nanocomposites 6 (1) (2020) 41–46.
[134] S.A. Vivek, K.P. Hardik, P.S. Mayur, Computational Analysis of Ultrasonic Treatment of Melt for Effective Dispersion of Reinforcement Particles. ICRISET2017. International Conference on Research and Innovations in Science, Engineering and Technology. Selected Papers in Engineering, 2017, pp. 287–293.
[135] T. Cao, M. Elimelech, Colloidal stability of cellulose nanocrystals in aqueous solutions containing monovalent, divalent, and trivalent inorganic salts, J. Colloid Interface Sci. 584 (2021) 456–463.
[136] P. Rouster, M. Pavlovic, I. Szilagyi, Destabilization of titania nanosheet suspensions by inorganic salts: hofmeister series and Schulze-Hardy rule, J. Phys. Chem. B 121 (27) (2017) 6749–6758.
[137] T. Cao, T. Sugimoto, I. Szilagyi, et al., Heteroaggregation of oppositely charged particles in the presence of multivalent ions, Phys. Chem. Chem. Phys. 19 (23) (2017) 15160–15171.
[138] G. Trefalt, I. Szilagyi, G. Téllez, et al., Colloidal stability in asymmetric electrolytes: modifications of the schulze–hardy rule, Langmuir 33 (7) (2017) 1695–1704.
[139] C. Chen, W. Huang, Aggregation kinetics of diesel soot nanoparticles in wet environments, Environ. Sci. Technol. 51 (4) (2017) 2077–2086.
[140] Y. Cao, P. Zavattieri, J. Youngblood, et al., The relationship between cellulose nanocrystal dispersion and strength, Constr. Build. Mater. 119 (2016) 71–79.
[141] H. Kargarzadeh, M. Mariano, J. Huang, et al., Recent developments on nanocellulose reinforced polymer nanocomposites: A review, Polymer 132 (2017) 368–393.
[142] S. Geng, D. Wloch, N. Herrera, et al., Large-scale manufacturing of ultra-strong, strain-responsive poly(lactic acid)-based nanocomposites reinforced with cellulose nanocrystals, Compos. Sci. Technol. 194 (2020) 108144.
[143] M. Gu, C. Jiang, D. Liu, et al., Cellulose nanocrystal/poly(ethylene glycol) composite as an iridescent coating on polymer substrates: structure-color and interface adhesion, ACS Appl. Mater. Interfaces 8 (47) (2016) 32565–32573.
[144] C. Li, C. Sun, C. Wang, et al., Cellulose nanocrystal reinforced poly(lactic acid) nanocomposites prepared by a solution precipitation approach, Cellulose 27 (13) (2020) 7489–7502.
[145] M.R. Vakili, W. Mohammed-Saeid, A. Aljasser, et al., Development of mucoadhesive hydrogels based on polyacrylic acid grafted cellulose nanocrystals for local cisplatin delivery, Carbohydr. Polym. 255 (2021) 117332.
[146] Y.M. Kim, Y.S. Lee, T. Kim, et al., Cationic cellulose nanocrystals complexed with polymeric siRNA for efficient anticancer drug delivery, Carbohydr. Polym. 247 (2020) 116684.
[147] R. Ramírez-Casillas, M.D.C. López-López, B. Becerra-Aguilar, et al., Preparation and characterization of cellulose nanocrystals using soluble grade cellulose from acid hydrolysis of huizache (Acacia farnesiana L. Willd.), BioResources 14 (2) (2019) 2019.
[148] H. Hu, W. Yuan, F.-S. Liu, et al., Redox-responsive polycation-functionalized cotton cellulose nanocrystals for effective cancer treatment, ACS Appl. Mater. Interfaces 7 (16) (2015) 8942–8951.
[149] J. Zhou, H. Yao, J. Ma, Recent advances in RAFT-mediated surfactant-free emulsion polymerization, Polym. Chem. 9 (19) (2018) 2532–2561.
[150] J. Engström, F.L. Hatton, L. Wågberg, et al., Soft and rigid core latex nanoparticles prepared by RAFT-mediated surfactant-free emulsion polymerization for cellulose modification – a comparative study, Polym. Chem. 8 (6) (2017) 1061–1073.
[151] M. Haqani, H. Roghani-Mamaqani, M. Salami-Kalajahi, Synthesis of dual-sensitive nanocrystalline cellulose-grafted block copolymers of N-isopropylacrylamide and acrylic acid by reversible addition-fragmentation chain transfer polymerization, Cellulose 24 (5) (2017) 2241–2254.
[152] J. Zhou, H. Li, Y. Li, et al., V-Shaped amphiphilic polymer brushes grafted on cellulose nanocrystals: Synthesis, characterization and properties, J. Phys. Chem. Solids 154 (2021) 110056.
[153] C. Baek, Z. Hanif, S.-W. Cho, et al., Shape control of cellulose nanocrystals via compositional acid hydrolysis, J. Biomed. Nanotechnol. 9 (7) (2013) 1293–1298.
[154] Z. Hanif, F.R. Ahmed, S.W. Shin, et al., Size- and dose-dependent toxicity of cellulose nanocrystals (CNC) on human fibroblasts and colon adenocarcinoma, Colloids Surf. B: Biointerfaces 119 (2014) 162–165.
[155] T. Abitbol, H.S. Marway, S.A. Kedzior, et al., Hybrid fluorescent nanoparticles from quantum dots coupled to cellulose nanocrystals, Cellulose 24 (3) (2017) 1287–1293.
[156] T.S. Anirudhan, V. Chithra Sekhar, F. Shainy, et al., Effect of dual stimuli responsive dextran/nanocellulose polyelectrolyte complexes for chemophotothermal synergistic cancer therapy, Int. J. Biol. Macromol. 135 (2019) 776–789.
[157] A. Herreros-López, M. Carini, T. Da Ros, et al., Nanocrystalline cellulose-fullerene: Novel conjugates, Carbohydr. Polym. 164 (2017) 92–101.
[158] A. Boujemaoui, S. Mongkhontreerat, E. Malmström, et al., Preparation and characterization of functionalized cellulose nanocrystals, Carbohydr. Polym. 115 (2015) 457–464.
[159] L.R. Arcot, M. Lundahl, O.J. Rojas, et al., Asymmetric cellulose nanocrystals: thiolation of reducing end groups via NHS–EDC coupling, Cellulose 21 (6) (2014) 4209–4218.
[160] S.D. Hujaya, A. Manninen, K. Kling, et al., Self-assembled nanofibrils from RGD-functionalized cellulose nanocrystals to improve the performance of PEI/DNA polyplexes, J. Colloid Interface Sci. 553 (2019) 71–82.
[161] J. Xu, Z. Wu, Q. Wu, et al., Acetylated cellulose nanocrystals with high-crystallinity obtained by one-step reaction from the traditional acetylation of cellulose, Carbohydr. Polym. 229 (2020) 115553.
[162] J.-L. Huang, C.-J. Li, D. Gray, Cellulose nanocrystals incorporating fluorescent methylcoumarin groups, ACS Sustain. Chem. Eng. 1 (2013) 1160–1164.
[163] L. Colombo, L. Zoia, M.B. Violatto, et al., Organ distribution and bone tropism of cellulose nanocrystals in living mice, Biomacromolecules 16 (9) (2015) 2862–2871.
[164] J.W. Grate, K.-F. Mo, Y. Shin, et al., Alexa fluor-labeled fluorescent cellulose nanocrystals for bioimaging solid cellulose in spatially structured microenvironments, Bioconjug. Chem. 26 (3) (2015) 593–601.
[165] T. Abitbol, A. Palermo, J.M. Moran-Mirabal, et al., Fluorescent labeling and characterization of cellulose nanocrystals with varying charge contents, Biomacromolecules 14 (9) (2013) 3278–3284.
[166] M. Guo, S. Her, R. Keunen, et al., Functionalization of cellulose nanocrystals with PEG-metal-chelating block copolymers via controlled conjugation in aqueous media, ACS Omega 1 (1) (2016) 93–107.
[167] K.R. Colacino, C.B. Arena, S. Dong, et al., Folate conjugated cellulose nanocrystals potentiate irreversible electroporation-induced cytotoxicity for the selective treatment of cancer Cells, Technol. Cancer Res. 14 (6) (2015) 757–766.
[168] N. Drogat, R. Granet, C. Le Morvan, et al., Chlorin-PEI-labeled cellulose nanocrystals: Synthesis, characterization and potential application in PDT, Bioorg. Med. Chem. Lett. 22 (11) (2012) 3648–3652.
[169] L. Hou, J. Fang, W. Wang, et al., Indocyanine green-functionalized bottle brushes of poly(2-oxazoline) on cellulose nanocrystals for photothermal cancer therapy, J. Mater. Chem. B 5 (18) (2017) 3348–3354.
[170] G.M. Ndong Ntoutoume, V. Grassot, F. Bregier, et al., PEI-cellulose nanocrystal hybrids as efficient siRNA delivery agents-Synthesis, physicochemical characterization and in vitro evaluation, Carbohydr. Polym. 164 (2017) 258–267.
[171] L. Cellante, R. Costa, I. Monaco, et al., One-step esterification of nanocellulose in a Bronsted acid ionic liquid for delivery to glioblastoma cancer cells, New J. Chem. 42 (7) (2018) 5237–5242.
[172] X. Liu, R. Yang, M. Xu, et al., Hydrothermal Synthesis of Cellulose Nanocrystal-Grafted-Acrylic Acid Aerogels with Superabsorbent Properties, Polymers 10 (10) (2018) 1168.
[173] F. Yin, L. Lin, S. Zhan, Preparation and properties of cellulose nanocrystals, gelatin, hyaluronic acid composite hydrogel as wound dressing, J. Biomater. Sci. Polym. Ed. 30 (3) (2019) 190–201.
[174] Y. Esparza, T.-D. Ngo, Y. Boluk, Preparation of powdered oil particles by spray drying of cellulose nanocrystals stabilized Pickering hempseed oil emulsions, Coll. Sur. A Physicochem. Eng. Aspects 598 (2020) 124823.
[175] I. Lugoloobi, X. Li, Y. Zhang, et al., Fabrication of lignin/poly(3-hydroxybutyrate) nanocomposites with enhanced properties via a Pickering emulsion approach, Int. J. Biol. Macromol. 165 (2020) 3078–3087.
[176] M. Azizi Samir, F. Alloin, J.-Y. Sanchez, et al., Cellulose nanocrystals reinforced poly(oxyethylene), Polymer 45 (12) (2004) 4149–4157.
[177] D. Musino, C. Rivard, G. Landrot, et al., Hydroxyl groups on cellulose nanocrystal surfaces form nucleation points for silver nanoparticles of varying shapes and sizes, J. Colloid Interface Sci. 584 (2021) 360–371.
[178] Q. Xu, L. Jin, Y. Wang, et al., Synthesis of silver nanoparticles using dialdehyde cellulose nanocrystal as a multi-functional agent and application to antibacterial paper, Cellulose 26 (2) (2019) 1309–1321.

[179] C. Amara, A. El Mahdi, R. Medimagh, et al., Nanocellulose-based composites for packaging applications, Curr. Opin. Green Sustain. Chem. 100512 (2021).
[180] H. Hu, X.-J. Hou, X.-C. Wang, et al., Gold nanoparticle-conjugated heterogeneous polymer brush-wrapped cellulose nanocrystals prepared by combining different controllable polymerization techniques for theranostic applications, Polym. Chem. 7 (18) (2016) 3107–3116.
[181] Y. Hu, C. Wen, L. Song, et al., Multifunctional hetero-nanostructures of hydroxyl-rich polycation wrapped cellulose-gold hybrids for combined cancer therapy, J. Control. Release 255 (2017) 154–163.
[182] N. Li, W. Lu, J. Yu, et al., Rod-like cellulose nanocrystal/cis-aconityl-doxorubicin prodrug: A fluorescence-visible drug delivery system with enhanced cellular uptake and intracellular drug controlled release, Mater. Sci. Eng. C 91 (2018) 179–189.
[183] M. Salajková, L.A. Berglund, Q. Zhou, Hydrophobic cellulose nanocrystals modified with quaternary ammonium salts, J. Mater. Chem. 22 (37) (2012) 19798–19805.
[184] J.K. Jackson, K. Letchford, B.Z. Wasserman, et al., The use of nanocrystalline cellulose for the binding and controlled release of drugs, Int. J. Nanomedicine 6 (2011) 321–330.
[185] W. Qing, Y. Wang, Y. Wang, et al., The modified nanocrystalline cellulose for hydrophobic drug delivery, Appl. Surf. Sci. 366 (2016) 404–409.
[186] G.M.A. Ndong Ntoutoume, R. Granet, J.P. Mbakidi, et al., Development of curcumin–cyclodextrin/cellulose nanocrystals complexes: new anticancer drug delivery systems, Bioorg. Med. Chem. Lett. 26 (3) (2016) 941–945.
[187] M. Caillaud, Z. Msheik, G.M.A. Ndong-Ntoutoume, et al., Curcumin–cyclodextrin/cellulose nanocrystals improve the phenotype of Charcot-Marie-Tooth-1A transgenic rats through the reduction of oxidative stress, Free Radic. Biol. Med. 161 (2020) 246–262.
[188] G.M.A.N. Ntoutoume, R. Granet, J.P. Mbakidi, et al., Development of curcumin-cyclodextrin/cellulose nanocrystals complexes: New anticancer drug delivery systems, Bioorg. Med. Chem. Lett. 26 (3) (2016) 941–945.
[189] J. Tang, Y. Li, Y. Song, et al., Carbodiimide coupling versus click chemistry for nanoparticle surface functionalization: A comparative study for the encapsulation of sodium cholate by cellulose nanocrystals modified with beta-cyclodextrin, Carbohydr. Polym. 244 (2020) 116512.
[190] M. Caillaud, B. Chantemargue, L. Richard, et al., Local low dose curcumin treatment improves functional recovery and remyelination in a rat model of sciatic nerve crush through inhibition of oxidative stress, Neuropharmacology 139 (2018) 98–116.
[191] Z. Zhao, X. Li, Q. Li, Curcumin accelerates the repair of sciatic nerve injury in rats through reducing Schwann cells apoptosis and promoting myelinization, Biomed. Pharmacother. 92 (2017) 1103–1110.
[192] V. Mohanta, G. Madras, S. Patil, Layer-by-layer assembled thin films and microcapsules of nanocrystalline cellulose for hydrophobic drugdelivery, ACS Appl. Mater. Interfaces 6 (22) (2014) 20093–20101.
[193] H. Wang, J. He, M. Zhang, et al., A new pathway towards polymer modified cellulose nanocrystals via a “grafting onto” process for drug delivery, Polym. Chem. 6 (23) (2015) 4206–4209.
[194] S. Ehsanimehr, P. Najafi Moghadam, W. Dehaen, et al., Synthesis of pH-sensitive nanocarriers based on polyacrylamide grafted nanocrystalline cellulose for targeted drug delivery to folate receptor in breast cancer cells, Eur. Polym. J. 150 (2021) 110398.
[195] U.D. Hemraz, K.A. Campbell, J.S. Burdick, et al., Cationic poly(2-aminoethylmethacrylate) and poly(N-(2-aminoethylmethacrylamide)) modified cellulose nanocrystals: synthesis, characterization, and cytotoxicity, Biomacromolecules 16 (1) (2015) 319–325.
[196] C. Xing, S. Chen, X. Liang, et al., Two-Dimensional MXene (Ti3C2)-integrated cellulose hydrogels: toward smart three-dimensional network nanoplatforms exhibiting light-induced swelling and bimodal photothermal/chemotherapy anticancer activity, ACS Appl. Mater. Interfaces 10 (33) (2018) 27631–27643.
[197] J. MartíNez-Guerra, New insights on the chemical stability of curcumin in aqueous media at different pH: influence of the experimental conditions, Int. J. Electrochem. Sci. (2019) 5373–5385.
[198] M. Rahimi, V. Shafiei-Irannejad, K. Safa, et al., Multi-branched ionic liquid-chitosan as a smart and biocompatible nano-vehicle for combination chemotherapy with stealth and targeted properties, Carbohydr. Polym. 196 (2018) 299–312.
[199] L. Wang, M. Zheng, Z. Xie, Nanoscale metal–organic frameworks for drug delivery: a conventional platform with new promise, J. Mater. Chem. B 6 (5) (2018) 707–717.
[200] J. Zhao, Y. Yang, X. Han, et al., Redox-sensitive nanoscale coordination polymers for drug delivery and cancer theranostics, ACS Appl. Mater. Interfaces 9 (28) (2017) 23555–23563.
[201] C. You, H. Wu, Z. Gao, et al., Enhanced reactive oxygen species levels by an active benzothiazole complex-mediated fenton reaction for highly effective antitumor therapy, Mol. Pharm. 16 (12) (2019) 4929–4939.
[202] C. You, H. Wu, R. Zhang, et al., Dendritic mesoporous organosilica nanoparticles: A pH-triggered autocatalytic fenton reaction system with self-supplied H2O2 for generation of high levels of reactive oxygen species, Langmuir 36 (19) (2020) 5262–5270.
[203] Y. Dai, S. Cheng, Z. Wang, et al., Hypochlorous acid promoted platinum drug chemotherapy by myeloperoxidase-encapsulated therapeutic metal phenolic nanoparticles, ACS Nano 12 (1) (2018) 455–463.
[204] F.A. Ngwabebhoh, S.I. Erdagi, U. Yildiz, Pickering emulsions stabilized nanocellulosic-based nanoparticles for coumarin and curcumin nanoencapsulations: In vitro release, anticancer and antimicrobial activities, Carbohydr. Polym. 201 (2018) 317–328.
[205] L.E. Low, L.T.-H. Tan, B.-H. Goh, et al., Magnetic cellulose nanocrystal stabilized Pickering emulsions for enhanced bioactive release and human colon cancer therapy, Int. J. Biol. Macromol. 127 (2019) 76–84.
[206] V.T. Devita, E. Chu, A history of cancer chemotherapy, Cancer Res. 68 (21) (2008) 8643–8653.
[207] R. Oun, Y.E. Moussa, N.J. Wheate, The side effects of platinum-based chemotherapy drugs: a review for chemists, Dalton Trans. 47 (19) (2018) 6645–6653.
[208] K. Nurgali, R.T. Jagoe, R. Abalo, Editorial: adverse effects of cancer chemotherapy: anything new to improve tolerance and reduce sequelae? Front. Pharmacol. 9 (245) (2018).
[209] S.T. Sanjay, W. Zhou, M. Dou, et al., Recent advances of controlled drug delivery using microfluidic platforms, Adv. Drug Deliv. Rev. 128 (2018) 3–28.
[210] S. Senapati, A.K. Mahanta, S. Kumar, et al., Controlled drug delivery vehicles for cancer treatment and their performance, Signal Trans. Targeted Ther. 3 (1) (2018) 7.
[211] N. Li, H. Zhang, Y. Xiao, et al., Fabrication of cellulose-nanocrystal-based folate targeted nanomedicine via layer-by-layer assembly with lysosomal pH-controlled drug release into the nucleus, Biomacromolecules 20 (2) (2019) 937–948.
[212] M. Roman, Toxicity of cellulose nanocrystals: a review, Ind. Biotechnol. 11 (1) (2015) 25–33.
[213] Y.Y. Khine, M.H. Stenzel, Surface modified cellulose nanomaterials: a source of non-spherical nanoparticles for drug delivery, Materials Horizons 7 (7) (2020) 1727–1758.
[214] W. Tao, X. Ji, X. Zhu, et al., Two-dimensional antimonene-based photonic nanomedicine for cancer theranostics, Adv. Mater. 30 (38) (2018) 1802061.
[215] S. Behzadi, V. Serpooshan, W. Tao, et al., Cellular uptake of nanoparticles: journey inside the cell, Chem. Soc. Rev. 46 (14) (2017) 4218–4244.
[216] J.V. Jokerst, D. Van De Sompel, S.E. Bohndiek, et al., Cellulose nanoparticles are a biodegradable photoacoustic contrast agent for use in living mice, Photoacoustics 2 (3) (2014) 119–127.
[217] S. Salatin, Khosroushahi A. Yari, Overviews on the cellular uptake mechanism of polysaccharide colloidal nanoparticles, J. Cell. Mol. Med. 21 (9) (2017) 1668–1686.
[218] W. He, X. Xin, Y. Li, et al., Rod-shaped drug particles for cancer therapy: the importance of particle size and participation of caveolae pathway, Part. Part. Syst. Charact. 34 (6) (2017) 1600371.
[219] I.S. Mohammad, H. Hu, L. Yin, et al., Drug nanocrystals: fabrication methods and promising therapeutic applications, Int. J. Pharm. 562 (2019) 187–202.
[220] P. Foroozandeh, A.A. Aziz, Insight into cellular uptake and intracellular trafficking of nanoparticles, Nanoscale Res. Lett. 13 (1) (2018) 339.
[221] C. Shen, B. Shen, X. Liu, et al., Nanosuspensions based gel as delivery system of nitrofurazone for enhanced dermal bioavailability, J. Drug Deliv. Sci. Technol. 43 (2018) 1–11.
[222] K.A. Mahmoud, J.A. Mena, K.B. Male, et al., Effect of surface charge on the cellular uptake and cytotoxicity of fluorescent labeled cellulose nanocrystals, ACS Appl. Mater. Interfaces 2 (10) (2010) 2924–2932.
[223] K.R. Bittleman, S. Dong, M. Roman, et al., Folic acid-conjugated cellulose nanocrystals show high folate-receptor binding affinity and uptake by KB and breast cancer cells, ACS Omega 3 (10) (2018) 13952–13959.
[224] S. Dong, H.J. Cho, Y.W. Lee, et al., Synthesis and cellular uptake of folic acid-conjugated cellulose nanocrystals for cancer targeting, Biomacromolecules 15 (5) (2014) 1560–1567.
[225] S.A. Mohd Zuki, N. Abd Rahman, N.F. Abu Bakar, Nanocrystal cellulose as drug excipient in transdermal patch for wound healing: an overview, IOP Conf. Ser. Mate. Sci. Eng. 334 (2018), 012046.
[226] K.R. Colacino, S. Dong, M. Roman, et al., Cellulose nanocrystals: a novel biomaterial for targeted drug delivery applications, FASEB J. 25 (1_supplement) (2011) 762.3.
[227] B. Rioux, C. Pouget, G.M.A. Ndong-Ntoutoume, et al., Enhancement of hydrosolubility and in vitro antiproliferative properties of chalcones following encapsulation into β-cyclodextrin/cellulose-nanocrystal complexes, Bioorg. Med. Chem. Lett. 29 (15) (2019) 1895–1898.
[228] L. Tang, F. Lin, T. Li, et al., Design and synthesis of functionalized cellulose nanocrystals-based drug conjugates for colon-targeted drug delivery, Cellulose 25 (2018) 1–12.
[229] S.-Y. Wu, H.-Y. Chou, H.-C. Tsai, et al., Amino acid-modified PAMAM dendritic nanocarriers as effective chemotherapeutic drug vehicles in cancer treatment: a study using zebrafish as a cancer model, RSC Adv. 10 (35) (2020) 20682–20690.
[230] F. Bessone, M. Argenziano, G. Grillo, et al., Low-dose curcuminoid-loaded in dextran nanobubbles can prevent metastatic spreading in prostate cancer cells, Nanotechnology 30 (21) (2019) 214004.
[231] L.E. Low, B.T. Tey, B.H. Ong, et al., Unravelling pH-responsive behaviour of Fe3O4@CNCs-stabilized Pickering emulsions under the influence of magnetic field, Polymer 141 (2018) 93–101.
[232] K. Shanmugapriya, H. Kim, Y.W. Lee, et al., Cellulose nanocrystals/nanofibrils loaded astaxanthin nanoemulsion for the induction of apoptosis via ROS-dependent mitochondrial dysfunction in cancer cells under photobiomodulation, Int. J. Biol. Macromol. 149 (2020) 165–177.
[233] N. Meghani, P. Patel, K. Kansara, et al., Formulation of vitamin D encapsulated cinnamon oil nanoemulsion: Its potential anti-cancerous activity in human alveolar carcinoma cells, Colloids Surf. B: Biointerfaces 166 (2018) 349–357.

[234] M.S. Jangdey, A. Gupta, S. Saraf, Fabrication, in-vitro characterization, and enhanced in-vivo evaluation of carbopol-based nanoemulsion gel of apigenin for UV-induced skin carcinoma, Drug Deliv. 24 (1) (2017) 1026–1036.
[235] S.Y. Teo, M.Y. Yew, S.Y. Lee, et al., In vitro evaluation of novel phenytoin-loaded alkyd nanoemulsions designed for application in topical wound healing, J. Pharm. Sci. 106 (1) (2017) 377–384.
[236] X. Chen, J. Wei, C. Li, et al., Blocking interleukin-6 signaling inhibits cell viability/proliferation, glycolysis, and colony forming activity of human medulloblastoma cells, Int. J. Oncol. 52 (2) (2018) 571–578.
[237] S. Fu, X. Chen, H.J. Lin, et al., Inhibition of interleukin 8/C-X-C chemokine receptor 1,/2 signaling reduces malignant features in human pancreatic cancer cells, Int. J. Oncol. 53 (1) (2018) 349–357.
[238] J.C. Villanova, E. Ayres, S.M. Carvalho, et al., Pharmaceutical acrylic beads obtained by suspension polymerization containing cellulose nanowhiskers as excipient for drug delivery, Eur. J. Pharm. Sci. 42 (4) (2011) 406–415.
[239] K.J. De France, K.J.W. Chan, E.D. Cranston, et al., Enhanced mechanical properties in cellulose nanocrystal–poly(oligoethylene glycol methacrylate) injectable nanocomposite hydrogels through control of physical and chemical cross-linking, Biomacromolecules 17 (2) (2016) 649–660.
[240] S.K. Nair, S. Basu, B. Sen, et al., Colloidal gels with tunable mechanomorphology regulate endothelial morphogenesis, Sci. Rep. (2019) 9(1).
[241] M.I.H. Mondal, M.O. Haque, Cellulosic hydrogels: a greener solution of sustainability, in: M.I.H. Mondal (Ed.), Cellulose-Based Superabsorbent Hydrogels, Springer International Publishing, Cham, 2019, pp. 3–35.
[242] A. Olad, H. Zebhi, D. Salari, et al., Water retention and slow release studies of a salep-based hydrogel nanocomposite reinforced with montmorillonite clay, New J. Chem. 42 (4) (2018) 2758–2766.
[243] J. Nam, I.-B. Jung, B. Kim, et al., A colorimetric hydrogel biosensor for rapid detection of nitrite ions, Sensors Actuators B Chem. 270 (2018) 112–118.
[244] Y.-J. Lin, J.A. Shatkin, F. Kong, Evaluating mucoadhesion properties of three types of nanocellulose in the gastrointestinal tract in vitro and ex vivo, Carbohydr. Polym. 210 (2019) 157–166.
[245] C.A. Garcia-Gonzalez, A. Sosnik, J. Kalmar, et al., Aerogels in drug delivery: From design to application, J. Control. Release 332 (2021) 40–63.
[246] M. Tamborini, E. Locatelli, M. Rasile, et al., A combined approach employing chlorotoxin-nanovectors and low dose radiation to reach infiltrating tumor niches in glioblastoma, ACS Nano 10 (2) (2016) 2509–2520.
[247] Y. Dong, D.J. Siegwart, D.G. Anderson, Strategies, design, and chemistry in siRNA delivery systems, Adv. Drug Deliv. Rev. 144 (2019) 133–147.
[248] H. Kim, Y.K. Lee, K.H. Han, et al., BRC-mediated RNAi targeting of USE1 inhibits tumor growth in vitro and in vivo, Biomaterials 230 (2020) 119630.
[249] J.H. Lee, S.H. Ku, M.J. Kim, et al., Rolling circle transcription-based polymeric siRNA nanoparticles for tumor-targeted delivery, J. Control. Release 263 (2017) 29–38.
[250] D.F. Williams, On the mechanisms of biocompatibility, Biomaterials 29 (20) (2008) 2941–2953.
[251] S. Naahidi, M. Jafari, F. Edalat, et al., Biocompatibility of engineered nanoparticles for drug delivery, J. Control. Release 166 (2) (2013) 182–194.
[252] P. Aggarwal, J.B. Hall, C.B. Mcleland, et al., Nanoparticle interaction with plasma proteins as it relates to particle biodistribution, biocompatibility and therapeutic efficacy, Adv. Drug Deliv. Rev. 61 (6) (2009) 428–437.
[253] A. Mahapatro, D.K. Singh, Biodegradable nanoparticles are excellent vehicle for site directed in-vivo delivery of drugs and vaccines, J. Nanobiotechnol. 9 (2011) 55.
[254] S.A. Ali, P.J. Doherty, D.F. Williams, Mechanisms of polymer degradation in implantable devices. 2. Poly(DL-lactic acid), J. Biomed. Mater. Res. 27 (11) (1993) 1409–1418.
[255] R. Sunasee, E. Araoye, D. Pyram, et al., Cellulose nanocrystal cationic derivative induces NLRP3 inflammasome-dependent IL-1β secretion associated with mitochondrial ROS production, Biochem. Biophys. Rep. 4 (2015) 1–9.
[256] L. Dai, C.-L. Si, Cellulose-graft-poly(methyl methacrylate) nanoparticles with high biocompatibility for hydrophobic anti-cancer drug delivery, Mater. 207 (2017) 213–216.
[257] R.M.A. Domingues, M.E. Gomes, R.L. Reis, The potential of cellulose nanocrystals in tissue engineering strategies, Biomacromolecules 15 (7) (2014) 2327–2346.
[258] K. Kümmerer, J. Menz, T. Schubert, et al., Biodegradability of organic nanoparticles in the aqueous environment, Chemosphere 82 (10) (2011) 1387–1392.
[259] M. Ogonowski, U. Edlund, E. Gorokhova, et al., Multi-level toxicity assessment of engineered cellulose nanofibrils in Daphnia magna, Nanotoxicology 12 (6) (2018) 509–521.
[260] S. Camarero-Espinosa, C. Endes, S. Mueller, et al., Elucidating the potential biological impact of cellulose nanocrystals, Fibers 4 (3) (2016) 21.
[261] N. Yanamala, M.T. Farcas, M.K. Hatfield, et al., In vivo evaluation of the pulmonary toxicity of cellulose nanocrystals: a renewable and sustainable nanomaterial of the future, ACS Sustain. Chem. Eng. 2 (7) (2014) 1691–1698.
[262] Z. Hosseinidoust, M.N. Alam, G. Sim, et al., Cellulose nanocrystals with tunable surface charge for nanomedicine, Nanoscale 7 (40) (2015) 16647–16657.
[263] C. Endes, S. Camarero-Espinosa, S. Mueller, et al., A critical review of the current knowledge regarding the biological impact of nanocellulose, J. Nanobiotechnol. 14 (1) (2016) 78.
[264] WHO, World health statistics; a wealth of information on global public health, 2013.
[265] M.J.D. Clift, E.J. Foster, D. Vanhecke, et al., Investigating the interaction of cellulose nanofibers derived from cotton with a sophisticated 3D human lung cell coculture, Biomacromolecules 12 (10) (2011) 3666–3673.
[266] B.J. Harper, A. Clendaniel, F. Sinche, et al., Impacts of chemical modification on the toxicity of diverse nanocellulose materials to developing zebrafish, Cellulose (London, England) 23 (3) (2016) 1763–1775.
[267] R. Sunasee, M. Carson, H.W. Despres, et al., Analysis of the immune and antioxidant response of cellulose nanocrystals grafted with B2;-cyclodextrin in myeloid cell lines, J. Nanomater. 2019 (2019) 9.
[268] D. Shuping, A. Anjali, R.C. Katelyn, et al., Cytotoxicity and cellular uptake of cellulose nanocrystals, Nano LIFE 02 (03) (2012) 1241006.
[269] E. Kamelnia, A. Divsalar, M. Darroudi, et al., Production of new cellulose nanocrystals from Ferula gummosa and their use in medical applications via investigation of their biodistribution, Ind. Crop. Prod. 139 (2019) 111538.
[270] M. Roman, S. Dong, A. Hirani, et al., Cellulose nanocrystals for drug delivery, 2010, pp. 81–91.
[271] N.A.H. Shazali, N.E. Zaidi, H. Ariffin, et al., Characterization and cellular internalization of spherical cellulose nanocrystals (CNC) into normal and cancerous fibroblasts, Materials (Basel) (2019) 12(19).
[272] K.B. Male, A.C. Leung, J. Montes, et al., Probing inhibitory effects of nanocrystalline cellulose: inhibition versus surface charge, Nanoscale 4 (4) (2012) 1373–1379.
[273] H. Ni, S. Zeng, J. Wu, et al., Cellulose nanowhiskers: Preparation, characterization and cytotoxicity evaluation, Biomed. Mater. Eng. 22 (2012) 121–127.
[274] Y. Li, M. Kröger, W.K. Liu, Shape effect in cellular uptake of PEGylated nanoparticles: comparison between sphere, rod, cube and disk, Nanoscale 7 (40) (2015) 16631–16646.
[275] T. Liebert, M. Kostag, J. Wotschadlo, et al., Stable cellulose nanospheres for cellular uptake, Macromol. Biosci. 11 (10) (2011) 1387–1392.
[276] M.T. Farcas, E.R. Kisin, A.L. Menas, et al., Pulmonary exposure to cellulose nanocrystals caused deleterious effects to reproductive system in male mice, J. Toxicol. Environ. Health A 79 (21) (2016) 984–997.
[277] S.D.Á. Gonçalves, R.P. Vieira, Current status of ATRP-based materials for gene therapy, React. Funct. Polym. 147 (2020) 104453.
[278] S. Ahmed, K. Alhareth, N. Mignet, Advancement in nanogel formulations provides controlled drug release, Int. J. Pharm. 584 (2020) 119435.
[279] L. Syedmoradi, M.L. Norton, K. Omidfar, Point-of-care cancer diagnostic devices: From academic research to clinical translation, Talanta 225 (2021) 122002.
[280] S. Sharma, R. Zhuang, M. Long, et al., Circulating tumor cell isolation, culture, and downstream molecular analysis, Biotechnol. Adv. 36 (4) (2018) 1063–1078.
[281] I.S. Mohammad, W. He, L. Yin, A smart paclitaxel-disulfiram nanococrystals for efficient MDR reversal and enhanced apoptosis, Pharm. Res. (2018) 35(4).
[282] M. Curcio, L. Mauro, G.D. Naimo, et al., Facile synthesis of pH-responsive polymersomes based on lipidized PEG for intracellular co-delivery of curcumin and methotrexate, Colloids Surf. B: Biointerfaces 167 (2018) 568–576.
[283] N. Sanoj Rejinold, G. Choi, J.-H. Choy, Recent trends in nano photo-chemo therapy approaches and future scopes, Coord. Chem. Rev. 411 (2020) 213252.